

สมรรถนะในการเร่งปฏิกิริยาของตัวเร่งปฏิกิริยาซัลเฟตเซอร์โคเนียในการสังเคราะห์ไอโซบิวทีน

จากแก๊สสังเคราะห์



นางสาวณิชา ตั้งชูพงศ์

สถาบันวิทยบริการ

วิทยานิพนธ์นี้เป็นส่วนหนึ่งของการศึกษาตามหลักสูตรปริญญาวิศวกรรมศาสตรมหาบัณฑิต

สาขาวิชาวิศวกรรมเคมี ภาควิชาวิศวกรรมเคมี

คณะวิศวกรรมศาสตร์ จุฬาลงกรณ์มหาวิทยาลัย

ปีการศึกษา 2550

ลิขสิทธิ์ของจุฬาลงกรณ์มหาวิทยาลัย

CATALYTIC PERFORMANCE OF SULFATED ZIRCONIA CATALYSTS IN
ISOBUTENE SYNTHESIS FROM SYNTHESIS GAS



Miss. Nicha Tangchupong

สถาบันวิทยบริการ
จุฬาลงกรณ์มหาวิทยาลัย

A Thesis Submitted in Partial Fulfillment of the Requirements
for the Degree of Master of Engineering Program in Chemical Engineering

Department of Chemical Engineering

Faculty of Engineering

Chulalongkorn University

Academic Year 2007

Copyright of Chulalongkorn University

Thesis Title CATALYTIC PERFORMANCE OF SULFATED ZIRCONIA
CATALYSIS IN ISOBUTENE SYNTHESIS FROM
SYNTHESIS GAS

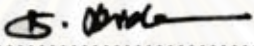
By Miss. Nicha Tangchupong

Field of study Chemical Engineering

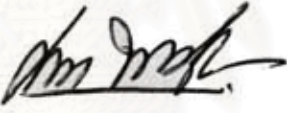
Thesis Advisor Associate Professor Suttichai Assabumrungrat, Ph.D.

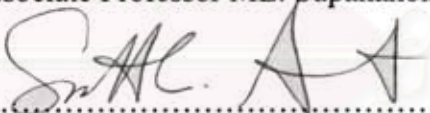
Thesis Co-advisor Assistant Professor Bunjerd Jongsomjit, Ph.D.

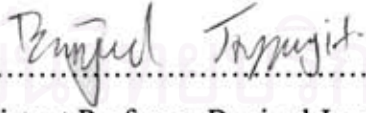
Accepted by the Faculty of Engineering, Chulalongkorn University in Partial
Fulfillment of the Requirements for the Master's Degree

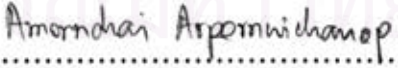

..... Dean of the Faculty of Engineering
(Associate Professor Boonsom Lerthirunwong, Dr.Ing.)

THESIS COMMITTEE


..... Chairman
(Associate Professor ML. Supakanok Thongyai, Ph.D.)


..... Thesis Advisor
(Associate Professor Suttichai Assabumrungrat, Ph.D.)


..... Thesis Co-advisor
(Assistant Professor Bunjerd Jongsomjit, Ph.D.)


..... Member
(Assistant Professor Amornchai Arpornwichanop, D.Eng.)


..... External Member
(Assistant Professor Worapon Kiatkittipong, D.Eng.)

นิชิต ตั้งชูพงศ์: พฤติกรรมในการเร่งปฏิกิริยาของตัวเร่งปฏิกิริยาซัลเฟตเซอร์โคเนียในการสังเคราะห์ไอโซบิวทีนจากแก๊สสังเคราะห์ (CATALYTIC PERFORMANCE OF SULFATED ZIRCONIA CATALYSIS IN ISOBUTENE SYNTHESIS FROM SYNTHESIS GAS) อ.ที่ปรึกษา: รศ.ดร.สุทธิชัย อัสสะบำรุงรัตน์, อ.ที่ปรึกษาร่วม: ผศ.ดร.บรรเจิด จงสมจิตร, 99 หน้า.

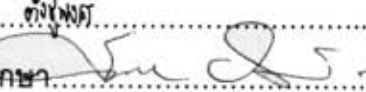
วิทยานิพนธ์นี้ศึกษาพฤติกรรมในการเร่งปฏิกิริยาของตัวเร่งปฏิกิริยาเซอร์โคเนีย ที่มีปริมาณซัลเฟอร์ที่แตกต่างกัน ซึ่งส่งผลกระทบต่อปฏิกิริยาสังเคราะห์ไอโซบิวทีน การศึกษาคุณลักษณะของตัวเร่งปฏิกิริยาเหล่านี้ทำโดยการใช้วิธีการวัดพื้นที่ผิว การกระเจิงรังสีเอ็กซ์ การคายซับของแอมโมเนียและคาร์บอนไดออกไซด์แบบโปรแกรมอุณหภูมิ และการส่องผ่านด้วยกล้องจุลทรรศน์อิเล็กตรอน สำหรับตัวเร่งปฏิกิริยาเซอร์โคเนียนั้นพบว่าตัวเร่งปฏิกิริยาที่สังเคราะห์จากเซอร์โคเนียในเตรตให้ความว่องไวและการเลือกเกิดของไอโซบิวทีนในไฮโดรคาร์บอนสูงกว่าเซอร์โคเนียคลอไรด์ คุณสมบัติความเป็นกรด-เบสและอัตราส่วนเฟสของเซอร์โคเนียสามารถส่งผลกระทบต่อพฤติกรรมในการเร่งปฏิกิริยาได้ นอกจากนี้ยังได้มีการปรับปรุงตัวเร่งปฏิกิริยาโดยการเติมซัลเฟอร์ลงไปบนตัวเร่งปฏิกิริยาเซอร์โคเนีย พบว่าตัวเร่งปฏิกิริยาซัลเฟตเซอร์โคเนียมีค่าการเลือกเกิดของไอโซบิวทีนในไฮโดรคาร์บอนสูงกว่าตัวเร่งปฏิกิริยาเซอร์โคเนีย เนื่องจากคุณสมบัติความเป็นกรด-เบส พื้นที่ผิวและอัตราส่วนเฟสของเซอร์โคเนีย และได้มีการศึกษาถึงผลของอุณหภูมิในการให้ความร้อนของการเผา สำหรับตัวเร่งปฏิกิริยาซัลเฟตเซอร์โคเนียทางการค้าพบว่าเมื่อเพิ่มอุณหภูมิในการให้ความร้อนจะได้เฟสโมโนคลินิกเพิ่มขึ้น และคุณสมบัติความเป็นกรดลดลง จากผลเหล่านี้พบว่าการเลือกเกิดไอโซบิวทีนลดลง สำหรับตัวเร่งปฏิกิริยาซัลเฟตเซอร์โคเนียจากการสังเคราะห์ที่เติมซัลเฟอร์ปริมาณ 0.75% พบว่าปัจจัยหลักที่มีผลต่อการเลือกเกิดไอโซบิวทีนคืออัตราส่วนเฟสของซัลเฟตเซอร์โคเนีย และคุณสมบัติความเป็นกรด-เบส ดังนั้นสามารถสรุปได้ว่าอุณหภูมิในการให้ความร้อนของการเผานั้นมีผลกระทบต่อปริมาณซัลเฟอร์ พื้นที่ผิว อัตราส่วนเฟส และความเป็นกรด-เบส ส่งผลต่อพฤติกรรมในการเร่งปฏิกิริยา นอกจากนี้อุณหภูมิในการทำปฏิกิริยาที่เหมาะสมคือ 400 องศาเซลเซียส


ภาควิชา.....วิศวกรรมเคมี.....

สาขาวิชา.....วิศวกรรมเคมี.....

ปีการศึกษา.....2550.....

ลายมือชื่อนิสิต.....นิชิต ตั้งชูพงศ์.....

ลายมือชื่ออาจารย์ที่ปรึกษา..........

ลายมือชื่ออาจารย์ที่ปรึกษาร่วม..........

4970313921: MAJOR CHEMICAL ENGINEERING

KEY WORDS: SULFATED ZIRCONIA / ISOBUTENE / ISOSYNTHESIS

NICHA TANGCHUPONG: CATALYTIC PERFORMANCE OF SULFATED ZIRCONIA CATALYSIS IN ISOBUTENE SYNTHESIS FROM SYNTHESIS GAS. THESIS ADVISOR: ASSOC. PROF. SUTTICHA ASSABUMRUNGRAT, Ph.D. THESIS CO-ADVISOR: ASST. PROF. BUNJERD JONGSOMJIT, Ph.D. 99 pp.

The catalytic performances of zirconia catalysts with various content of sulfur on isosynthesis were studied. The characteristics of the catalysts were determined by using various techniques including BET surface area, XRD, NH₃- and CO₂-TPD, and SEM. For zirconia catalysts, it was found that zirconia catalysts synthesized from zirconyl nitrate showed the highest activity and selectivity of isobutene in hydrocarbons among other ones. The acid-base properties and phase composition of sulfated zirconia influenced the catalytic performance. Moreover, the catalysts were improved by sulfur loading. It revealed that sulfated zirconia catalysts exhibited higher selectivity of isobutene in hydrocarbons than zirconia due to difference in acid-base properties, specific surface area and phase composition. Effect of calcination temperature was also investigated. For the commercial sulfated zirconia, it found that increased calcination temperature resulted in increased monoclinic phase in sulfated zirconia, but decreased acid sites. The result revealed that lower selectivity of isobutene in hydrocarbons. The 0.75% sulfated zirconia synthesized from zirconyl nitrate showed the major factor determining the activity and selectivity of isobutene in terms of phase composition. Therefore, it was concluded that the difference in the calcination temperatures influenced the catalytic performance, sulfur content, specific surface area, phase composition and acid-base properties of the catalysts. In addition, the suitable reaction temperature for isosynthesis was 400°C.

Department ... Chemical Engineering...	Student's signature... NICHA TANGCHUPONG
Field of study... Chemical Engineering...	Advisor's signature..... <i>Suttichai Assabumrungrat</i>
Academic year.....2007.....	Co-advisor's signature... <i>Bunjerd Jongsomjit</i>

ACKNOWLEDGEMENTS

The author would like to express her greatest gratitude to her advisor, Associate Professor Suttichai Assabumrungrat, and co-advisor, Assistant Professor Bunjerd Jongsomjit, for their invaluable suggestion and guidance throughout this study. In addition, I would also grateful to thank to Associate Professor ML. Supakanok Thongyai who has been the chairman of the committee for this thesis, Amornchai Arpornwichanop and Assistant Professor Woraphon Kaitkittipong, members of the thesis committee for their kind cooperation.

Moreover, the author would like to thank the Thailand Research Fund (TRF), as well as the Graduate School of Chulalongkorn University and Center of Excellence in Catalysis and Catalytic Reaction Engineering for their financial support. Finally, she also would like to dedicate this thesis to her parents for their worthy support and encouragement at all times.



สถาบันวิทยบริการ
จุฬาลงกรณ์มหาวิทยาลัย

CONTENTS

	PAGE
ABSTRACT (IN THAI).....	iv
ABSTRACT (IN ENGLISH).....	v
ACKNOWLEDGEMENTS.....	vi
CONTENTS.....	vii
LIST OF TABLES.....	xi
LIST OF FIGURES.....	xii
CHAPTER	
I INTRODUCTION.....	1
II THEORY.....	4
2.1 Fischer-Tropsch synthesis (FTS).....	4
2.2 Isosynthesis.....	5
2.3 General feature of zirconia.....	7
2.4 Preparation method of catalysts.....	9
2.4.1 Precipitation and Coprecipitation	9
2.4.1.1 General Principles Governing Precipitation from Solution.....	10
2.4.1.2 Chemical Considerations.....	11
2.4.1.3 Process Considerations.....	12
2.4.1.4 Influences on Properties of the Final Product..	15
2.5 Preparation of SO ₄ -ZrO ₂	15
III LITERATURE REVIEWS.....	17
3.1 Mechanism of isosynthesis over oxide catalysts.....	17
3.2 Effect of preparation of oxide catalysts.....	18
3.2.1 Precipitation method.....	18
3.2.2 Mechanical mixing method.....	19
3.2.3 Coprecipitation method.....	20
3.3 Effect of reactor material.....	20
3.4 Effect of acidic and basic properties.....	21

CHAPTER	PAGE
3.5	Effect of redox properties..... 21
3.6	Effect of preparation parameters..... 22
3.6.1	Effect of precipitation pH..... 22
3.6.2	Effect of calcinations temperatures..... 22
3.6.3	Effect of precursor and sulfating agent..... 24
3.6.4	Effect of activation temperature..... 27
3.7	Mechanism of <i>n</i> -butene isosynthesis over sulfated zirconia..... 28
3.8	Nature of active sites..... 28
3.9	Effect of additives on sulfated zirconia-based catalysts..... 37
IV	EXPERIMENTS..... 39
4.1	Catalyst Preparation..... 39
4.1.1	Chemicals..... 39
4.1.2	Preparation of zirconia..... 39
4.1.3	Preparation Sulfated zirconia..... 40
4.2	Catalyst Characterization..... 40
4.2.1	X-ray Photoelectron Spectroscopy (XPS)..... 40
4.2.2	N ₂ Physisorption..... 41
4.2.3	X-ray Diffraction (XRD)..... 41
4.2.4	Electron Spin Resonance Spectroscopy (ESR)..... 41
4.2.5	Scanning Electron Microscopy (SEM)..... 41
4.2.6	Temperature-Programmed Desorption (TPD)..... 42
4.3	Reaction Study in Isosynthesis via CO Hydrogenation..... 42
4.3.1	Materials..... 42
4.3.2	Apparatus..... 42
4.3.2.1	Reactor..... 43
4.3.2.2	Gas Controlling System..... 43
4.3.2.3	Automatic Temperature Controller..... 43
4.3.2.4	Electric Furnace..... 43
4.3.2.5	Gas Chromatography..... 43
4.3.3	Procedure..... 44

	PAGE
CHAPTER	
V RESULTS AND DISCUSSION.....	47
5.1 Characteristics of Zirconia and Sulfated Zirconia Catalysts and Their Catalytic Properties toward Isosynthesis via CO Hydrogenation.....	47
5.1.1 Catalyst Characterization.....	47
5.1.1.1 X-ray Diffraction (XRD).....	47
5.1.1.2 N ₂ Physisorption.....	50
5.1.1.3 Temperature Programmed Desorption (TPD)..	52
5.1.1.4 Electron Spin Resonance Spectroscopy (ESR).	57
5.1.1.5 Scanning Electron Microscopy (SEM).....	60
5.1.2 Catalytic Performance of Isosynthesis over Zirconia and Sulfated Zirconia Catalysts.....	61
5.2 The Effect of temperature during Calcinations on Characteristics of Sulfated Zirconia and Their Application as a Catalyst for Isosynthesis.....	64
5.2.1 Catalyst Characterization.....	65
5.2.1.1 X-ray Diffraction (XRD).....	65
5.2.1.2 N ₂ Physisorption.....	67
5.2.1.3 Temperature Programmed Desorption (TPD)..	69
5.2.1.4 Electron Spin Resonance Spectroscopy (ESR).	73
5.2.1.5 X-ray Photoelectron Spectroscopy(XPS).....	73
5.2.2 Catalytic Performance of Isosynthesis over Sulfated Zirconia Catalysts.....	74
VI CONCLUSIONS AND RECOMMENDATIONS.....	79
6.1 Conclusions.....	79
6.2 Recommendations for future studies.....	80
REFERENCES.....	81

	PAGE
APPENDICES.....	84
APPENDIX A: Calculation of crystallite size.....	85
APPENDIX B: Calculation of fraction of crystal phase of zirconia	88
APPENDIX C: Calibration curves	90
APPENDIX D: Calculations of carbon monoxide conversion, reaction rate and selectivity.....	97
VITA.....	99



สถาบันวิทยบริการ
จุฬาลงกรณ์มหาวิทยาลัย

LIST OF TABLES

TABLE	PAGE
3.1 Effect of calcination temperature before and after sulfation on acid strength.....	23
3.2 Physico-chemical characteristics of S-ZrO ₂ catalysts and conversions in <i>n</i> -butane isomerization at 150°C, WHSV=2 h ⁻¹	24
3.3 Properties of S-ZrO ₂ obtained with different sulfur compounds in the percolating solution and after heating for 3 h in nitrogen at 893 K.....	26
3.4 Catalytic activities for 1-butene isomerization.....	26
3.5 Percentage of acid sites on the SO ₄ ²⁻ -ZrO ₂ catalysts that are of the Bronsted type.....	27
3.6 H MAS NMR shifts, δH (ppm), of S-ZrO ₂ and zeolites and their shifts, ΔδH, upon adsorption of bases	35
4.1 Operating conditions for gas chromatography.....	44
5.1 Summary of catalyst characteristics obtained from XRD measurement...	49
5.2 N ₂ Physisorption results.....	52
5.3 Results from NH ₃ - and CO ₂ -TPD measurements	56
5.4 ESR parameters of Zr ³⁺ observed from different references	59
5.5 Catalytic activity results from isosynthesis	62
5.6 Product selectivity results from isosynthesis	63
5.7 Characteristics of ZrO ₂ with various calcination temperatures.....	66
5.8 N ₂ Physisorption results	68
5.9 Results from NH ₃ - and CO ₂ -TPD	71
5.10 Results from XPS	74
5.11 The catalytic activity results from isosynthesis	76
5.12 Production selectivity results from isosynthesis.....	76
B.1 Calculation of the fraction of crystal phase of zirconia.....	89
C.1 Conditions of Gas chromatography, Shimadzu model GC-8A and GC-14B.....	91

LIST OF FIGURES

FIGURE	PAGE
1.1 Isobutene synthesis from non-petroleum sources.....	1
2.1 The unit cells of the crystal systems.....	8
2.2 Crystal structure of cubic, tetragonal and monoclinic zirconia.....	8
2.3 Preparation scheme for precipitated catalysts (optional preparation steps are indicated by square brackets).....	12
2.4 Possible implementations of precipitation processes. Note that in the batchwise process (a) the pH and all other parameters except for the temperature change continuously during the precipitation due to consumption of the metal species. Coprecipitation should be carried out in the reversed arrangement by addition of the metal species to the precipitating agent to avoid sequential precipitation. In process (b) the pH is kept constant, but the batch composition and the residence time of the precipitate change continuously. In process (c) all parameters are kept constants.....	14
3.1 Model proposed by Kumbhar <i>et al.</i>	29
3.2 Model proposed by Yamaguchi	31
3.3 Model proposed by Davis <i>et al.</i>	31
3.4 Model proposed by Arata and Hino	32
3.5 Model proposed by Clearfield <i>et al.</i>	33
3.6 Model proposed by Kustov <i>et al.</i>	34
3.7 Model proposed by Babou <i>et al.</i>	35
3.8 Model proposed by Adeeva <i>et al.</i>	36
4.1 Flow diagram of lab-scale gas phase isobutene synthesis system.....	46
5.1 XRD patterns of ZrO ₂ and SO ₄ -ZrO ₂ catalysts synthesized from ZrOCl ₂	48
5.2 XRD patterns of ZrO ₂ and SO ₄ -ZrO ₂ catalysts synthesized from ZrO(NO ₃) ₂	49
5.3 Pore size distribution of ZrO ₂ and SO ₄ -ZrO ₂ catalysts synthesized from ZrOCl ₂	51

FIGURE	PAGE
5.4 Pore size distribution of ZrO_2 and SO_4-ZrO_2 catalysts synthesized from $ZrO(NO_3)_2$	51
5.5 NH_3 -TPD profiles of ZrO_2 and SO_4-ZrO_2 catalysts synthesized from $ZrOCl_2$	54
5.6 NH_3 -TPD profiles of ZrO_2 and SO_4-ZrO_2 catalysts synthesized from $ZrO(NO_3)_2$	54
5.7 CO_2 -TPD profiles of ZrO_2 and SO_4-ZrO_2 catalysts synthesized from $ZrOCl_2$	55
5.8 CO_2 -TPD profiles of ZrO_2 and SO_4-ZrO_2 catalysts synthesized from $ZrO(NO_3)_2$	55
5.9 Relationship between amount of acid and base sites and percent of sulfur content in ZrO_2 and SO_4-ZrO_2 catalysts synthesized from $ZrOCl_2$	56
5.10 Relationship between amount of acid and base sites and percent of sulfur content in ZrO_2 and SO_4-ZrO_2 catalysts synthesized from $ZrO(NO_3)_2$	57
5.11 ESR spectrum of ZrO_2	58
5.12 Relative ESR intensity of various ZrO_2 catalysts.....	59
5.13 SEM micrograph of ZrO_2-Cl	60
5.14 SEM micrograph of 0.75% SZ (ZrO_2-Cl).....	60
5.15 SEM micrograph of ZrO_2-N	61
5.16 SEM micrograph of 0.75% SZ (ZrO_2-N).....	61
5.17 Relationship between CO conversion and selectivity of isobutene with sulfur content in SO_4/ZrO_2-Cl	63
5.18 Relationship between CO conversion and selectivity of isobutene with sulfur content in SO_4/ZrO_2-N	64
5.19 XRD patterns of 0.75%SZ (N) various calcination temperatures.....	66
5.20 XRD patterns of SO_4/ZrO_2 commercial various calcination temperature..	67
5.21 Surface areas of the catalysts as a function of calcination temperature....	68
5.22 Pore size distribution of sulfated zirconia catalysts	69
5.23 NH_3 -TPD profiles of SO_4-ZrO_2 catalysts.....	70
5.24 CO_2 -TPD profiles of SO_4-ZrO_2 catalysts.....	71

FIGURE	PAGE
5.25 Relationship between calcinations temperature and base/acid site in sulfated zirconia.....	72
5.26 Relationship between percentage of monoclinic phase and base sites on 0.75% SZ (ZrO ₂ -N).....	72
5.27 Relative ESR intensity of various calcination temperatures in sulfated zirconia catalysts.....	73
5.28 Relationship between reaction rate and time on stream.....	77
5.29 Relationship between CO conversion and selectivity of isobutene in commercial sulfated zirconia various calcination temperatures.....	77
5.30 Relationship between CO conversion and selectivity of isobutene in 0.75% SZ (ZrO ₂ -N) various calcinations temperature.....	78
5.31 Relationship between percentage of monoclinic phase and acid sites.....	78
A.1 The 111 _m diffraction peak of zirconia for calculation of the crystallite size.....	87
A.2 The plot indicating the value of line broadening due to the equipment (data were obtained by using α -alumina as a standard).....	87
B.1 The X-ray diffraction peaks of zirconia (nanopowder) for calculation of the fraction of crystal phase of zirconia.....	89
C.1 The calibration curve of carbon monoxide.....	92
C.2 The calibration curve of carbon dioxide.....	92
C.3 The calibration curve of methane.....	93
C.4 The calibration curve of ethane.....	93
C.5 The calibration curve of ethylene.....	94
C.6 The calibration curve of propane.....	94
C.7 The calibration curve of propylene.....	95
C.8 The calibration curve of n-butane.....	95
C.9 The calibration curve of isobutane.....	96
C.10 The calibration curve of isobutene.....	96

CHAPTER I

INTRODUCTION

1.1 Introduction

Isobutene is an important feedstock for production of oxygenated compounds, such as methyl *tert*-butyl ether (MTBE) and ethyl *tert*-butyl ether (ETBE), which are mainly used as gasoline blending components. The demands of oxygenated compounds are greatly increased with the growth of world economy. However, the production of MTBE and ETBE is limited by a worldwide shortage of *i*-C₄ (MTBE and ETBE are produced by the catalytic reaction of isobutene with methanol and ethanol, respectively, over an acidic ion-exchange resin) since the amount of *i*-C₄ extracted from C₄ stream of petroleum stream cracking process is inadequate to meet the expected demand. It is expected that production *i*-C₄ from non-petroleum sources such as biomass, coal and natural gas is essential. This route is attractive due to the following reasons; (i) the chosen resource of isobutene production is renewable, then being more green than the conventional petroleum sources, which are about to shortage in the near future, (ii) carbon dioxide, a by-product of fermentation process, is substantially consumed to produce syngas, thus reducing the CO₂ emission to the atmosphere, and (iii) the ratio of carbon monoxide to hydrogen of 1:1 for the syngas from fermentation of biomass is suitable for the reaction of isobutene synthesis. Figure 1.1 shows the synthesis routes of isobutene from various non-petroleum sources.

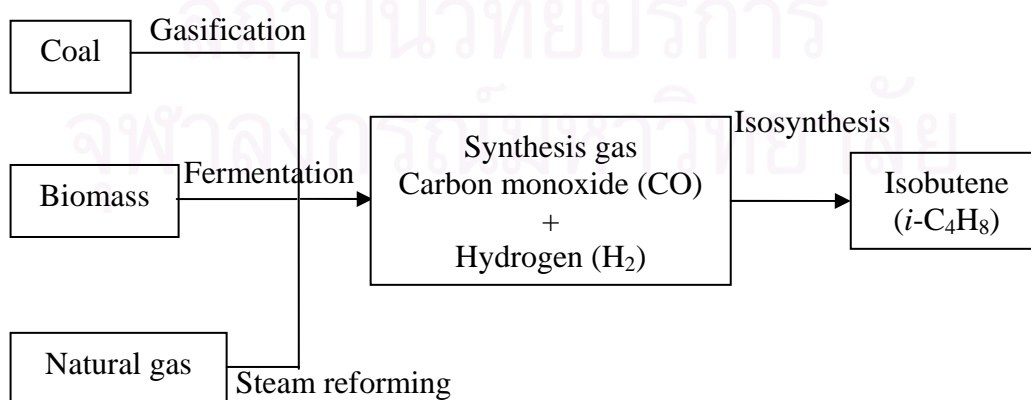
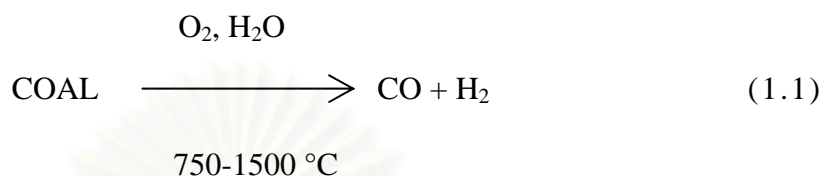


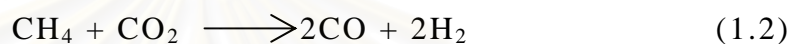
Figure 1.1 Isobutene synthesis from non-petroleum sources

Firstly, synthesis gas, a mixture of carbon monoxide and hydrogen, is synthesized by various possible routes, for example, gasification of coal (Eq. 1.1), fermentation of biomass to biogas (mixture of CH₄ and CO₂) which is subsequently reformed to synthesis gas (Eq. 1.2) and steam reforming of natural gas (Eq. 1.3).

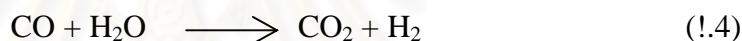
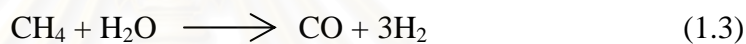
Coal gasification:



Dry reforming of biogas:



Natural gas:



Then isosynthesis reaction is carried out via CO hydrogenation to convert the synthesis gas to branched chain hydrocarbons, especially isobutene and isobutene.



This reaction was first reported by Pichler and Ziesecke (1949) using several transition metal oxides (ThO₂, CeO₂) or mixed-oxide systems (ThO₂-Al₂O₃, ThO₂-ZnO and so on) to catalyze CO hydrogenation under very several condition (150-1000 atm). Thorium dioxide (ThO₂) and zirconium dioxide (ZrO₂) have been reported as the most active catalysts for this reaction. However, zirconia-based catalysts have attracted much interest because of their absence of radioactivity and high selectivity to isobutene.

Sulfated zirconia (SO₄-ZrO₂ abbreviated as SZ) has been the subject of extensive research work since its ability to catalyze the isomerization of linear to branched light hydrocarbons was discovered. Metal oxides, such as ZrO₂, Al₂O₃, and TiO₂, are acid catalysts. Their acidity could be enhanced by sulfation. Sulfated zirconia (SO₄-ZrO₂), a

solid super acid, was reported to be active for *n*-butene isosynthesis even at low temperature, giving high selectivity. It is therefore interesting and becomes the focus of this work to apply this SO₄-ZrO₂ catalyst for the CO hydrogenation reaction for synthesis of isobutene. It is expected that the use of SO₄-ZrO₂ would offer the following advantages: 1) the reaction temperature should be lower than zirconia or mixed oxide zirconia, and 2) the amount of catalyst for formation of isobutene is less than other type of catalyst.

1.2 Objectives

1. To investigate the characteristics and the catalytic properties of various sulfated zirconia catalysts for isosynthesis.
2. To investigate the effect of sulfur content on catalytic performance.
3. To investigate the effect of calcination temperature on catalytic performance.



สถาบันวิทยบริการ
จุฬาลงกรณ์มหาวิทยาลัย

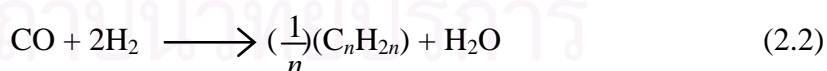
CHAPTER II

THEORY

This chapter focuses on carbon monoxide hydrogenation reactions particularly on Fischer-Tropsch synthesis (FTS) and isosynthesis. It consists of five main sections. Details of Fischer-Tropsch synthesis (FTS) and isosynthesis are described in Sections 2.1 and 2.2, respectively. General features of zirconia are detailed in Sections 2.3. The last two sections describe preparation method of catalysts (Section 2.4) and preparation of S-ZrO₂ (Section 2.5).

2.1 Fischer-Tropsch synthesis (FTS)

Fischer-Tropsch synthesis (FTS) or CO hydrogenation reaction was originally intended for production of synthetic liquid fuels from synthesis gases (CO and H₂). After the Second World War, FTS has been developed continuously by several researchers, although the rise and fall in research intensity on this process has been highly related to demands for cheap oil-based hydrocarbons. This synthesis is basically the reductive polymerization (oligomerization) of carbon monoxide by hydrogen to produce heavier saturated hydrocarbons or lower olefins or oxygenated hydrocarbons. The main reactions of FTS are:



Equation (2.1) is the formation of methane, Equation (2.2) is the synthesis of hydrocarbons higher than methane, Equation (2.3) is the water-gas shift reaction, and Equation (2.4) is the Boudouard reaction resulting in deposition of carbon.

For FTS, it is desired to obtain high molecular weight, straight chain hydrocarbons. Nevertheless, methane and other light hydrocarbons are always present as less desirable product distribution, typically 10 to 20% of products from the synthesis are usually light hydrocarbons (C_1 - C_4). The disadvantages of light alkanes are inconvenient for transportation because byproducts have low boiling points and exist in the gas phase at room temperature. Many attempts have been made to minimize these by-products and increase the yield of long chain liquid hydrocarbons by improving chain growth probability. It would be more efficient to be able to convert these less desirable products into more useful forms, rather than re-reforming them into the synthesis gas and recycling them (Farrauto and Bartholomew, 1997). The distribution of the molecular weight of the hydrocarbon products can be remarkably varied, depending on types of catalyst used, promoters, reaction conditions (pressure, temperature and H_2/CO ratios), gas hour space velocity and type of reactors.

2.2 Isosynthesis

The Fischer-Tropsch process is consisted of isosynthesis, that is part of the more generalized reaction systems. During World War II, the synthesis gas reaction was improved by Pichler and Ziesecke (1949). Details of the project, actually started in 1941, were kept secret because its primary goal was the catalytic production of isobutane and isobutene, important raw materials for high octane gasoline synthesis (Pichler, 1952).

Synthesis gas was converted over reducible oxide catalysts to form branched chain hydrocarbons. Development of the process was rapid but its commercial use was cut off by the successful development of new catalysts for the production of high octane gasoline from readily available petroleum.

Although both isosynthesis and FTS use synthesis gas as the feed, the isosynthesis differs from the FTS in several ways

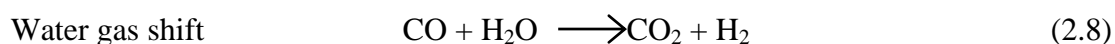
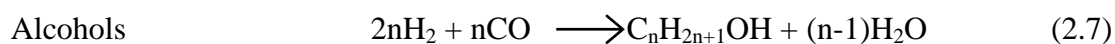
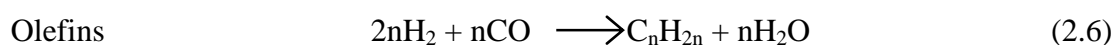
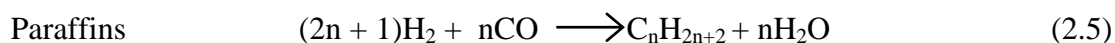
- The isosynthesis gives high yields of isoparaffins rather than normal paraffins.

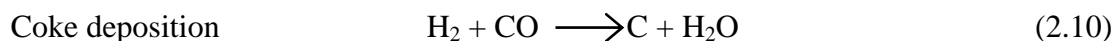
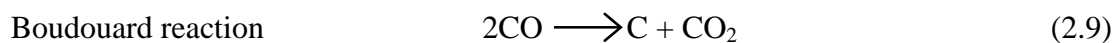
- The catalysts are difficultly reducible oxides such as ThO₂ or ZrO₂ rather than reduced transition metals.
- Isosynthesis temperatures and pressure are considerably higher than those used in FTS.
- Isosynthesis catalysts are not poisoned by sulfur to any great extent.

Very few attempts have been reported about the isosynthesis process since the early work by Picher and Ziesecke (1949), but interest in this reaction has been revived, chiefly because of the increasing demand for isobutene and other branched hydrocarbons. Sofianos (1992) has reviewed the isosynthesis. The existing literature indicated that the main products of the isosynthesis reaction were isobutane and isobutene which can be obtained in sufficiently high yields only at mild condition (high temperatures and pressures). The operation of the isosynthesis reaction is not favorable at low pressures as the formations of DME, lower alcohols and isobutanol predominate under these conditions.

Pichler and Ziesecke (1949) reported that there was a relationship between the Isosynthesis and higher alcohol synthesis particularly isobutanol which is used as a solvent, an additive in lubricating oils and for the production of amide resins. When operating the catalytic system under milder condition, the production of isobutanol and other higher alcohols is more favorable than that of iso-C₄ compounds from the Isosynthesis. Large amount of methanol is always present and it becomes a driving force to realize a direct reaction between methanol and isobutanol or isobutene derived from isobutanol to form MTBE.

A large number of reactions taking place during the FTS reaction or isosynthesis can be summarized as follows:





Noted that the best yields are obtained with a CO: H₂ ratio of 1.0-1.2: 1.0.

2.3 General feature of zirconia

Early researchers reported that the crystal structures of zirconia have three different phases: monoclinic, tetragonal, and cubic. Figure 2.1 depicts the typical unit cells of different phases. Crystal structures of cubic, tetragonal and monoclinic zirconia are shown in Figure 2.2. The temperature is an important factor, which makes phase transform to another phase. The temperature transform of the monoclinic phase is 1170 °C, below this the crystal structures is stable, then the monoclinic transform into the tetragonal phase, which is stable up to 2370°C (Cormack and Parker, 1990). The stabilization of the tetragonal phase below 1100°C is important in the use of zirconia as a catalyst in some reactions. The cubic phase is stable up to 2370°C and exists up to the melting point of 2680°C. A result of the martensitic nature of the transformations, neither the high temperature tetragonal nor cubic phase can be quenched in rapid cooling to room temperature. However, at low temperature, a metastable tetragonal zirconia phase is usually observed when the zirconia is prepared by certain methods, such as precipitation from aqueous salt solution or thermal decomposition of zirconium salts. This is not the expected behavior according to the phase diagram of zirconia (i.e., monoclinic phase is the stable phase at low temperatures). At low temperatures, the exist of the tetragonal phase can be attributed to several factors for example chemical effects, (the presence of anionic impurities) (Srinivasan *et al.*, 1990, Tani *et al.*, 1982) structural similarities between the tetragonal phase and the precursor amorphous phase (Livage *et al.*, 1968, Osendi *et al.*, 1985, Tani *et al.*, 1982) as well as particle size effects based on the lower surface energy in the tetragonal phase compared to the monoclinic phase (Garvie, 1978, Osendi *et al.*, 1985, Tani *et al.*, 1982). The transformation of the metastable tetragonal form into the monoclinic form is generally complete by 650-700°C.

Crystal system	Unit cell shape
Cubic	$a = b = c, \alpha = \beta = \gamma = 90^\circ$
Tetragonal	$a = b \neq c, \alpha = \beta = \gamma = 90^\circ$
Monoclinic	$a \neq b \neq c, \alpha = \gamma = 90^\circ, \beta \neq 90^\circ$

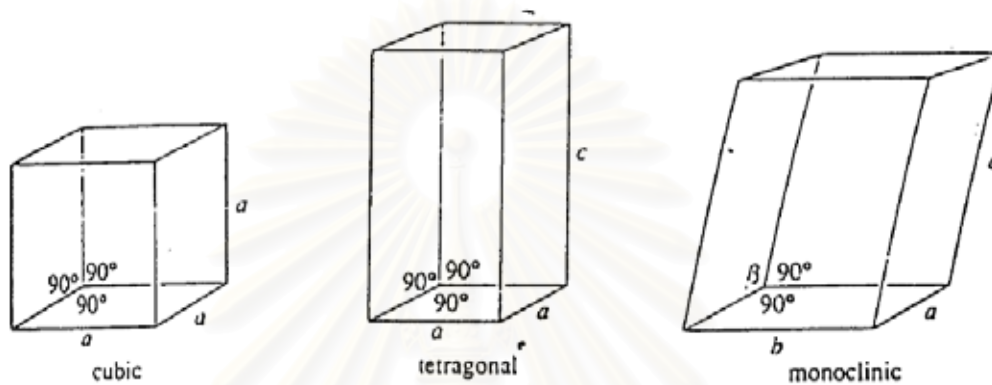


Figure 2.1 The unit cells of the crystal systems (West, 1997).

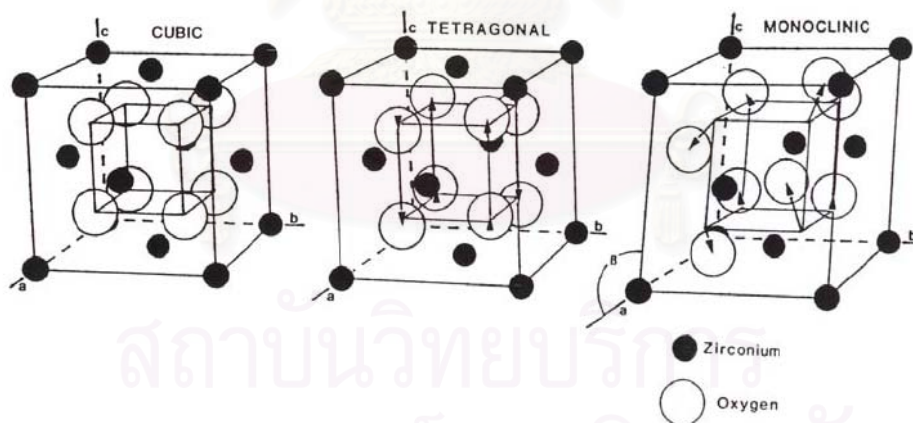


Figure 2.2 Crystal structure of cubic, tetragonal and monoclinic zirconia (Heuer, 1987)

2.4 Preparation method of catalysts

2.4.1 Precipitation and Coprecipitation

The catalyst and support is prepared by precipitation or coprecipitation, which is technically very important (Thomas, 1970 and Stiles, 1983). However, the precipitation method is generally more demanding than several other preparation techniques, due to the need of product separation after precipitation and the tremendous volumes of salt containing solutions generated in precipitation processes. Techniques for catalyst manufacture have to produce catalysts with better performance in order to compensate for the higher cost of production in comparison, for instance, to solid-state reactions for catalyst preparation.

Nonetheless, for various catalytically suitable materials, especially for support materials, precipitation is the most frequently applied method of preparation. These materials include mainly aluminum and silicon oxides. In other systems precipitation techniques are also used, for instance in the production of iron oxides, titanium oxides or zirconias. The main advantages of precipitation for the preparation of such materials are the possibility of creating very pure materials and the flexibility of the process with respect to final product quality.

Other catalysts, based on more than one component, can be prepared by coprecipitation. According to IUPAC nomenclature, coprecipitation is the simultaneous precipitation of a normally soluble component with a macrocomponent from the same solution by formation of mixed crystals, by adsorption, occlusion or mechanical entrapment. However, in catalyst preparation technology, the term is usually used in a more general sense in that the requirement of one species being soluble is dropped. In many cases, both components to be precipitated are essentially insoluble under precipitation conditions, although their solubility products might differ substantially. We will therefore use the term coprecipitation for the simultaneous precipitation of more than one component. Such systems prepared by coprecipitation include Ni/Al₂O₃, Cu/Al₂O₃, Cu/ZnO, and Sn-Sb oxides.

Coprecipitation is very relevant for the generation of a homogeneous distribution of catalyst components or for the creation of precursors with a definite stoichiometry, which can be easily converted to the active catalyst. If the precursor for the final catalyst is a stoichiometrically defined compound of the later constituents of the catalyst, a calcination and/or reduction step to generate the final catalyst usually creates very small and intimately mixed crystallites of the components. Such a good dispersion of catalyst components is difficult to achieve by other means of preparation, and thus coprecipitation still remains an important technique in the manufacture of heterogeneous catalysts in spite of the disadvantages associated with such processes. These disadvantages are the higher technological demands, the difficulties in following the quality of the precipitated product during the precipitation, and the problems in maintaining a constant product quality throughout the whole precipitation process, if the precipitation is carried out discontinuously.

2.4.1.1 General Principles Governing Precipitation from Solutions

Precipitation processes are not only relevant for catalysis, but also for other industries, as for instance the production of pigments. However, in spite of the tremendous importance of precipitation from solution, many basic questions in this field are still unsolved and the production of a precipitate with properties that can be adjusted at will is still rather more an art than a science. This is primarily due to the fact that the key step, nucleation of the solid from a homogeneous solution, is a very elusive one, and is difficult to study using the analytical tools currently available.

Spectroscopy using local probes is not sensitive enough to study larger arrangements of atoms on the one hand. In addition, diffraction methods are not suitable for analysis either, since a nucleus is not large enough to produce a distinctive diffraction pattern. Thus, investigations of crystallization and precipitation processes from solution often have to rely on indirect and theoretical methods. Figure 2.3 depicts a general flow scheme for the preparation of a precipitated catalyst.

2.4.1.2 Chemical Considerations

It is generally desirable to precipitate the desired material in such a form, that the counter-ions of the precursor salts and the precipitation agent, which can be occluded in the precipitate during the precipitation, can easily be removed by a calcination step. If precipitation is induced by physical means, i.e. cooling or evaporation of solvent to reach super-saturation of the solution, only the counter-ion of the metal salt is relevant. If precipitation is induced by addition of a precipitating agent, ions introduced into the system via this route also have to be considered. Favorable ions are nitrates, carbonates, or ammonium, which decompose to volatile products during the calcination. For catalytic applications usually hydroxides, oxohydrates, oxides (in the following the term “hydroxides” is used in a rather general sense, comprising hydroxides and oxides with different degrees of hydration) are precipitated; in some cases carbonates, which are subsequently converted to the oxides or other species in the calcination step, are formed. In addition, the precipitation of oxalates as precursors for spinel-type catalysts has occasionally been reported to give good results (Peshev *et al.*, 1989). If the ions do not decompose to volatile products, careful washing of the precipitate is necessary.

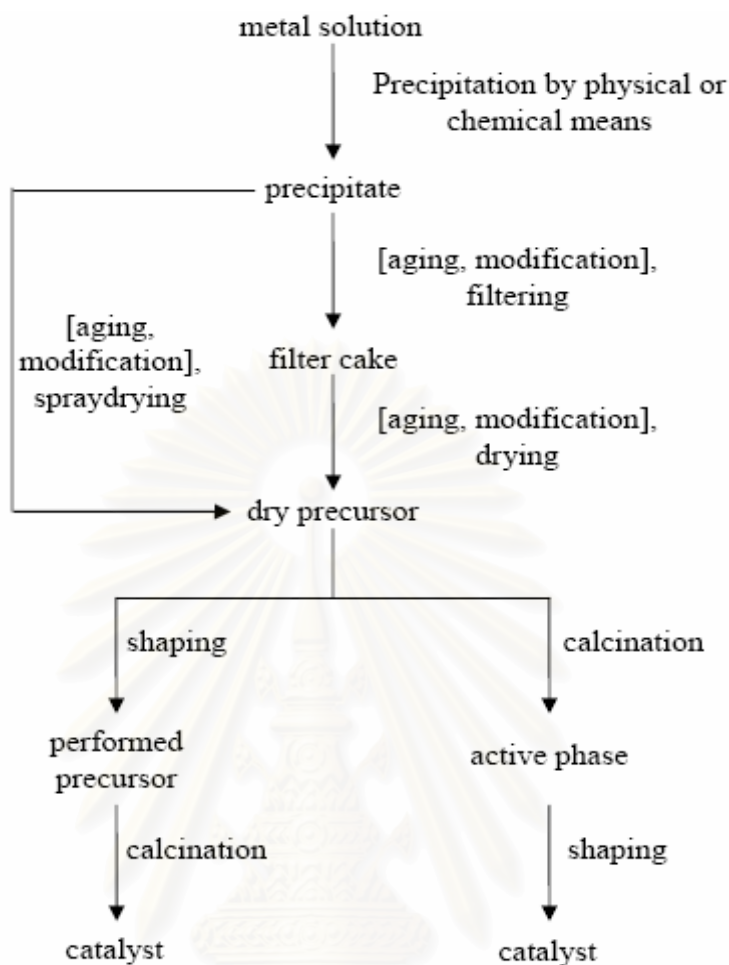


Figure 2.3 Preparation scheme for precipitated catalysts (optional preparation step are indicated by square brackets).

In many cases it has been found advantageous to work at low and relatively constant super-saturation which is achieved homogeneously in the whole solution (precipitation from homogeneous solution, PFHS). This can also be employed for deposition-precipitation processes. This can be reached by using a precipitating agent which slowly decomposes to form the species active in the precipitation.

2.4.1.3 Process Considerations

There are several ways to carry out the precipitation process (Figure 2.4) (Courty and Marcilly, 1983). The simplest implementation of the precipitation reaction is the batch operation where the solution from which the salt is to be precipitated is usually

present in the precipitation vessel and the precipitating agent is added. The advantage of this mode of operation is the simple way in which the product can be obtained; the most severe disadvantage is the variation of batch composition during the precipitation process. This can lead to differences between the product formed during the initial stages of the precipitation and the precipitate formed at the end of process. If a coprecipitation is carried out this way, it is important to decide which compounds are present in the vessel and which compounds are to be added. If the precipitating agent is present in the precipitator and the mixed metal solutions are added, the product tends to be homogeneous, since the precipitation agent is always present in large excess. If, on the other hand, the precipitating agent is added to a mixed metal solution, the precipitate with the lower solubility tends to precipitate first, thus resulting in the formation of an inhomogeneous product.

A slightly more complex process is the simultaneous addition of both reagents under strict control of the pH and the reagent ratios. If the precipitation is carried out following this procedure, the ratio of the metal salt and precipitating agent remains constant; all other concentrations, however, change during the process. Homogeneity of the product is usually better than in the first process described, but might still vary between the first precipitate and the precipitate formed last. This is due to the different concentrations of the other ions which are not precipitated and might be occluded in the precipitate to a larger extent during the final stages of the procedure. Moreover, the precipitates first formed are aged for a longer time in the solution. Thus, phase transitions might have already occurred, while fresh precipitates are still formed.

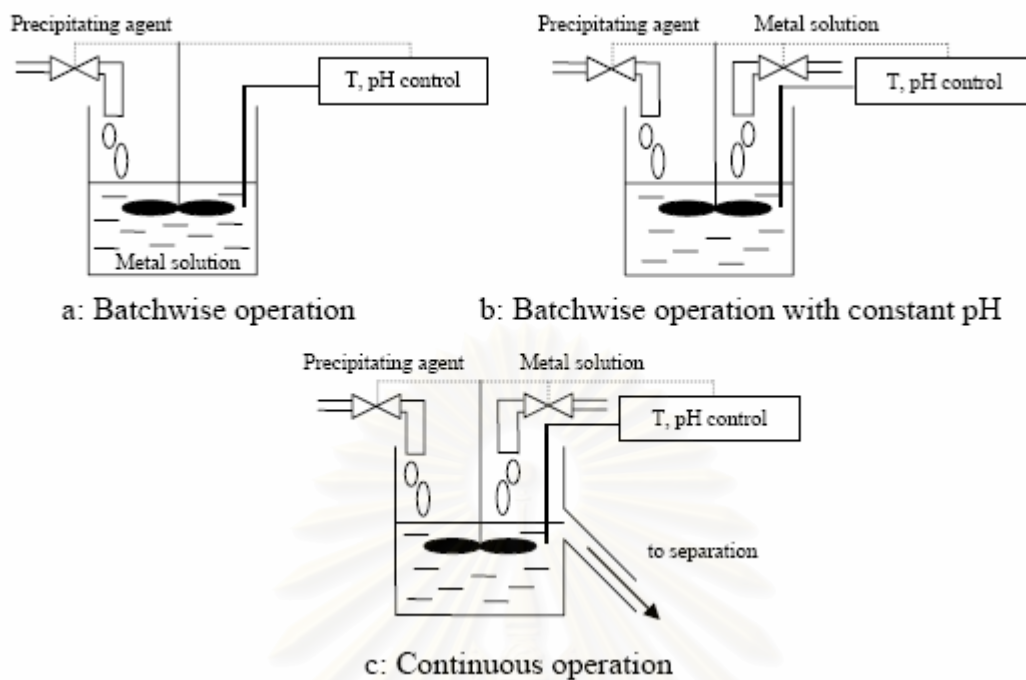


Figure 2.4 Possible implementations of precipitation processes.

Note that in the batchwise process (a) the pH and all other parameters except for the temperature change continuously during the precipitation due to consumption of the metal species. Coprecipitation should be carried out in the reversed arrangement by addition of the metal species to the precipitating agent to avoid sequential precipitation. In process (b) the pH is kept constant, but the batch composition and the residence time of the precipitate change continuously. In process (c) all parameters are kept constants.

These problems are avoided if a continuous process is employed for the precipitation; however, this makes higher demands on the process control. In a continuous process all parameters as temperature, concentrations, pH, and residence times of the precipitate can be kept constant or altered as desired.

The continuous process usually allows precipitation at low supersaturation conditions, since seeds are already present in the precipitation vessel. Thus, no homogeneous precipitation, which needs high levels of super-saturation, is necessary, and nucleation occurs heterogeneously with the associated lower supersaturation levels.

2.4.1.4 Influences on Properties of the Final Product

Basically all process parameters, some of which are fixed and some which are variable, influence the quality of the final product of the precipitation. Usually precipitates with specific properties are desired. These properties could be the nature of the phase formed, chemical composition, purity, particle size, surface area, pore sizes, pore volumes, separability from the mother liquor, and many more, including the demands which are imposed by the requirements of downstream processes, like drying, palletizing, or calcination. It is therefore necessary to optimize the parameters in order to produce the desired material. Figure 2.5 summarizes the parameters which can be adjusted in precipitation process and the properties which are mainly influenced by these parameters. The following discussion attempts to give some general guidelines concerning the influence of certain process parameters on the properties of the resulting precipitate. It should, however, be stressed, that the stated tendencies are only trends which might vary in special cases. The exact choice of precipitation parameters is usually the result of a long, empirically driven optimization procedure and a well-guarded secret of catalyst manufacturers or the producers of precursors for catalysts.

2.5 Preparation of $\text{SO}_4\text{-ZrO}_2$

The catalytic properties of $\text{SO}_4\text{-ZrO}_2$ significantly depend upon the preparation method and the activating treatment. A variety of methods have been reported for the preparation of $\text{SO}_4\text{-ZrO}_2$. These methods differ mainly in the type of precursor, type of precipitating agent, type of sulfating agent, method of impregnation, calcination temperature. Various methods have been used for the characterization of these catalysts.

The method of preparation significantly affects the activity of $\text{SO}_4\text{-ZrO}_2$. Major factors that affect the catalyst performance are pH of the solution during sol-gel precipitation, solution concentration, drying and calcination temperatures.

The type of precursor for preparing $\text{SO}_4\text{-ZrO}_2$ plays a vital role in the final texture and, hence, in the performance of the catalyst. Various zirconium compounds, such as $\text{Zr}(\text{NO}_3)_4$, ZrCl_4 , zirconium isopropoxide, zirconyl chloride, zirconium oxychloride and

sometimes zirconia itself, are used to prepare these catalysts. Various precipitating agents, like aqueous ammonium hydroxide and urea, have been reported (Yamaguchi, *et al.*, 1986). The type of hydrolyzing agent also has a significant effect on the catalyst activity. Amorphous zirconium hydroxide obtained by the alkaline hydrolysis of the zirconia precursor is usually sulfated before it is crystallized by thermal treatment. Although this is the general way of preparing the catalyst, sometimes hydrous zirconia is first crystallized by thermal treatment and then sulfated. The sulfating isomerization species most commonly used are H_2SO_4 and $(\text{NH}_4)_2\text{SO}_4$ (Sohn *et al.*, 1989). Some sulfur compounds, like H_2S and SO_2 , have also been used. The sulfated species is then thermally crystallized, whereby it undergoes a phase transformation, the tetragonal phase being stabilized as a result of sulfate incorporation.



สถาบันวิทยบริการ
จุฬาลงกรณ์มหาวิทยาลัย

CHAPTER III

LITERATURE REVIEWS

3.1 Mechanism of isosynthesis over oxide catalysts

CO hydrogenation over oxide catalysts selectively forms branched-chain compounds such as isobutane, isobutene, isoprene, methylpropanal, and isobutanol. The formation of isobutene is favorable over ZrO_2 catalyst (Maehashi *et al.*, 1992). The formation of isobutene (chain-branching mechanism) over ZrO_2 was proposed by early researcher (Ekerdt *et al.*, 1988 and 1990). The mechanism consisted of two paths (i) CO insertion into the zirconium-carbon bond of adsorbed aldehydic intermediate and (ii) condensation between η -enolate and methoxide species. The results by Maruya *et al.* (1996) presented the reaction path which consists of the sequence of (i) conversion of methoxide species to η^2 -formaldehyde species, (ii) formation of methyl or methylene species from the η^2 -formaldehyde species by hydrogenation or thermolysis, (iii) carbonylation of the methyl or methylene species to form C_2 oxygenate, (iv) aldol condensation type reaction to form branched C_4 oxygenates, and (v) formation of branched hydrocarbons from the hydrogenation followed by dehydration.

Furthermore, Maruya *et al.* (1998) studied reaction path of methoxy species to isobutene over oxide catalysts such as ZrO_2 , CeO_2 , ZrO_2-CeO_2 , ZrO_2-CeO_2-CoO and $ZrO_2-CeO_2-Fe_2O_3$ in CO hydrogenation. The reaction conditions are as follows: amount of catalyst of 2.0 g, reaction temperature of 643 K, and ratio of CO:H₂ in feed flow rate of 1:1. The conclusion of formation of isobutene in CO hydrogenation over oxide catalysts is explained by paths: (1) formation of methoxy species from CO and H₂, (2) conversion of methoxy species to methyl species, (3) insertion of CO into a methyl-metal bond, and (4) aldol condensation of C_2 oxygenates with formaldehyde. Besides, the results from experiments disclosed that effect of dimethyl ether (DME) addition to CO and H₂ over oxide catalysts. ZrO_2 , ZrO_2-CeO_2 , and ZrO_2-CeO_2-CoO are catalysts that increase in formation rate of hydrocarbons with high isobutene selectivity (isobutene selectivity in C_4 hydrocarbons of about 92-97%) and large decrease of CO₂. CeO_2 revealed no effect when

adding DME. The last one is $\text{ZrO}_2\text{-CeO}_2\text{-Fe}_2\text{O}_3$ which proposed lower isobutene but higher methane and the moderate increase of the other hydrocarbons.

3.2 Effect of preparation of oxide catalysts

3.2.1 Precipitation method

Early researchers prepared zirconia by precipitation method. Hydrous zirconia was prepared by addition dropwise a zirconium salt precursors, for example ZrOCl_2 , ZrCl_4 , $\text{Zr}(\text{NO}_3)_4$, and $\text{Zr}(\text{SO}_4)_2$, into well-stirred precipitate solution such as ammonium solution (NH_4OH) at room temperature. The pH value of solution during precipitation was carefully controlled at 10. Then the resulting precipitate was separated by filtering, followed by washing with deionized water until no Cl^- was detected with AgNO_3 solution. The resultant was dried overnight and calcined (Li *et al.*, 2001, Li *et al.*, 2002, Li *et al.*, 2003, Li *et al.*, 2004, Su *et al.*, 2000).

Maruya *et al.* (2000) studied effect of phase structure and active sites over ZrO_2 catalysts in isosynthesis. CO hydrogenation was carried out using a conventional flow system at 673 K and atmospheric pressure with ratio of CO: H_2 is 1:1. The results indicated that ZrO_2 catalysts, that were prepared by changing pH value during precipitation, having different fraction of monoclinic phase. The rate of isobutene formation and the *i*- C_4 selectivity increased with an increase in the fraction of monoclinic phase, while other hydrocarbons such as C_1 , C_2 , C_3 and C_{5+} were independent fraction. If zirconia were prepared at pH range 2.1 to 10.5, the increase in the value of pH leads to increase of volumetric fraction of monoclinic phase. The selectivity of isobutene in C_4 hydrocarbons and total hydrocarbons for precipitation pH range of 7-10.5 were 94% and 77%, respectively. The amounts of adsorbed methoxy and formate species during the reaction and also of the surface sites with strong basicity increase in the fraction of monoclinic phase. The strong basicity on monoclinic phase is available for the aldol condensation reaction to form C_3 hydrocarbons from C_2 oxygenate and branched C_4 compounds from C_3 oxygenate.

Nanosize zirconium oxides were prepared by other methods e.g. supercritical fluid drying (SCFD) and freeze-drying (FD) method (Su *et al.*, 2000). The hydrogenation of CO was carried out using a flow-type fixed-bed pressurized tubular reactor at 623-723 K, mixed gas of CO and H₂ (CO/H₂ = 1), 5.0 MPa and amount of catalysts of 2.0 g. The results showed that the crystal phase, acidic and basic properties of the catalyst of nanosize zirconia depend remarkably on the drying condition. The highest basic/acidic ratios and selectivity of isobutene were obtained over nanosize zirconia, which were prepared by precipitation method.

Moreover, Su *et al.* (2000) investigated influences of preparation parameters (for example, precipitation pH, salt precursor and the calcination temperatures) on the structural and catalytic performance of zirconia in isosynthesis. The zirconium salt precursor had tremendous effect on the crystal structure because the involvement of precursor anions in the hydroxide. Highest selectivity to isobutene was obtained over the catalysts prepared from Zr(NO₃)₄.

3.2.2 Mechanical mixing method

Early researchers (Li *et al.*, 2000 and 2001) were prepared mixed oxides catalysts by mechanical mixing method, the promoters (Al₂O₃, KOH and calcium salts) were milled together with ZrO₂-based catalyst thoroughly and then the mixture was calcined again.

Reaction, occurred under relatively mild operation conditions (673 K, 5.0 MPa and 650 h⁻¹), was carried out in a fixed-bed flow type pressurized stainless steel tubular reactor that packed 2.1 g of catalysts. The performance of zirconia-based catalysts varied with calcium salts added. The results showed that CaF₂ and CaSO₄ could enhance the isobutene selectivity in total hydrocarbons and meanwhile surely maintain the activity of pure ZrO₂. Selectivity of *i*-C₄ in total hydrocarbons from CaF₂-ZrO₂ and CaSO₄-ZrO₂ were 50.5% and 50.6%, respectively. After that Li *et al.* (2002) studied the type of promoters which affected acidic and basic properties. Promoted zirconia with various additives markedly changed the activity and the distribution of hydrocarbons. The test results show that the promoters affected both the amount of acid-base site and the strength

of acid and base catalysts as well as activity and selectivity of reaction. Al_2O_3 -KOH showed to be effective promoters, which could remarkably enhance *i*-C₄ selectivity in total hydrocarbons.

3.2.3 Coprecipitation method

Coprecipitation method is one method for synthesis mixed oxide catalyst. Li *et al.* (2004) were prepared mixed oxide catalysts by coprecipitation of mixed zirconium salt precursor, ZrOCl_2 , and various additives, such as cerium or yttrium nitrate salts, with ammonia solution. The experimental results indicated that the activity and selectivity of CeO_2 - ZrO_2 and Y_2O_3 - ZrO_2 varied with the quantity of additives. The highest values of selectivity to isobutene in total hydrocarbons were 66.8% and 63.7% over 50% CeO_2 -doped ZrO_2 and 6.2% Y_2O_3 -doped ZrO_2 , respectively.

3.3 Effect of reactor material

Li *et al.* (2003) investigated the effect of reactor on the catalytic performance of isosynthesis. The research compared the isosynthesis performance from two reactors, quartz lined stainless steel tubular reactor and stainless steel tubular reactor. Reaction was carried out in high-pressure flow fixed-bed reactors at 5.0 MPa, 623-723 K, 650 h^{-1} , and catalyst were Al_2O_3 and various calcium salts (CaCO_3 , CaO , CaF_2 , and CaSO_4) promoted ZrO_2 -based prepared by mill together and then the mixture calcined again, mechanical mixing method. The investigation revealed that stainless steel tubular reactor seriously affected the selectivity of isosynthesis, while quartz line stainless steel tubular reactor was favorable for the formation of *i*-C₄ hydrocarbons and subdued the formation of CO_2 . The CO conversion in quartz line stainless steel tubular reactor (16%) was just lower than in the other reactor (19%). The selectivity to *i*-C₄ in total hydrocarbons was largely enhanced (53%) with lower percentage of CO_2 in the products (38%) in the isosynthesis over ZrO_2 in stainless steel tubular reactor, but the selectivity to *i*-C₄ in total hydrocarbons was 40% over ZrO_2 in quartz line stainless steel tubular reactor. Moreover, the content Al_2O_3 into ZrO_2 based catalysts could largely enhance the activity while maintain the *i*-C₄ selectivity of pure ZrO_2 . CaF_2 and CaSO_4 proved to be effective promoters, which could remarkably enhance the *i*-C₄ selectivity in total hydrocarbons and

meanwhile surely maintain the activity of pure ZrO_2 . Furthermore, the formation of by product, especially CO_2 , was suppressed. Further, the effect of reaction temperature on performance of the catalyst that proposed the suitable reaction temperatures for the formation of $i\text{-C}_4$ were about 673-698 K.

3.4 Effect of acidic and basic properties

The experiments of temperature-programmed desorption (TPD) of ammonia and carbon dioxide indicated that both the amount of acid-base sites. Su *et al.* (2000) studied nanosize zirconia catalysts. The acidic sites of the catalysts are responsible for the activation of the reactant molecules, while the basic sites are responsible for the chain propagation to form $i\text{-C}_4\text{H}_8$. (Li *et al.*, 2001) The surface acidic-basic properties play important role in determining the performance of the catalysts in the isosynthesis. The results indicated that the acidic sites are responsible for the activation of CO to start the reaction and the formation of $n\text{-C}_4$ hydrocarbons (by product). However, the basic sites are significant for the formation of $i\text{-C}_4$ hydrocarbons. $\text{CaF}_2\text{-ZrO}_2$ and $\text{CaSO}_4\text{-ZrO}_2$ offered increase in the $i\text{-C}_4$ selectivity in total hydrocarbons, so CaF_2 and CaSO_4 were effective promoters.

Furthermore, Li *et al.* (2002) proposed that both amount of acid-base sites and strength of acid and base of catalysts varied with the incorporation of promoters including various calcium salts. The amount of acidic sites on ZrO_2 and activity are related and especially formation of linear C_4 hydrocarbons, and the basic sites are responsible for the formation of $i\text{-C}_4$ hydrocarbons. However, the ratio of base to acid sites on catalyst would determine the ratio of $i\text{-C}_4$ to $n\text{-C}_4$ hydrocarbons in total hydrocarbons

3.5 Effect of redox properties

Li *et al.* (2004) was conducted to investigate the effect of redox properties and acid-base properties on isosynthesis over incorporation of CeO_2 or Y_2O_3 with ZrO_2 by coprecipitation method. Temperature-programmed reduction (TPR) of H_2 measurements showed that the addition of CeO_2 or Y_2O_3 into ZrO_2 enhanced the reduction properties of catalysts. The highest activities and C_4 selectivity in total hydrocarbons were obtained

over the catalysts which maximum amount of H₂ consumption for both CeO₂- and Y₂O₃-doped ZrO₂-based catalysts. The reduction behavior of the catalysts was mostly developed compared to that of pure ZrO₂ catalyst. Higher reduction behavior is suggested to be related to increasing mobility of lattice oxygen of the catalysts that would be likely to play important role in the isosynthesis. Moreover, the acid-base properties would determine the activation of reactant molecules and selectivity of the catalysts.

3.6 Effect of preparation parameters

3.6.1 Effect of precipitation pH

Su *et al.* (2000) studied the influences of precipitation pH and the calcinations temperature on the catalytic performance of ZrO₂. The results showed that the pH values of the precipitating solutions are responsible for the amount of acid and base sites on the catalyst surface and specific surface area. The highest selectivity isobutene (60%) was obtained over zirconia, which was prepared in the pH range of 3 to 10. However, ZrO₂ that was prepared at pH range of 6 to 7 showed highest activity.

3.6.2 Effect of calcination temperatures

Apart from the catalysts properties, calcination temperature is other factor that influenced activity and selectivity of isosynthesis. The XRD results demonstrated that the dominant crystal phase of zirconia, calcined from 673-1073 K, was all monoclinic. Higher calcined temperature leads to better crystallization. Furthermore, the acidic and basic properties of ZrO₂ may be changed with the change of calcination temperatures, but acidity and basicity of the catalyst is not only dependent on the calcination temperatures. The formation of *i*-C₄ was favored over the catalyst calcined at 773-973 K. The highest selectivity for isobutene was obtained over catalyst that was obtained over the catalyst that was calcined at 873 K (Su *et al.*, 2000).

The catalytic activity of SO₄-ZrO₂ is found to depend on the calcination temperature as well as the pre-calcination temperature of ZrO₂. Table 3.1 suggests that the superacidic SO₄-ZrO₂ is produced when the pre-calcination temperature is between 110

and 400°C and the calcination temperature upon sulfation with sulfuric acid is 650°C. Pre-calcination temperatures beyond 400°C, lead to a reduction in superacidity. In fact, the test reaction of isomerization of *n*-butane to isobutane (Guo et al., 1994) has shown that there is a combination of calcinations temperature and concentration of sulfuric acid to give a better catalyst; for example, 600°C and 0.3 N H₂SO₄ or 650°C and 0.5 N H₂SO₄, produce almost identical activities (Table 3.2).

Table 3.1 Effect of calcination temperature before and after sulfation on acid strength (Guo *et al.*, 1994)

Pre-calcination temp. ZrO ₂ (°C)	Calcination temp. S-ZrO ₂ (°C)	Acid strength H ₀
200	650	≤-16.12
400	650	≤-16.12
500	650	≤-13.75
600	650	≤-12.70
800	650	>-12.70
110	200	>-12.70
110	400	≤-12.70
110	650	≤-16.12
110	800	≤-12.70

สถาบันวิทยบริการ
จุฬาลงกรณ์มหาวิทยาลัย

Table 3.2 Physico-chemical characteristics of S-ZrO₂ catalysts and conversions in *n*-butane isomerization at 150°C, WHSV=2 h⁻¹ (Nascimento *et al.*, 1993)

Temp. (°C)	H ₂ SO ₄ concentration (N)	Sulfur contents (% wt)	Surface area (m ² g ⁻¹)	<i>k</i> (mol h ⁻¹ m ⁻² × 106)
500	1.0	5.36	147	n.d.
	0.1	1.14	117	0.45
	0.2	1.95	128	40
550	0.3	2.41	126	44
	0.5	3.90	156	15.5
	1.0	5.70	136	3.8
600	0.1	1.09	95	0.8
	0.2	1.55	114	7
	0.3	1.99	115	46.5
	0.5	2.95	133	33
650	0.2	1.22	83	10
	0.3	1.17	93	20.3
	0.5	1.33	116	43.5
700	1.0	1.50	112	36.5
	1.0	1.14	90	26.5

3.6.3 Effect of precursor and sulfating agent

It has been found that the use of ammonia or urea for precipitation of hydrated zirconium dioxide significantly affects the surface area of the final catalyst (Yamaguchi *et al.*, 1986). Precipitation with ammonia yields catalysts with higher surface areas. The specific surface area obtained by sulfating precrystallized zirconia is somewhat lower than that obtained by sulfating amorphous hydrous zirconia (Sarzanini *et al.*, 1995). Moreover, catalysts obtained by sulfating the amorphous hydrated ZrO₂ possess a significantly higher activity than that obtained by sulfating the microcrystalline samples (Guo *et al.*, 1995). Sohn and Kim have studied the effect of using various sulfating agents, such as H₂SO₄, (NH₄)₂SO₄, H₂S, SO₂ and CS₂. The effects of different sulfating

agents, and their post-treatment with oxygen and hydrogen, have been studied for 1-butene isomerization (Table 3.3). These authors have observed that the superacidity obtained in these catalysts is independent of the sulfur source used for the sulfation of the metal oxide precursor. It has been also found that, for sulfate concentrations above an average half monolayer, sulfation with H_2SO_4 leads to contents of sulfate that are appreciably lower than the nominal concentration. On the other hand, sulfation with ammonium sulfate produces high nominal sulfate concentration. The previous study has compared the surface sulfate concentration and the surface area of the catalysts when the sulfation is accomplished using sulfuric acid and ammonium sulfate. It is seen that higher sulfate concentrations and surface area are obtained with sulfuric acid than ammonium sulfate. The somewhat lower rate constant obtained with the latter, for the isomerization of 1-butene (Table 3.4) is thus explainable on the basis of surface area. This catalyst also shows significantly higher activity for the *n*-butane isomerization reaction at room temperature. Even typical solid acid catalysts, such as zeolites, show no activity at such low temperature. Zeng *et al.* (1994) have found that higher concentrations of the solutions used for carrying out sulfation result in higher tetragonal content of the catalyst. Higher concentrations also increase the sulfur content of the catalyst samples (Chen *et al.*, 1993). Most of the excess sulfate is, however, lost during the thermal activation of the catalyst. These sulfates thus represent the thermally most labile forms of the grafted sulfates (Yamaguchi *et al.*, 1986). With the use of high-resolution transmission electron microscopy (TEM) and X-ray diffraction (XRD) techniques, it has been found that the nature of the surface sulfates grafted by any of the techniques on amorphous or precrystallized zirconia is much the same. When monoclinic microcrystalline ZrO_2 is doped with sulfuric acid, the first doses of the acid selectively graft sulfate groups on to the crystal defects (Morterra *et al.*, 1993). The latter doses react with the regular crystal faces of the crystallites. It has been found that the relative amounts of the Lewis and Bronsted sites depend largely on the surface concentration of the sulfates and their nature (Nascimento *et al.*, 1993). At low sulfate loadings, when only sulfates located in the crystallographically defective sites are present, there is a fair amount of Lewis acidity formed, but no Bronsted acidity is formed. Isolated sulfate species observed for higher sulfate loadings and the existence of pyrosulfates on a few low index planes lead to the formation of Bronsted acid sites. Morterra *et al.* (1991) have studied the effect of sulfate concentration on the Bronsted acidity of the catalyst. Their results suggest an increase in

the Bronsted acidity with an increase in sulfate concentration up to a certain maximum, after which the amount of Bronsted acidity remains constant. This trend has also been reported by Nascimento *et al.* (1993). Thus, sulfates present above this concentration are lost during the thermal activation and represent the thermally more labile fraction.

Table 3.3 Properties of S-ZrO₂ obtained with different sulfur compounds in the percolating solution and after heating for 3 h in nitrogen at 893 K

Sulfur compound	Sulfur concentration (wt%)	Surface area (m ² g ⁻¹)
H ₂ SO ₄	1.48	104.1
(NH ₄) ₂ SO ₄	0.81	95.3
(NH ₄) ₂ S ₂ O ₃	0.45	45.4
(NH ₄) ₂ S	0.16	45.6

Table 3.4 Catalytic activities for 1-butene isomerization

Catalyst ^a	Rate constant $k \times 10^2$ (s ⁻¹ g ⁻¹)
ZrO ₂	0
ZrO ₂ /SO ₄ ²⁻ (S)	2.48
ZrO ₂ /SO ₄ ²⁻ (A)	2.41
ZrO ₂ /SO ₄ ²⁻ (S)-H ₂ ^b	0
ZrO ₂ /SO ₂	0
ZrO ₂ /SO ₂ -O ₂ ^c	2.38
ZrO ₂ /H ₂ S	0
ZrO ₂ /H ₂ S-O ₂ ^c	2.35
ZrO ₂ /CS ₂	0
ZrO ₂ /CS ₂ -O ₂ ^c	2.32

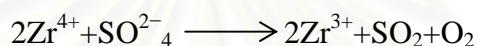
^a Sulfating agent: (S), sulfuric acid; (A), ammonium sulfate.

^b Reduced with H₂ at 500°C for 2 h.

^c Oxidized with O₂ at 400°C for 2 h.

3.6.4. Effect of activation temperature

Thermal treatment of the catalyst under vacuum below 723 K affects only the surface hydration degree, which in turn affects the covalency of the surface sulfates, thus altering the Bronsted:Lewis (B:L) site ratio (Morterra *et al.*, 1993). This effect is depicted in Table 3.5. Activation temperatures above 723 K under vacuum start affecting the overall surface hydration degree as well as the concentration of the surface sulfates (Bensitel *et al.*, 1988 and Morterra *et al.*, 1994). At higher temperatures, some of the sulfates decompose to form SO₂. A possible pathway for this decomposition has been suggested by Chen *et al.* (1993) as:



Comelli *et al.* (1995) have found that calcination temperatures above 753 K lead to a reduction in surface area. For instance, calcination at 663 K produces a surface area of 117 m² g⁻¹, which decreases to 104 m² g⁻¹ at 893 K. Similar results have been reported by Chen *et al.* (1993).

Table 3.5 Percentage of acid sites on the SO₄²⁻-ZrO₂ catalysts that are of the Bronsted type^a

Treatment temperature (°C)		Bronsted acid sites (% of total)			
Pre-	Post-	0 wt% SO ₄ ²⁻	1.17 wt% SO ₄ ²⁻	9.87 wt% SO ₄ ²⁻	13.6 wt% SO ₄ ²⁻
100	100	0	47	98	98 (97) ^c
100	400	0	49	93	95 (89) ^c
400	100	42	– (45) ^b	68	68 (70) ^c
400	400	46	– (52) ^b	80	83 (64) ^c

^a All samples were calcined at 625°C, exposed to air prior to the pretreatment in situ at 100 or 400°C prior to pyridine adsorption.

^b SO₄²⁻ content of the precursor before 650°C calcination.

^c Numbers in parentheses are for Pt-containing material.

3.7 Mechanism of *n*-butene isosynthesis over sulfated zirconia

The literature (Lohitharn *et al.*, 2006) reported a comprehensive mechanistic for *n*-butene isomerization on sulfated zirconia (SO₄-ZrO₂). The reaction occurs via a bimolecular mechanism, while others have suggested that a monomolecular pathway is dominant. The other mechanism for *n*-butane isomerization on SO₄-ZrO₂ proposed by numerous researchers is bimolecular mechanism. The bimolecular pathway is considered to occur via formation the formation of butane, which subsequently oligomerizes with adsorbed C₄⁺ carbenium ions to produce C₈⁺ oligomeric species. The SO₄-ZrO₂ catalyst was prepared by calcining the sulfated-doped zirconium hydroxide [Zr(OH)₄] precursor at 600°C under static air for 2 h. The *n*-butane isosynthesis, that reaction over SZ has been proposed based on the results from the use of added nonspecific olefins as molecular probe, was carried out with 0.2 g of the SO₄-ZrO₂, and wide range of reaction temperatures from 20 to 250°C. The addition of other olefins, such as ethylene, propylene, isobutene, and 1-pentene, besides the intermediate butane promoted catalytic activity. The results indicated that not only C₄ olefins, but also any olefins with the ability to form carbenium ion species on the surface, which can promote catalytic activity. The reaction mechanism is proposed involving a bimolecular pathway with the characteristics of a monomolecular pathway (dual-nature mechanism) using “olefin-modified sites” as the centers of reaction. The major observations made for the isomerization of *n*-butane (i.e., isotropic scrambling, nonspecific olefin activity promotion, high isobutene selectivity, and catalyst deactivation) are discussed in light of the proposed molecular pathway, and seeming duality of the mechanism is addressed.

3.8 Nature of active sites

The various techniques used for the characterization of these catalysts to throw light on the origin and nature of active sites activity, which have been the subject of intense debate. Technological advances to date still seem to be inadequate for the complete characterization of the complex nature of these solid superacidic anion treated transition metal oxides. As a result, the exact structure of the active sites, as well as their nature (Lewis or Bronsted type), is a subject of debate. Attempts have, however, been made to unearth these features of the catalysts. Kumbhar *et al.* (1989) had speculated the

structure of $\text{SO}_4\text{-ZrO}_2$ as given in Figure 3.1. Chen *et al.* (1993) have proposed a possible mechanism for the generation of the acid sites on the surface of $\text{SO}_4\text{-ZrO}_2$. This mechanism suggests the formation of acid sites to be a two-step chemical reaction between the superficial hydroxyl groups and the sulfate anions being adsorbed. The first chemical reaction occurs during the impregnation with sulfates and the subsequent drying:

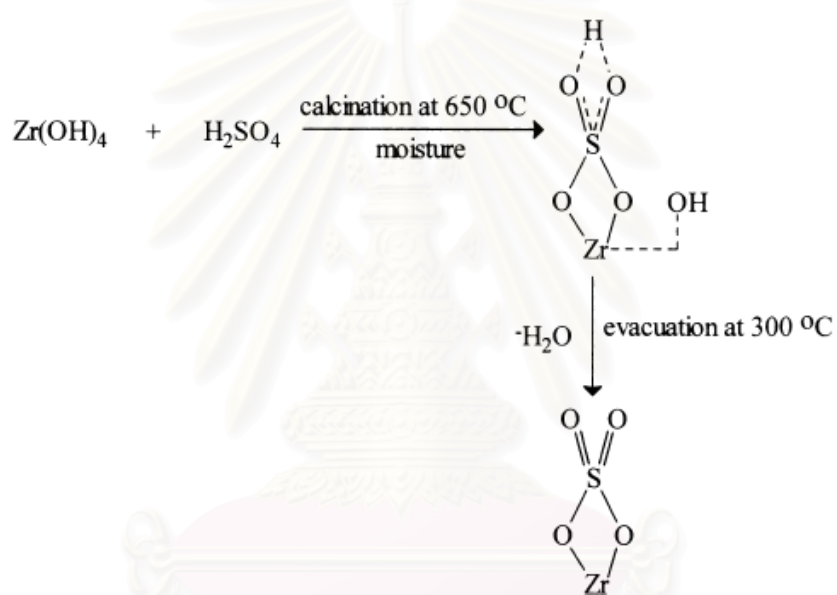
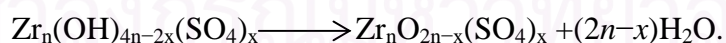


Figure 3.1 Model proposed by Kumbhar *et al.* (1989)

The second part of the formation occurs during the calcination of the catalyst:



Several observations, such as higher surface area, increased sintering resistance and stability of tetragonal phase and smaller crystallite size as a result of presence of sulfate anions, support this type of mechanism. The incorporation of the sulfate anions on the surface of ZrO_2 has been found to probably increase the number and strength of the Lewis acid sites [Yamaguchi *et al.* (1990), Papera *et al.* (1992), Zhang *et al.* (1994), Jin *et al.* (1986) and Corma *et al.* (1994)]. Yamaguchi has proposed a possible scheme for the

formation of acid sites (Figure 3.2). According to this hypothesis, whatever the starting materials used for sulfation is the oxidation during the thermal treatment results in the formation of the structure II. This structure is essential for the catalysis of reactions by such catalysts. It has further been suggested that such a structure may develop at the edge or corner of the metal oxide surfaces. This latter view is supported by the fact that the first doses during a stepwise loading of the acid on microcrystalline ZrO_2 selectively form sulfate groups on crystal defects such as corners and edges (Morterra *et al.*, 1993). For an S- ZrO_2 sample dehydrated to a medium to high degree, Morterra *et al.* (1994) have observed the surface sulfates to exhibit a highly covalent character. It has further been observed that the adsorption of basic molecules, like pyridine, on the central metal cation causes a large shift in the IR band for S=O from 1370 to 1330 cm^{-1} (Jin *et al.*, 1986). Similar results have been presented by Morterra *et al.* (1994). These observations suggest that the highly covalent surface sulfates tend, under the influence of basic molecules, to exhibit a lesser covalent character. Further, the partial rehydration (water acting as a weak Lewis base) of the catalyst initially tends to convert the surface sulfates to a lesser covalent form and then into an ionic form. This results in the transformation of the strong Lewis sites to Bronsted acid sites. The subsequent decrease in the catalytic activity towards *n*-butane isomerization suggests that the strong Lewis sites associated with these highly covalent sulfates are catalytically active. These covalent sulfates in structure II of the Yamaguchi model (Figure 3.2) possess a strong ability to accept electrons from a basic molecule and hence are responsible for the generation of superacidic sites. Even though this model for the structure of active sites explains the above-mentioned observations, it does not provide a possible explanation for the decomposition of the sulfate species as SO_2 or SO_3 from structure II at high temperatures (above 923 K). In this context, Davis *et al.* (1994) suggested that the changes in the structure and valence occurring during the catalyst preparation and thermal activation do not seem to confirm with the chemical bonding. Hence, they have proposed a different scheme that is able to explain the loss of surface sulfates as SO_3 on heating above 923 K (Figure 3.3).

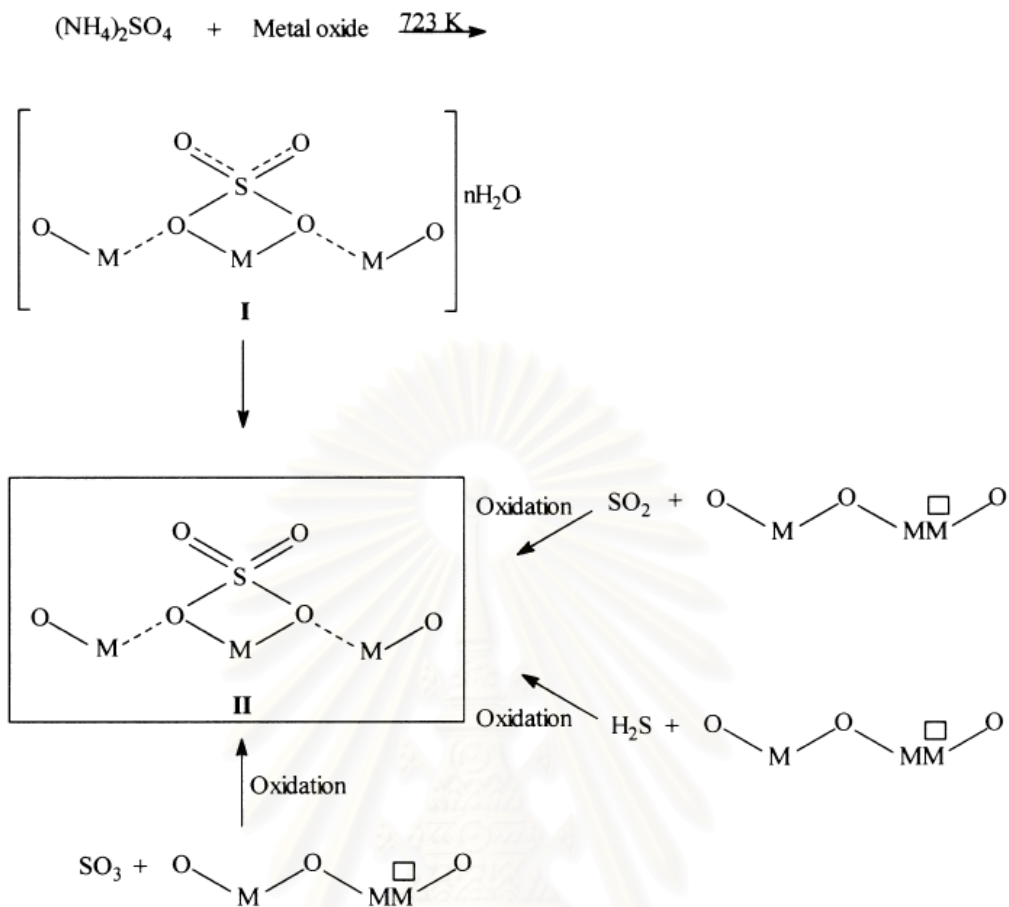


Figure 3.2 Model proposed by Yamaguchi (1990).

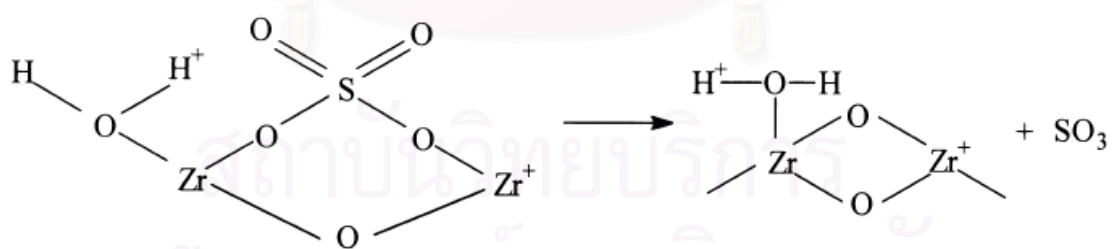


Figure 3.3 Model proposed by Davis *et al.* (1994).

The model in Figure 3.3, however, is incapable of providing an explanation for the loss of sulfates as SO_2 , because this involves the reduction of S^{6+} to S^{4+} with a corresponding oxidation of some Zr or O species.

Another model has been proposed by Arata and Hino (1990) for the structure of the active site, wherein the sulfate bridges across two zirconium atoms (Figure 3.4).

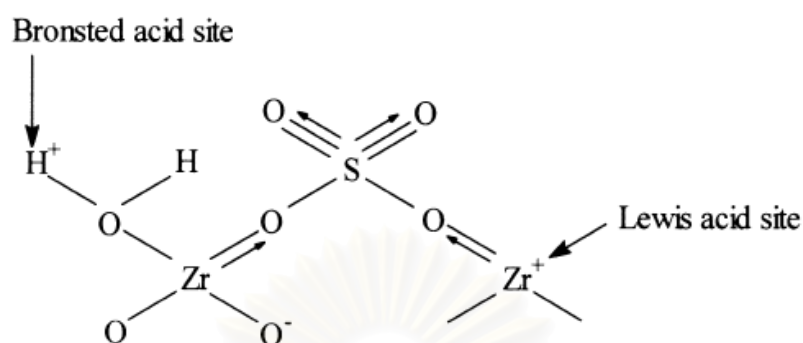


Figure 3.4 Model proposed by Arata and Hino (1990)

The Arata and Hino model takes into account the formation of Bronsted sites as a result of the uptake of water molecules as a weak Lewis base on the Lewis acid site, as has been evidenced by the IR studies. This model has also been accepted by Davies *et al.* (1995).

The models mentioned in the foregoing discussion for the structure of the active sites describe the formation of Lewis-type sites due to the highly covalent character of the adsorbed sulfates and the formation of Bronsted sites as a result of the interaction of water molecules with these sulfates. In fact, Morterra *et al.* have, for low sulfate loadings, claimed the presence of Lewis sites to be predominant, depending on the degree of dehydration. Their study reveals the presence of a very low number, though ever null, of Bronsted sites at high dehydration of the catalyst. Nevertheless, it seems that the formation of these Bronsted sites is due to the residual amounts of water. Contrary to the above models, Clearfield *et al.* (1994) have proposed a model that allows for the formation of Bronsted sites (Figure 3.5). This model is based on the assumption that the predominant species in sulfuric acid media is the bisulfate ion, which can displace a Zr-OH-Zr bridge during chemisorption on the surface of hydrated zirconia (I). On heating, either the bisulfate ion can react with an adjacent hydroxyl group or two adjacent hydroxyl groups can react with each other, liberating water and keeping the bisulfate ion intact. The former results in to the generation of Lewis-type acidity, whereas the latter

leads to the formation of a Bronsted-type site. The Clearfield *et al.* model thus describes the one step formation of both types of acidic site.

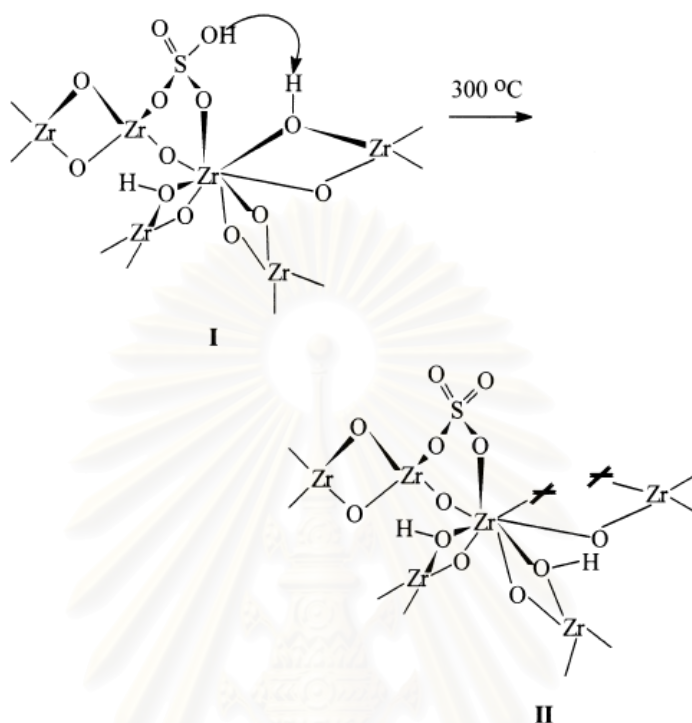


Figure 3.5 Model proposed by Clearfield *et al.* (1994).

This type of Bronsted acidity generation has also been proposed by Kustov *et al.* [33], who have postulated that the sulfate treatment of hydrous zirconia results in the elimination of the terminal ZrOH species (Hertl *et al.*, 1989) due to their substitution by bisulfate anions and enhances the acid strength of the bridging ZrOH groups (Figure 3.6). They have proposed schemes for both an ionic structure with a proton forming a multicenter bond with the SO_4^{2-} anion and a covalent structure with hydrogen-bonded hydroxyl groups.

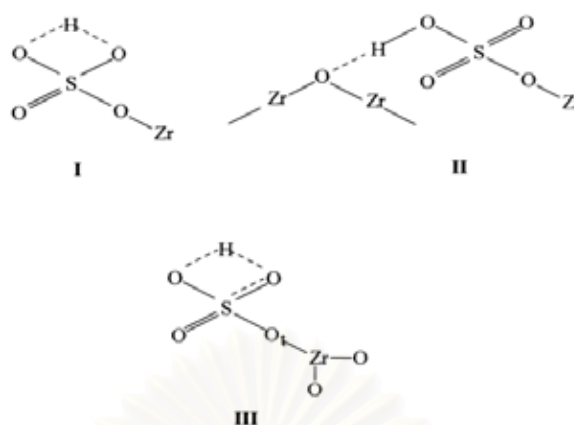


Figure 3.6 Model proposed by Kustov *et al.* (1994).

With this model, Kustov *et al.* have explained the modification of Lewis acid sites by HSO_4^- anions. The Lewis acidity enhancement was attributed to the increase of the electron-accepting properties of three-coordinate zirconium cations via the inductive effect of SO_4^{2-} anions, which withdraw electron density from the zirconium cations through the bridging oxygen atom. Furthermore, with the IR study of benzene adsorption, they have reported that the strength of the Bronsted sites of S-ZrO₂ is stronger than the silanol groups of silica gel, but weaker than the bridging OH groups in HX zeolites.

Babou *et al.* (1995) have postulated a different structure for the active sites at the surface of S-ZrO₂ (Figure 3.7). They have proposed that the interaction of the zirconia support with sulfuric acid solution results in the trapping of the protons by the zirconium hydroxide surface. Sulfate ions then get trapped on this ionized surface. Dehydration at temperatures below 473 K results in the loss of a first water molecule, leading to the formation of the structure II. Further dehydration at higher temperatures liberates a second water molecule with the formation of $(\text{SO}_3)_{\text{ads}}$ linked by dative bonds to the support. Such a model is based on quantum chemical calculations and describes the acidity to be near that of sulfuric acid but not to be superacidic. Similar arguments based on P-NMR studies have been put forward by Adeeva *et al.* (1995) (Figure 3.8), who have proposed that the acid strength of the Bronsted sites in S-ZrO₂ is similar to that of the lower OH-frequency protons in HY, but is weaker than that of the protons H-ZSM-5.

Table 3.6 ^1H MAS NMR shifts, δH (ppm), of S-ZrO₂ and zeolites and their shifts, $\Delta\delta\text{H}$, upon adsorption of bases

Sample	δH before ads.	δH after CCl ₃ CN ads.	$\Delta\delta\text{H}$ (CCl ₃ CN)	δH after CD ₃ CN ads.	$\Delta\delta\text{H}$ (CD ₃ CN)
ZrO ₂	4.5	8.5	4	-	-
ZrO ₂ /SO ₄	6.2	8.5	2.3	10	3.8
HY	4.7	7.7	3	9	4.3
	4.1	8.5	4.4	11	6.9
H-ZSM-5	4.1	9	4.9	11	6.9
H-ZSM-5	4.3	-	-	11.5	7.2

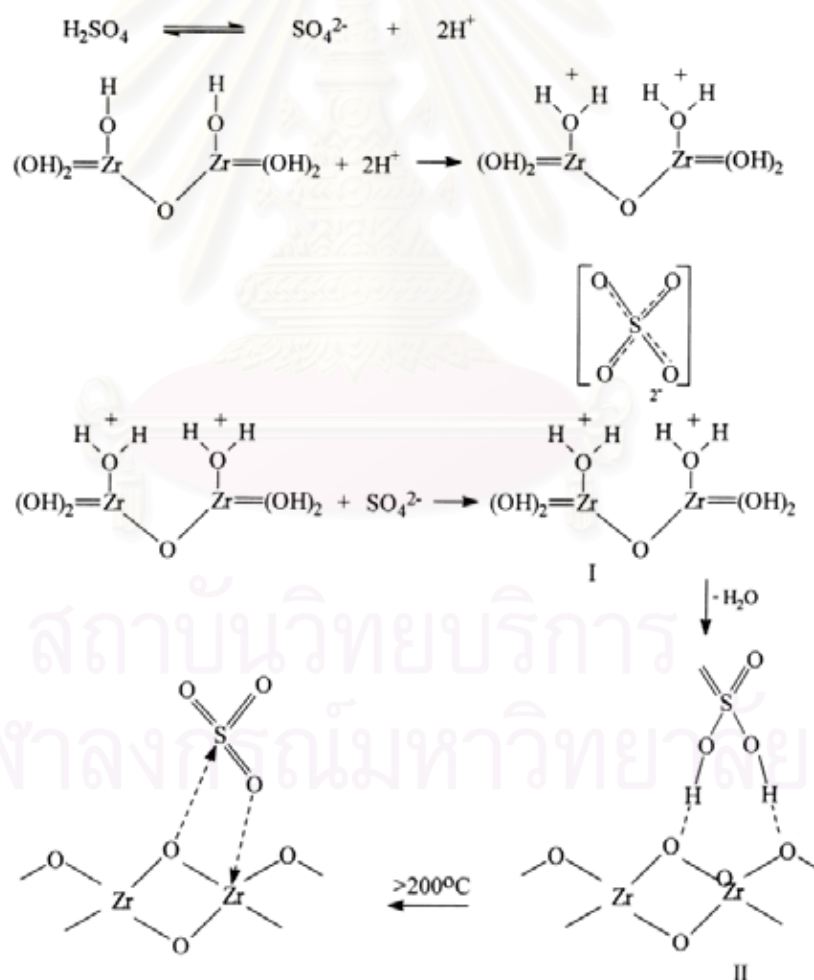


Figure 3.7 Model proposed by Babou *et al.* (1995).

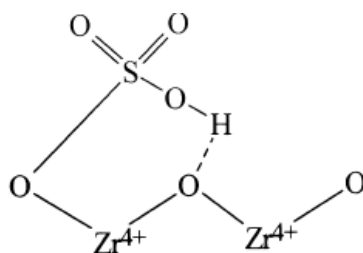


Figure 3.8 Model proposed by Adeeva *et al.* (1995).

It has also been speculated that the extraordinary activity of these catalysts is not due to its superacidity, but it results from the stabilization of the transition state complex as alkyl sulfates or surface alkoxy groups at the catalytic site. The H MAS NMR shifts for S-ZrO₂ and HY zeolite are given in Table 3.6. From spectroscopic studies, formation of such species has indeed been found in the case of zeolite catalysts wherein the oxygen from the zeolite framework is involved in the stabilization of the chemisorption complex Malkin *et al.*, (1990). Pinna *et al.* (1994), and Morterra and co-workers (1993 and 1994) have proposed that the sulfates responsible for the Bronsted acidity of these catalysts represent the most labile fraction of the overall sulfates and no Bronsted acidity is irreversibly lost for thermal activation temperatures above 923 K. Lewis acidity is shown by the sulfates located in the crystallographically defective sites such as edges and corners. Increasing surface sulfation results in the shielding of the surface Zr⁴⁺ cations located on the low index planes. Most of these sulfates have been proposed to induce Bronsted acidity, this effect being more pronounced if the sulfates are in the form of polynuclear pyrosulfates resulting from high loadings of sulfates. Yamaguchi and co-workers (1986 and 1987) have reported the existence of only the Lewis type of acidity on the surface of S-ZrO₂ catalysts. Microcalorimetric studies of ammonia adsorption on the catalyst by Fogash *et al.* have revealed the presence of a spectrum of acid sites with different acid strengths. Their study also reveals that the initial doses of ammonia are coordinately bound to the support. For higher amounts of ammonia dosed, IR spectroscopy shows the presence of NH⁴⁺ ions adsorbed on the surface which points to the existence of Bronsted acidity in association with the Lewis type acid sites. Lunsford and co-workers (1994) used P-NMR spectroscopy to probe the nature of the sites and have provided evidence for the existence of both types of acidities. Similarly with Arata and co-workers, Sohn and Kim, Guo *et al.*, and Clearfield *et al.* have supported the view

that both the Lewis and Bronsted types of acidity are present on the surface of S-ZrO₂. Babou *et al.* (1995) have found from IR studies of adsorbed bases, such as butane, CO, H₂O and pyridine that two types of Lewis site and one type of Bronsted site exist at the surface of sulfate- modified zirconia. Of these active sites, one Lewis- type site is associated with the zirconia support and the rest exist due to the presence of surface sulfates.

The foregoing discussion is indicative of the nature of acidic sites on the surface of S-ZrO₂, depending on the types of precursor and pretreatment. S-ZrO₂ can be prepared with superacidity, which will be useful in certain types of reaction.

3.9 Effect of additives on sulfated zirconia-based catalysts

Y. Kim *et al.* (2005) studied various promoters, for example Fe, Mn, and Pt, to enhance the activity of SZ. Furthermore, the addition of refractory oxides, such as SiO₂, Al₂O₃, and TiO₂, has also shown to increase the thermal stability and increase the surface area of zirconia. SZ promoted with Al₂O₃ indicated an approximately 30% increase in n-butane isomerization activity at 250°C. The n-butane isomerization was studied in quartz micro-reactor using 0.2-0.5 g of catalyst, total flow rate of reactant stream was 30 cm³/min are consisted of n-C₄:H₂:He = 0.75:6.75:22.5 cm³/min. The total pressure was kept constant at 1.5 atm. The results showed that SZ, contained Al₂O₃ 2.2 wt%, gave the highest formation rate of isobutene. The difference in the amount of Al₂O₃ indicated that dissimilarity catalyst stability, formation rate of isobutene, and selectivity of isobutene. Furthermore, addition of Al₂O₃ results in the formation of smaller crystallites of zirconia which stabilize the active tetragonal phase than those on the monoclinic may play a role in the changes in sulfated content with Al₂O₃ content. The results indicated that the presence of smaller crystallite sizes of the tetragonal phase of ZrO₂ present after Al₂O₃-promotion affects the total surface area, sulfur content and the number of active sites.

Moreover, Kim *et al.* (2001) investigated the effect of impact of Pt on n-butane isomerization over SZ. The research showed that a Pt-promoted SZ (PtSZ) catalyst does not function as a traditional bifunctional catalyst similar to the commercial n-butane

isomerization catalyst. *n*-Butane isomerization was studied using a quartz microreactor. The reaction was carried out with and without H₂ addition. The experiment indicated that H₂ in feed stream reduces rate of catalyst deactivation. Promotion of SZ with Pt did not improve the activity or the stability of the catalyst in the absence of H₂. The combined effects of Pt promotion and H₂ addition cause a significant increase in the concentration of active intermediates.



สถาบันวิทยบริการ
จุฬาลงกรณ์มหาวิทยาลัย

CHAPTER IV

EXPERIMENTAL

This chapter provides details on experimental systems and procedures used in this study. Section 4.1 describes catalyst preparation methods for preparing ZrO₂ and sulfated zirconia (SZ). Catalyst characterization techniques consisting of XPS, N₂ physisorption, XRD, ESR, SEM and TPD are explained in Section 4.2. The last section involves the reaction study of isosynthesis via CO hydrogenation.

4.1 Catalyst Preparation

4.1.1 Chemicals

1. Aluminium nitrate hydrate from Aldrich.
2. Ammonium hydroxide from Aldrich.
3. Ammonium sulfated from Aldrich.
4. Zirconyl nitrate hydrate from Aldrich.
5. Zirconyl chloride, 30 % solution in hydrochloric acid from Aldrich.
6. Zirconium (IV) oxide, powder, < 5 micro from Aldrich.
7. Zirconium (IV) hydroxide, sulfated from Aldrich.
8. Sulfuric acid 95-97% from Merck.

4.1.2 Preparation of Zirconia

Zirconia (ZrO₂) was prepared by the precipitation method. A solution of zirconium salt precursors such as zirconyl chloride (ZrOCl₂) or zirconyl nitrate [ZrO(NO₃)₂] (0.15 M) was slowly added into a well-stirred precipitating solution of ammonium hydroxide (NH₄OH) (2.5 wt%) at room temperature. The pH of the solution was controlled at 10. The resulting precipitate was removed, and then washed with deionized water until Cl⁻ was not detected by a silver nitrate (AgNO₃) solution. The

obtained sample was then dried overnight at 110°C and calcined at 450°C for 3 hours with a temperature ramping rate of 5°C/min.

4.1.3 Preparation of Sulfated Zirconia

Sulfated zirconia was prepared by the incipient wetness impregnation method. Sulfuric acid was doped on zirconia at room temperature. The obtained sample was then dried overnight at 110°C and calcined at 450, 650, and 700°C for 3 hours with a temperature ramp of 5°C/min.

For commercial sulfated zirconia, the catalyst was also calcined at 450, 600, and 750°C for 3 hours with a temperature ramp of 5°C/min.

4.2 Catalyst Characterization

4.2.1 X-ray Photoelectron Spectroscopy (XPS)

XPS surface analysis was performed using a Kratos Amicus X-ray photoelectron spectroscopy. The XPS spectra were measured using the following condition: Mg K α X-ray source at a current of 20 mA and 12 keV; a resolution of 0.1 eV/step; and a pass energy of 75 eV. The operating pressure was approximately 1×10^{-6} Pa. The surface of sulfated zirconia was cleaned *in situ* using an Ar ion gun sputtering for 30 seconds with 0.5 kV beam voltage and 50 mA emission current. A wide-scan survey spectrum was collected for each sample in order to determine the elements present on the surface. Then, window spectra were recorded for the C 1s, O 1s, Zr 3d and S 2p photopeaks of each sample. All the binding energies were calibrated internally with the carbon C 1s photoemission peak at 285.0 eV. Photoemission peak areas were determined after smoothing and background subtraction using a linear routine. Deconvolution of complex spectra were done by fitting with Gaussian (70%)-Lorentzian (30%) shape using a VISION 2 software equipped with the XPS system.

4.2.2 N₂ Physisorption

Measurement of BET surface area, cumulative pore volume and average pore diameter were performed by N₂ physisorption technique using the Micromeritics ASAP 2020 surface area and porosity analyzer.

4.2.3 X-ray Diffraction (XRD)

The X-ray diffraction (XRD) patterns of powder were performed by X-ray diffractometer. The crystallite size was estimated from line broadening according to the Scherrer equation and α -Al₂O₃ was used as a standard. In addition, the characteristic peaks of crystal phase from XRD spectra were used for calculating the fraction of crystal phase in catalyst.

4.2.4 Electron Spin Resonance Spectroscopy (ESR)

Electron spin configuration was detected by using Electron spin resonance spectroscopy (ESR) (JEOL model JES-RE2X) at the Scientific and Technological Research Equipment Center, Chulalongkorn University (STREC). The sample was degassed before measurement at room temperature.

4.2.5 Scanning Electron Microscopy (SEM/EDX)

Scanning electron microscopy (SEM) and Energy dispersive X-ray spectroscopy (EDX) were used to determine the catalyst granule morphology and elemental distribution of the catalyst particles using JEOL JSM-5800LV scanning electron microscope. The SEM was operated using the back scattering electron (BSE) mode at 20kV. After the SEM micrographs were taken, EDX was performed to determine the elemental concentration distribution on the catalyst granules using Link Isis Series 300 software at the Scientific and Technological Research Equipment Center, Chulalongkorn University (STREC).

4.2.6 Temperature-Programmed Desorption (TPD)

Temperature-programmed desorption techniques with ammonia and carbon dioxide (NH₃- and CO₂-TPD) were used to determine the acid-base properties of catalysts, respectively. TPD experiments were carried out using a flow apparatus. The catalyst sample (0.1g) was treated at its calcination temperature (450°C) in helium flow for 1 hour and then saturated with 15% NH₃/He mixture or pure CO₂ flow after cooling to 100°C. After purging with helium at 100°C for 1 hour to remove weakly physisorbed NH₃ or CO₂, the sample was heated to 650°C at a rate of 20°C/min in a helium flow of 50 cm³/min. The amount of acid-base sites on the catalyst surface was calculated from the desorption amount of NH₃ and CO₂, respectively. It was determined by measuring the areas of the desorption profiles obtained from the Micromeritics ChemiSorb 2750 Pulse Chemisorption System analyzer.

4.3 Reaction Study in Isosynthesis via CO Hydrogenation

4.3.1 Materials

The reactant gases used for the reaction study were carbon monoxide (99.3%), ultra high purity hydrogen (99.999%) and high purity nitrogen (99.99%) supplied by Thai Industrial Gas Limited (TIG). The total flow rate was fixed at 25 cm³/min with a CO: H₂: N₂ ratio of 10: 10: 5 cm³/min, corresponding to a H₂/CO ratio of 1.

4.3.2 Apparatus

Flow diagram of a lab-scale gas phase isobutene synthesis system is depicted in Figure 4.1. The system consisted of a reactor, an automatic temperature controller, an electrical furnace and a gas controlling system.

4.3.2.1 Reactor

The reaction was carried out in a quartz tube (O.D. 1/4"). Two sampling points were provided before and after the catalyst bed. Catalyst was placed between two quartz wool layers.

4.3.2.2 Gas Controlling System

The controlling system for each gas consisted of a pressure regulator, an on-off valve and a mass flow controller

4.3.2.3 Automatic Temperature Controller

This unit consisted of a magnetic switch connected to a variable voltage transformer and a solid state relay temperature controller connected to a thermocouple. Reactor temperature was measured at the centre of the catalyst bed in the reactor. The temperature control set point was adjustable within the range of 0-800°C at the maximum voltage output of 220 V.

4.3.2.4 Electric Furnace

The electric furnace with 2000 W heating coil was used to supply heat to the reactor for isosynthesis. The reactor could be operated from room temperature up to 600°C at the maximum voltage of 220 V.

4.3.2.5 Gas Chromatography

A gas chromatography Shimadzu model 8A (GC-8A) equipped with a thermal conductivity detector (TCD) was used to analyze compositions of carbon monoxide and hydrogen in the feed and product streams by using Molecular sieve column and used to analyze composition of carbon dioxide in the product stream by using Poropak-Q column. Hydrocarbons in the product stream were analyzed by a gas chromatography Shimadzu

model 14B (GC-14B) equipped with a flame ionization detector (FID) by using VZ-10 column. The operating conditions for each instrument are listed in Table 4.1.

Table 4.1 Operating conditions for gas chromatography

Gas Chromatography	Shimadzu GC-8A		Shimadzu GC-14B
Detector	TCD		FID
Column	Molecular sieve 5A	Porapak-Q	VZ-10
- Column material	SUS	SUS	SUS
- Length (m)	2	2	2
- Outer diameter (mm)	4	4	4
- Inner diameter (mm)	3	3	3
- Mesh range	60/80	60/80	60/80
- Maximum temperature (°C)	350	350	80
Carrier gas	Ar (99.999%)	Ar (99.999%)	N ₂ (99.999%)
Carrier gas flow (ml/min)	30	30	30
Column temperature			
- initial (°C)	70	70	70
- final (°C)	70	70	70
Injector temperature (°C)	100	100	100
Detector temperature (°C)	100	100	150
Current (mA)	70	70	-
Analyzed gas	N ₂ , H ₂ , CO	CO ₂	Hydrocarbon C ₁ -C ₄

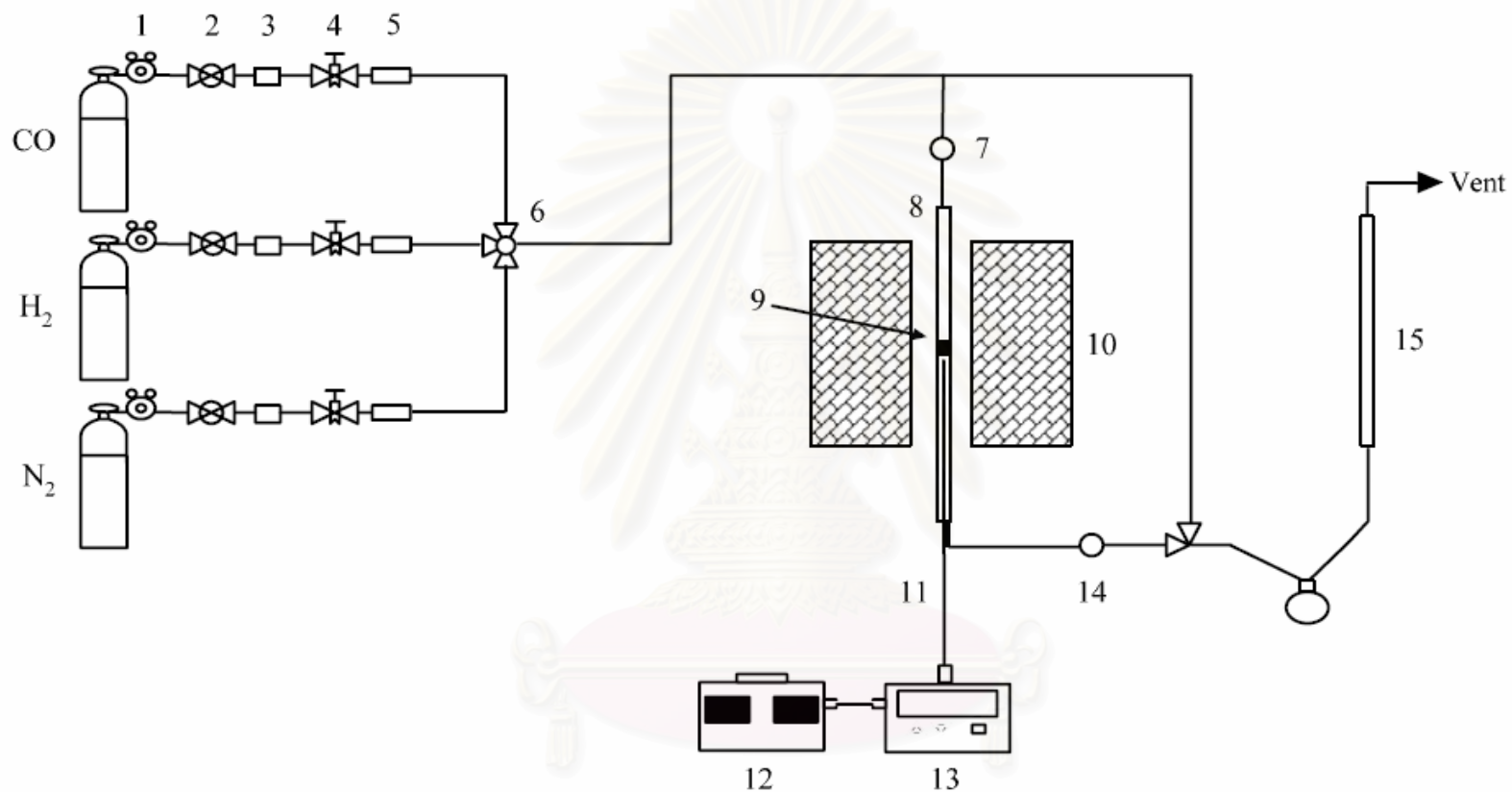
4.3.3 Procedure

Experiments were carried out using a lab-scale isobutene synthesis system as shown in Figure 4.1. A catalyst (0.2-0.5 g) was packed in the middle of the quartz tube reactor located in the center of the electric furnace. The total flow rate was 25 cm³/min with a H₂/CO ratio of 1. Isosynthesis was operated at 250-450°C and atmospheric pressure. The product gases were sampled to analyze the concentration of hydrocarbon (C₁-C₄) using GC-14B equipped with a VZ-10 column, whereas carbon monoxide and

carbon dioxide concentration were analyzed by GC-8A equipped with Molecular sieve column and Porapak-Q column, respectively. The calibration curves of reactant (CO) and products (hydrocarbon C₁-C₄) are illustrated in Appendix A.



สถาบันวิทยบริการ
จุฬาลงกรณ์มหาวิทยาลัย



- | | | | |
|----------------------------|--------------------|-----------------------|----------------------------------|
| 1. Pressure Regulator | 2. On-Off Valve | 3. Gas Filter | 4. Mass Flow Controller |
| 5. Back Pressure | 6. 3-way Valve | 7. Sampling Point | 8. Quartz Tubular Reactor |
| 9. Catalyst Bed | 10. Furnace | 11. Thermocouple | 12. Variable Voltage Transformer |
| 13. Temperature Controller | 14. Sampling Point | 15. Bubble Flow Meter | |

Figure 4.1 Flow diagram of a lab-scale gas phase isobutene synthesis system.

CHAPTER V

RESULTS AND DISCUSSION

This chapter has two sections. The characteristics of zirconia and sulfated zirconia catalysts and their catalytic properties towards isosynthesis via CO hydrogenation are described in Section 5.1. Secondly, Section 5.2 describes the effect of temperature during calcinations on characteristics of sulfated zirconia and their application as a catalyst for isosynthesis.

5.1 Characteristics of Zirconia and Sulfated Zirconia Catalysts and Their Catalytic Properties towards Isosynthesis via CO Hydrogenation.

In this section, ZrO_2 and SO_4-ZrO_2 catalysts were used and tested for the catalytic performance on isosynthesis. The synthesized ZrO_2 obtained from $ZrOCl_2$ and $ZrO(NO_3)_2$ were denoted as ZrO_2-Cl and ZrO_2-N , respectively. The amounts of sulfur loading in SO_4-ZrO_2 , was used in the study. The SO_4-ZrO_2 catalysts prepared by using various sulfur contents of 0.1, 0.25, 0.5 and 0.75% were denoted as 0.1%SZ (ZrO_2-N), 0.25%SZ (ZrO_2-N), 0.5%SZ (ZrO_2-N), 0.75%SZ (ZrO_2-N), 0.1%SZ (ZrO_2-Cl), 0.25%SZ (ZrO_2-Cl), 0.5%SZ (ZrO_2-Cl), and 0.75%SZ (ZrO_2-Cl), respectively

5.1.1 Catalyst Characterization

5.1.1.1 X-ray Diffraction (XRD)

The XRD patterns of the ZrO_2 and sulfated zirconia (SO_4-ZrO_2) catalysts synthesized from $ZrOCl_2$ are shown in Figure 5.1 and the other ones are shown in Figure 5.2. They showed that both ZrO_2 and SO_4-ZrO_2 catalysts exhibited the similar XRD peaks at $2\theta = 28.2^\circ$ and 31.5° , indicating the presence of the monoclinic phase. Besides the monoclinic characteristic peaks, they also exhibited the XRD characteristic peaks at $2\theta = 30.18, 35.3, 50.2$ and 60.2° , which indicates the presence of tetragonal crystalline phase. The crystallite size of the tetragonal phase of sulfated-zirconia was determined from the peak at $2\theta = 30.18$ for 111 plane. For all catalysts,

the contents of different phases are listed in Table 5.1. Typically, the monoclinic phase is stable up to ca. 1170°C and then, transforms into the tetragonal phase at higher temperature (Mercera *et al.*, 1991). The tetragonal phase is stable up to ca. 2370°C and finally transforms into the cubic phase at higher temperature. However, the metastable tetragonal phase in zirconia can usually be observed when the precipitation method from an aqueous salt solution is employed as seen in this work or when the thermal decomposition of zirconium salts is used. Sample obtained via incipient wetness impregnation, sulfated zirconia, contained more tetragonal phase compared with zirconia (Morterra *et al.*, 1993). Moreover, it was found that intensity apparently changed with different sulfur loading.

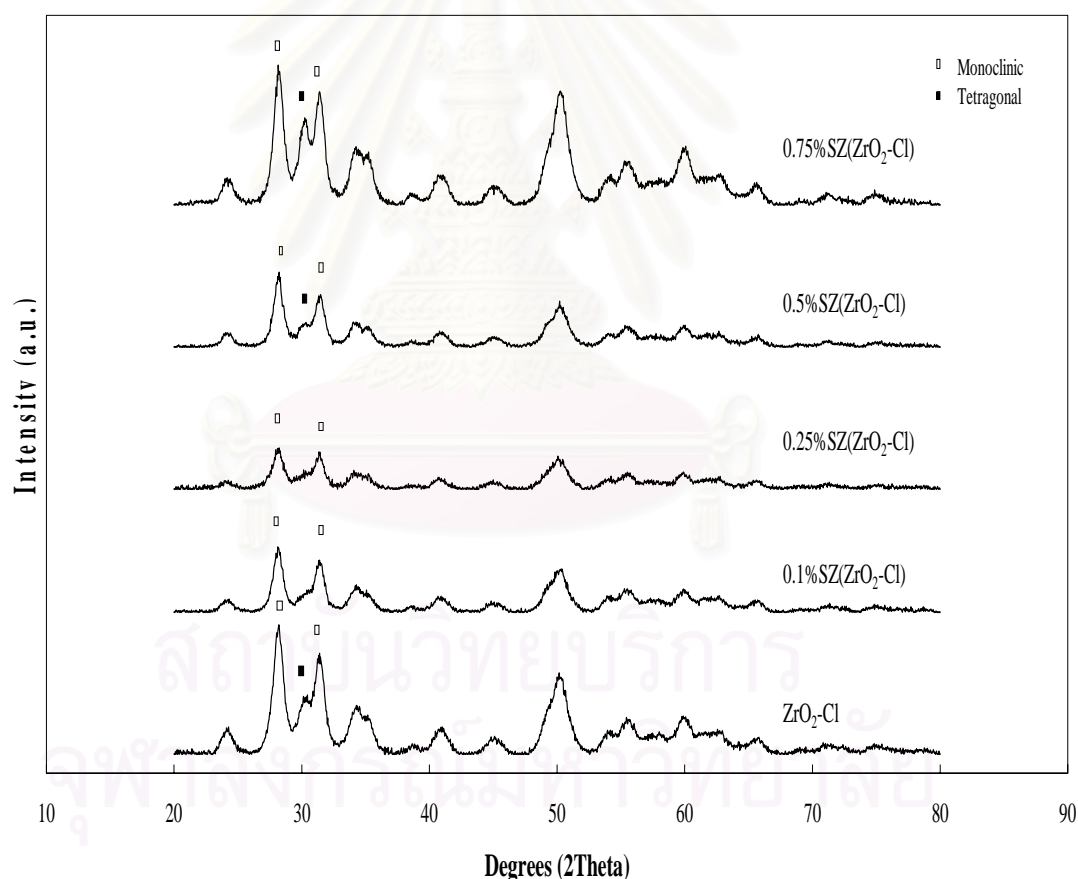


Figure 5.1 XRD patterns of ZrO₂ and SO₄-ZrO₂ catalysts synthesized from ZrOCl₂

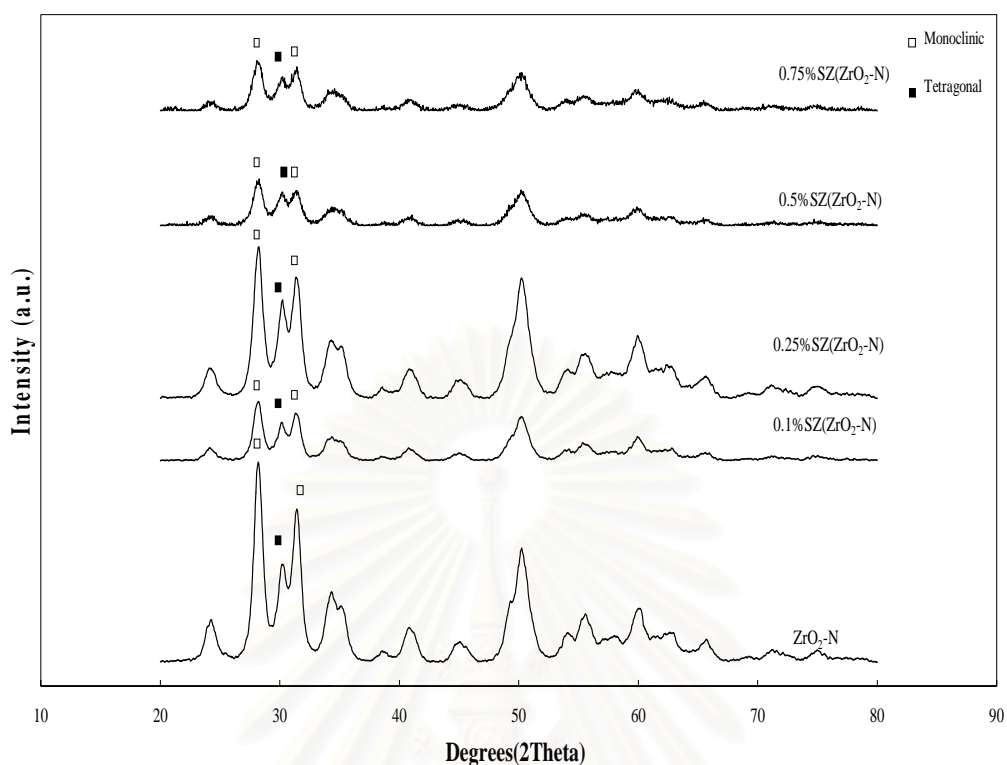


Figure 5.2 XRD patterns of ZrO_2 and SO_4 - ZrO_2 catalysts synthesized from $ZrO(NO_3)_2$

Table 5.1 Summary of catalyst characteristics obtained from XRD measurement

Catalysts	Phase	Average Crystal Size (nm)	Crystal Size (nm) ^a		% monoclinic phase ^a
			M ^b	T ^c	
ZrO_2 -N	M, T	9.5	8.7	4.7	67.3
0.1%SZ (ZrO_2 -N)	M, T	9.1	10.0	5.5	76.1
0.25%SZ (ZrO_2 -N)	M, T	8.9	10.2	13.8	84.1
0.5%SZ (ZrO_2 -N)	M, T	8.8	10.0	6.1	75.4
0.75%SZ (ZrO_2 -N)	M, T	8.7	9.1	9.5	71.1
ZrO_2 -Cl	M,T	8.7	9.5	7.5	73.2
0.1%SZ (ZrO_2 -Cl)	M, T	10.0	9.1	8.1	72.5
0.25%SZ (ZrO_2 -Cl)	M, T	10.2	8.9	7.5	70.3
0.5%SZ (ZrO_2 -Cl)	M, T	10.0	8.9	7.0	63.4
0.75%SZ (ZrO_2 -Cl)	M, T	9.1	8.7	7.0	67.5

^a Based on XRD line broadening

^b Monoclinic phase in ZrO₂

^c Tetragonal phase in ZrO₂

5.1.1.2 N₂ Physisorption

The other physical properties of catalysts such as BET surface area, cumulative pore volume, average pore diameter and pore size distribution were determined by the N₂ physisorption using the Micromeritics ASAP 2020 surface area and porosity analyzer. The values are summarized in Table 5.2. For the catalysts prepared by different zirconium salt precursors, the resulted crystal structure was probably changed (Srinivasan and Davis, 1992; Su *et al.*, 2000 and Wu and Yu, 1990) because SO₄²⁻ from zirconium salt precursor such as Zr(SO₄)₂ affected crystallization and phase transformation of ZrO₂. The ZrO₂ prepared from Zr(SO₄)₂ showed both tetragonal phase and amorphous, but the ZrO₂ prepared from other zirconium salt precursors such as Zr(NO₃)₄, ZrCl₄ and ZrOCl₂ showed monoclinic and tetragonal phase. The specific surface area of sulfated zirconia first increases with increase of quantity of sulfuric acid solution, then decreases when amount of sulfuric acid solution added is greater than 3 ml per gram of zirconium hydroxide (Fărcașiu *et al.*, 1997). The abrupt decrease in surface area for higher sulfur contents correlates with the alteration of crystal structure and sulfate migration into the bulk phase of the solid. Considering to the various %sulfur loadings, zirconia exhibited the smaller crystallite sizes, which influenced not only on the increase in the cumulative pore volume, but also on the reduction of the average pore diameter. In this case, ZrO₂-Cl and ZrO₂-N were prepared from ZrOCl₂ and ZrO(NO₃)₂ as zirconium salt precursors, respectively. It was found that different precursors slightly affected the crystal structure in the phase composition of monoclinic/tetragonal phase over ZrO₂ and the BET surface area as well. Considering pore size distribution of zirconia and sulfated zirconia catalysts as shown in Figures 5.3 and 5.4, no significant change was observed for those regarding pore size distribution.

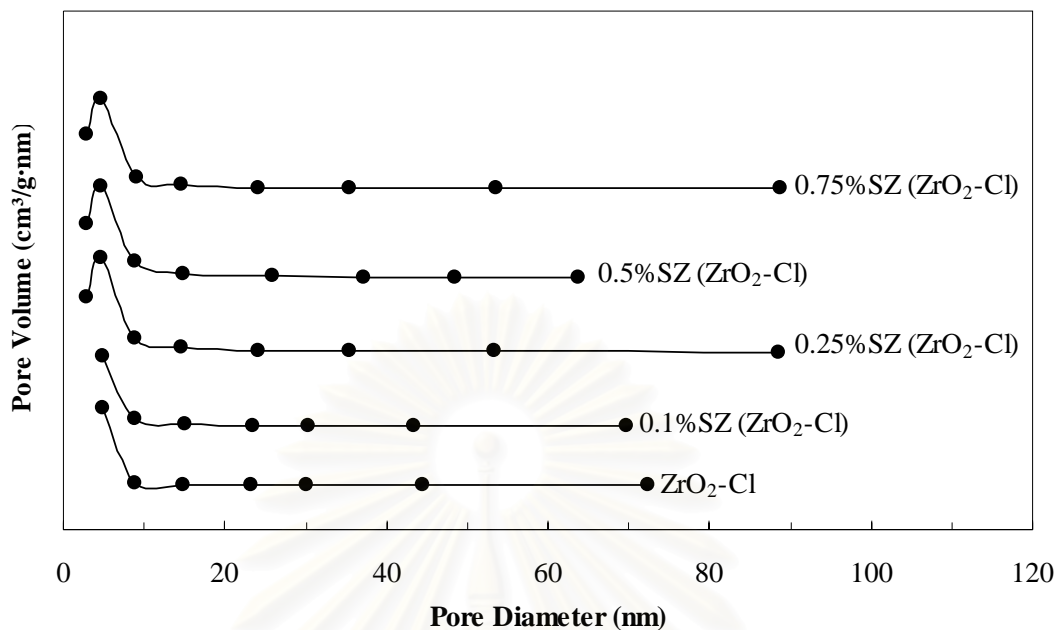


Figure 5.3 Pore size distribution of ZrO_2 and $\text{SO}_4\text{-ZrO}_2$ catalysts synthesized from ZrOCl_2

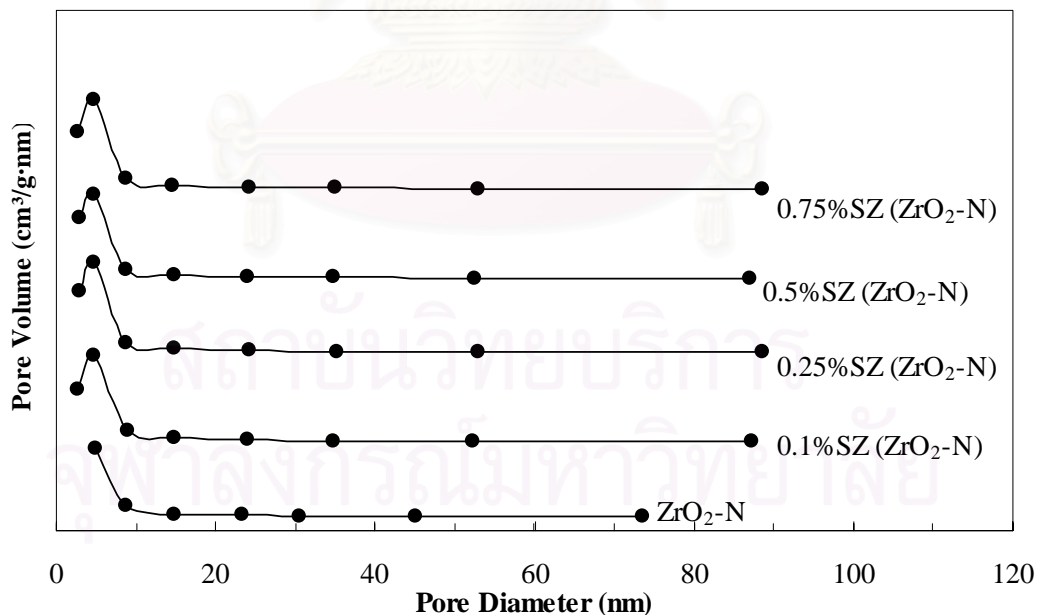


Figure 5.4 Pore size distribution of ZrO_2 and $\text{SO}_4\text{-ZrO}_2$ catalysts synthesized from $\text{ZrO}(\text{NO}_3)_2$

Table 5.2 N₂ Physisorption results

Catalysts	BET Surface Area ^a (m ² /g)	Cumulative Pore Volume ^b (cm ³ /g)	Average Pore Diameter ^c (nm)
ZrO ₂ -N	76.2	0.198	5.5
0.1%SZ (ZrO ₂ -N)	222.7	0.345	4.9
0.25%SZ (ZrO ₂ -N)	243.3	0.361	4.8
0.5%SZ (ZrO ₂ -N)	227.3	0.336	4.8
0.75%SZ (ZrO ₂ -N)	232.3	0.351	4.8
ZrO ₂ -Cl	89.8	0.194	5.0
0.1%SZ (ZrO ₂ -Cl)	89.2	0.205	5.4
0.25%SZ (ZrO ₂ -Cl)	236.6	0.380	4.5
0.5%SZ (ZrO ₂ -Cl)	239.2	0.388	5.0
0.75%SZ (ZrO ₂ -Cl)	238.1	0.372	4.4

^a Error of measurement = $\pm 5\%$.

^b BJH desorption cumulative volume of pores between 1.7 and 300 nm diameter.

^c BJH desorption average pore diameter.

5.1.1.3 Temperature Programmed Desorption (TPD)

The NH₃- and CO₂-TPD techniques were used to measure the acid-base properties of the catalysts, respectively. The NH₃- and CO₂-TPD profiles are shown in Figures 5.5, 5.6, 5.7 and 5.8. From the TPD profiles, the amounts of acid and base sites, which are also listed in Table 5.3, were calculated from the area below curves. The characteristic peaks of these profiles are assigned to their desorption temperatures indicating the strength of Lewis acid surface sites. From the NH₃-TPD results of Ma *et al.* (2005), it showed that NH₃ desorption peaks located at ca. 200°C and 300°C for ZrO₂ catalysts were corresponding to weak acid sites and moderate acid sites, respectively. Moreover, both peaks of monoclinic ZrO₂ exhibited slightly higher amount of acid sites compared to the tetragonal ZrO₂. A previous report indicated that the sulfated group on monoclinic SO₄-ZrO₂ should be more stable than sulfated group on tetragonal SO₄-ZrO₂ because the monoclinic phase may be more basic than the

tetragonal phase (Li *et al.*, 2006). In this work, not only ZrO_2 contained weak acid sites, but the moderate acid sites were also evident for the $\text{SO}_4\text{-ZrO}_2$. The adsorption of sulfur group has some effect on acid site. The higher sulfur contents were responsible for more acid sites present.

Based on CO_2 desorption peaks, the weak base sites, moderate and strong base sites can be identified (Ma *et al.*, 2005). It indicated that all kinds of base sites were presented in the tetragonal ZrO_2 , whereas only weak and moderate base sites were observed on the monoclinic ZrO_2 . For CO_2 -TPD profiles of ZrO_2 (Figure 5.7), the $\text{ZrO}_2\text{-Cl}$ exhibited higher desorption temperature than the other catalysts due to more tetragonal phase and no sulfur loading. Furthermore, for the zirconia and sulfated zirconia prepared by ZrO_2Cl had the higher amount of CO_2 desorption peaks was result of percentage of monoclinic phase and sulfur content, indicating higher basicity of monoclinic $\text{SO}_4\text{-ZrO}_2$ than tetragonal $\text{SO}_4\text{-ZrO}_2$.

For the other salt precursors, catalysts contained only the weak base sites and moderate base sites. From, Figure 5.8 and Table 5.3, they show that $\text{ZrO}_2\text{-N}$ exhibited higher base sites than sulfated zirconia. It should be mentioned that acid and base sites of $\text{ZrO}_2\text{-Cl}$ and $\text{ZrO}_2\text{-N}$ were less than those of the sulfated zirconia due to sulfated group on surface catalysts. It was suggested that differences in both acid and base sites can be attributed to the various fractions of crystal phases along with the crystallite sizes of catalysts. In fact, crystallite size also relates to BET surface area. Therefore, the amount of acid and base sites may be ascribed to affect the surface area. In order to give a better understanding, the relationship between acid-base sites and percent of sulfur content in ZrO_2 is illustrated in Figures 5.9 and 5.10. It was found that the amount of acid sites increased with increased percents of sulfur content in ZrO_2 . Considering the $\text{ZrO}_2\text{-Cl}$ and $\text{SO}_4/\text{ZrO}_2\text{-Cl}$ acid sites increased with increased percents of sulfur content up to a maximum at 0.25%, and then decreased with more sulfur loading, but base sites depended on sulfur content, too. In other catalysts, there was an optimum point at 0.25% of the sulfur loading in ZrO_2 , which can maximize the acid sites. Considering the base sites, the amount of base sites was apparently proportional to the percent of tetragonal phase and sulfur content in ZrO_2 .

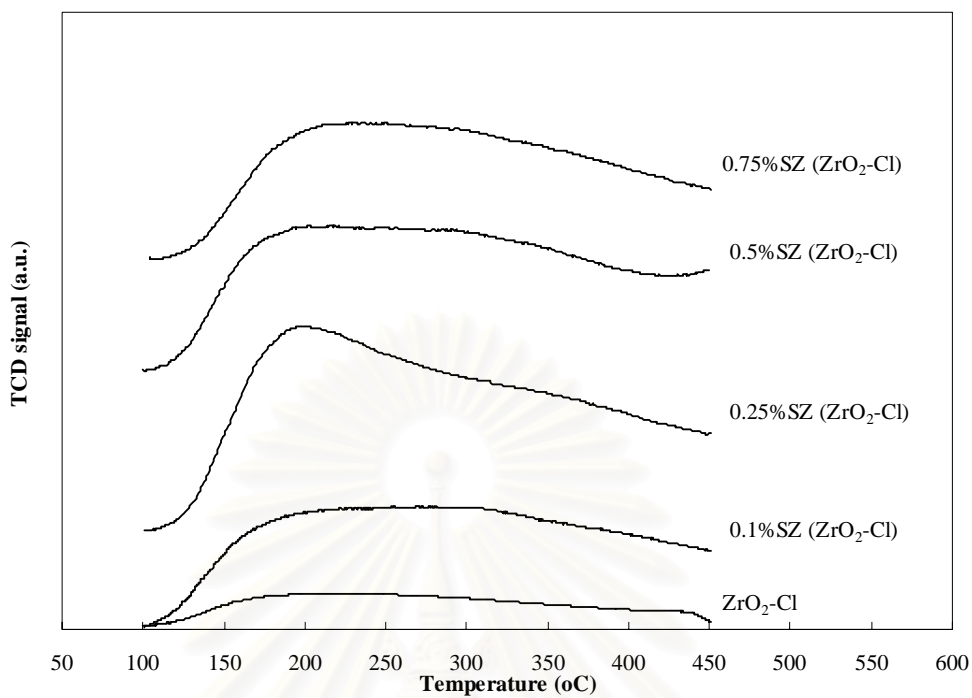


Figure 5.5 NH_3 -TPD profiles of ZrO_2 and SO_4 - ZrO_2 catalysts synthesized from $ZrOCl_2$

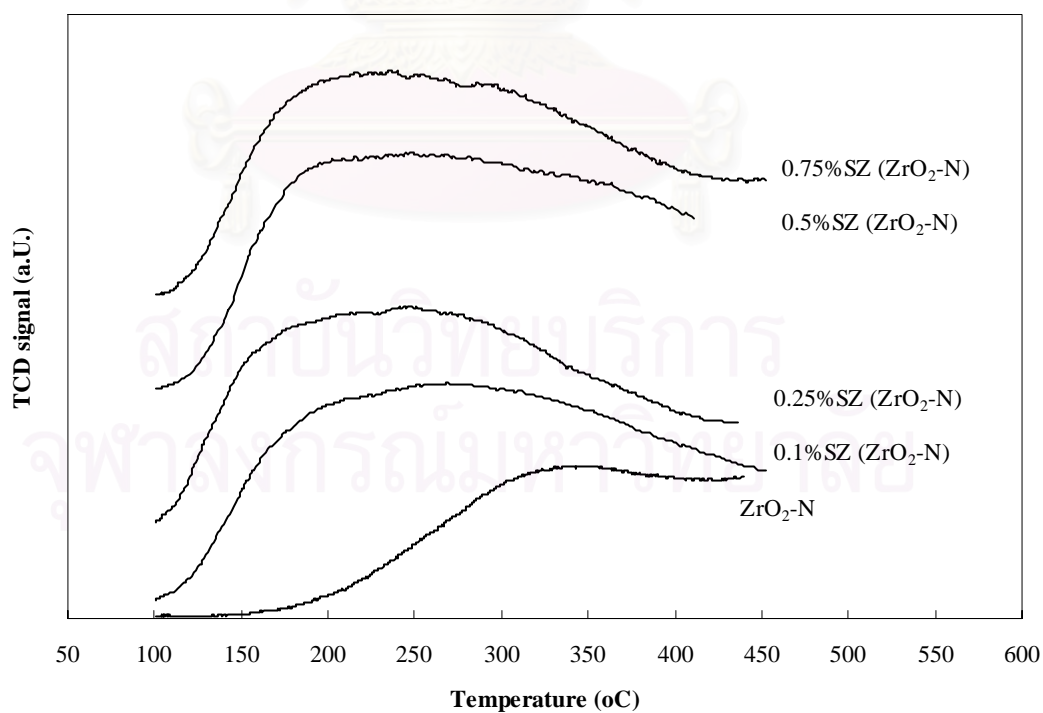


Figure 5.6 NH_3 -TPD profiles of ZrO_2 and SO_4 - ZrO_2 catalysts synthesized from $ZrO(NO_3)_2$

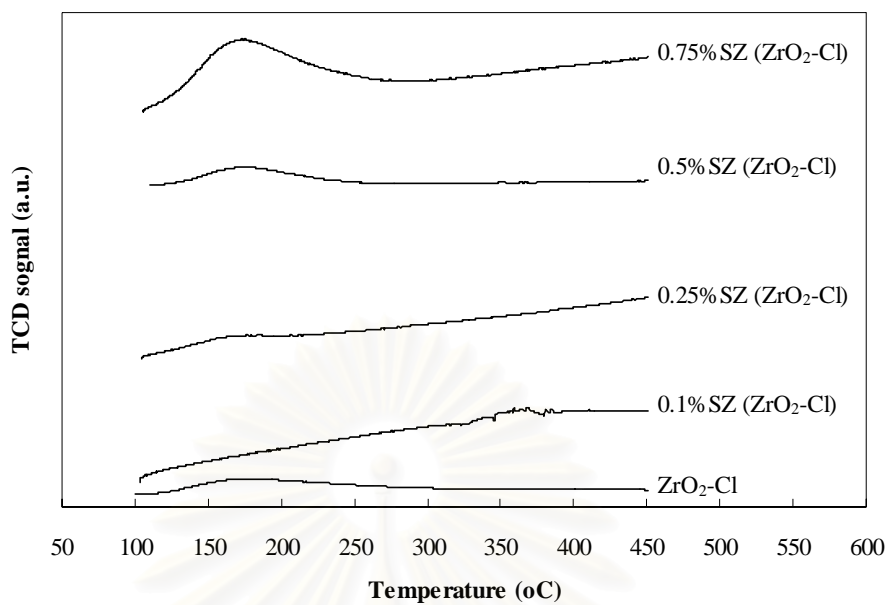


Figure 5.7 CO₂-TPD profiles of ZrO₂ and SO₄-ZrO₂ catalysts synthesized from ZrOCl₂

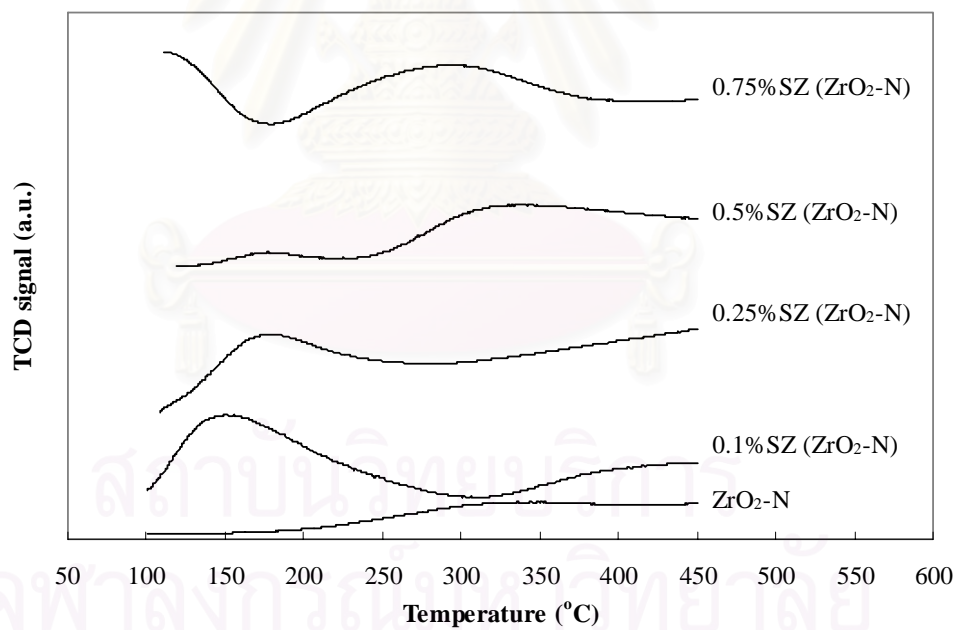


Figure 5.8 CO₂-TPD profiles of ZrO₂ and SO₄-ZrO₂ catalysts synthesized from ZrO(NO₃)₂

Table 5.3 Results from NH₃- and CO₂-TPD measurements

Catalysts	Total Sites ($\mu\text{mole/g}$)	
	Acid Sites ^a	Base Sites ^b
ZrO ₂ -N	197	257
0.1%SZ (ZrO ₂ -N)	959	76
0.25%SZ (ZrO ₂ -N)	1014	50
0.5%SZ (ZrO ₂ -N)	993	46
0.75%SZ (ZrO ₂ -N)	917	39
ZrO ₂ -Cl	594	55
0.1%SZ (ZrO ₂ -Cl)	978	25
0.25%SZ (ZrO ₂ -Cl)	1290	26
0.5%SZ (ZrO ₂ -Cl)	926	19
0.75%SZ (ZrO ₂ -Cl)	993	15

^a From NH₃-TPD.

^b From CO₂-TPD.

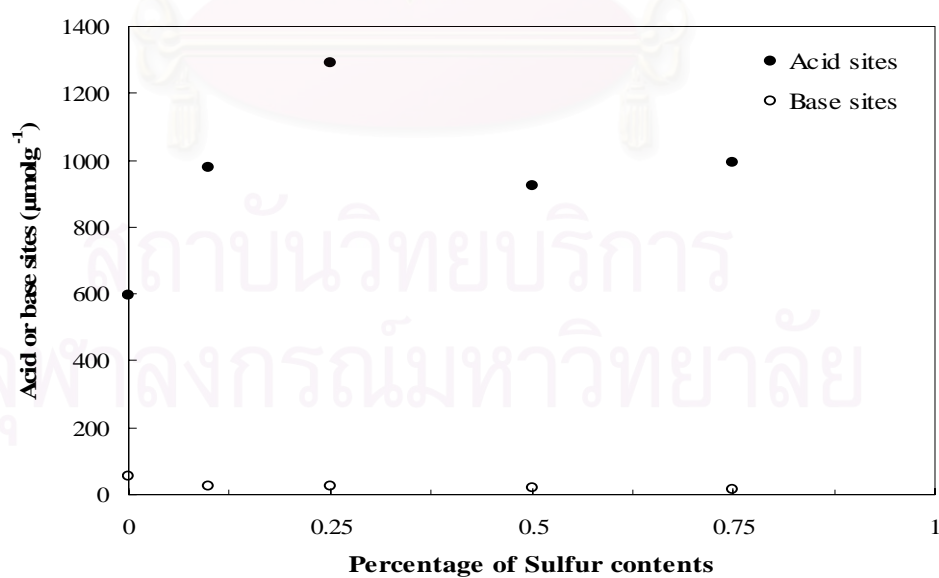


Figure 5.9 Relationship between amount of acid and base sites and percent of sulfur content in ZrO₂ and SO₄-ZrO₂ catalysts synthesized from ZrOCl₂

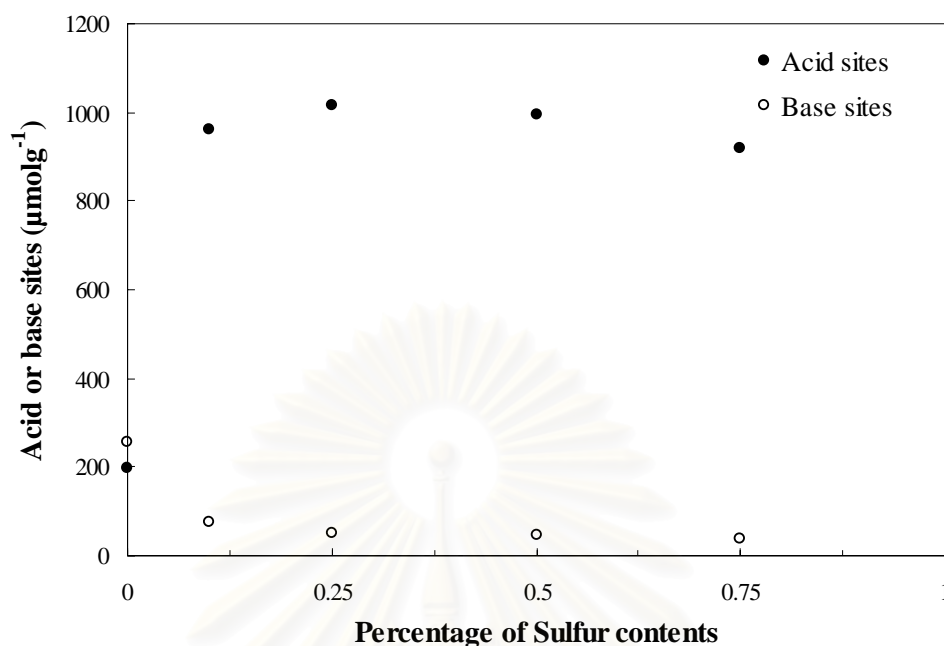


Figure 5.10 Relationship between amount of acid and base sites and percent of sulfur content in ZrO_2 and SO_4-ZrO_2 catalysts synthesized from $ZrO(NO_3)_2$

5.1.1.4 Electron Spin Resonance Spectroscopy (ESR)

A spin of unpaired electron was detected by means of ESR to identify defect center of zirconia considerably assumed as the existence of Zr^{3+} sites. Zr^{3+} signals represented at $g_{\perp} \sim 1.97$ and $g_{\parallel} \sim 1.95$ as shown the example in Figure 5.11 were very close to the positions of Zr^{3+} on ZrO_2 surface observed by many researchers as reported in Table 5.4. Only g_{\perp} was considered in this work due to the apparent signal. The relative ESR intensity at various zirconia and sulfated zirconia is shown in Figure 5.12. It was found that quantity of Zr^{3+} ascended on amount of sulfuric acid during sulfation step. The result of ESR showed that g -value from zirconia and sulfated zirconia were different. The Zr^{3+} gradually increased with increased sulfur content in incipient wetness impregnation step. For ZrO_2-Cl , having the highest intensity was deserved at 0.25% sulfur content, and then rapidly decreased beyond that value. The other zirconium salt precursor, exhibited the similar trend. The optimum point of Zr^{3+} intensity is 0.5%SZ (ZrO_2-N) after that the value decreased. From the early researches (Zhao *et al.*, 2004, Anpo and Nomura, 1990), it reasonably suggested that the Zr^{3+}

center to ESR can be described as the oxygen coordinatively unsaturated zirconium sites on ZrO_2 surface. In addition, they proposed that the removal of the surface hydroxyl accounted for the formation of the new Zr^{3+} sites. It was possibly due to the presence of hydroxyl groups combined in a position of coordinatively unsaturated sites resulting in less Zr^{3+} intensity. Therefore, changing of Zr^{3+} intensity in this case may be attributed to loss of the surface O atoms, especially hydroxyl groups, on ZrO_2 surface. The surface structure of SO_4 combined with Zr elements in the bridging bidentate state. The S=O double bond nature in the sulfate complex is much stronger than that of a simple metal sulfate, thus the Lewis acid strength of Zr^{3+} becomes remarkably greater by the inductive effect of S=O in the complex.

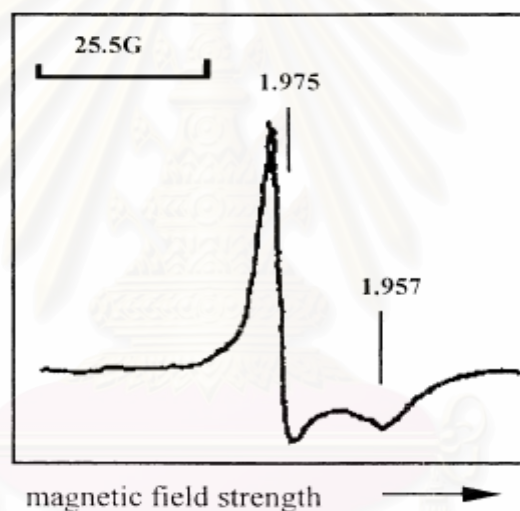


Figure 5.11 ESR spectrum of ZrO_2 (Zhao *et al.*, 2004)

Table 5.4 ESR parameters of Zr^{3+} observed from different references

Paramagnetic ion	g-value	Reference
Zr^{3+} in ZrO_2	$g_{\parallel} = 1.956$	Torralvo and Alario, 1984
	$g_{\perp} = 1.981$	
Zr^{3+} in ZrO_2	$g_{\parallel} = 1.953$	Moterra <i>et al.</i> , 1990
	$g_{\perp} = 1.978$	
Zr^{3+} in sulfated zirconia	$g_{\parallel} = 1.951$	Chen <i>et al.</i> , 1993
	$g_{\perp} = 1.979$	
Zr^{3+} in ZrO_2	$g_{\parallel} = 1.961$	Liu <i>et al.</i> , 1995
	$g_{\perp} = 1.974$	
Zr^{3+} in V_2O_5/ZrO_2	$g_{\perp} = 1.97$	Adamski <i>et al.</i> , 1999
Zr^{3+} in sulfated zirconia	$g_{\parallel} = 1.967$	Carlos <i>et al.</i> , 1999
	$g_{\perp} = 1.982$	
Zr^{3+} in $Pt/WO_x/ZrO_2$	$g_{\parallel} = 1.96$	Punnoose and Seehra, 2002
	$g_{\perp} = 1.98$	
Zr^{3+} in ZrO_2	$g_{\parallel} = 1.957$	Zhao <i>et al.</i> , 2004
	$g_{\perp} = 1.975$	

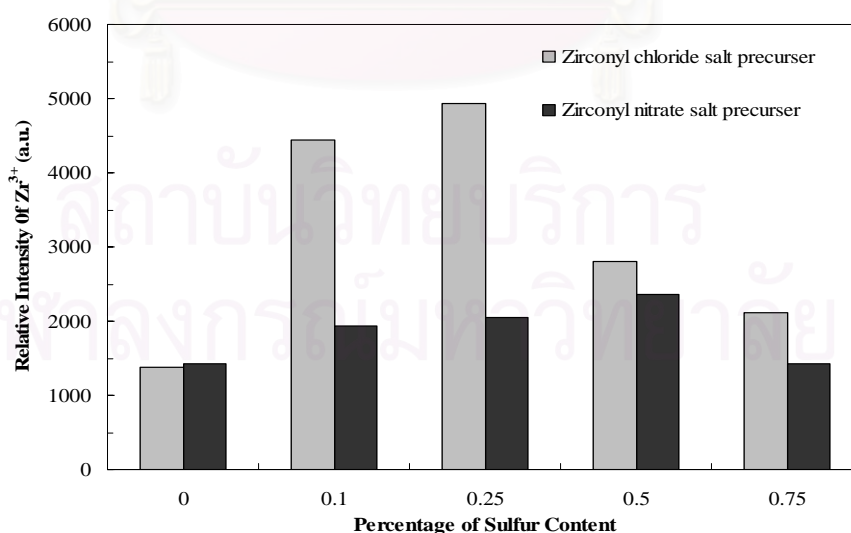


Figure 5.12 Relative ESR intensity of various ZrO_2 catalysts

5.1.1.5 Scanning Electron Microscopy (SEM)

SEM is used to study the morphologies of catalysts. Figures 5.13-5.14, showed characteristic of catalysts that synthesized from zirconyl chloride. It observed that fine particles, nanocrystallize catalysts. The particle size of other catalysts, ZrO_2-N and 0.75% SZ (ZrO_2-N) was bigger than previous ones.

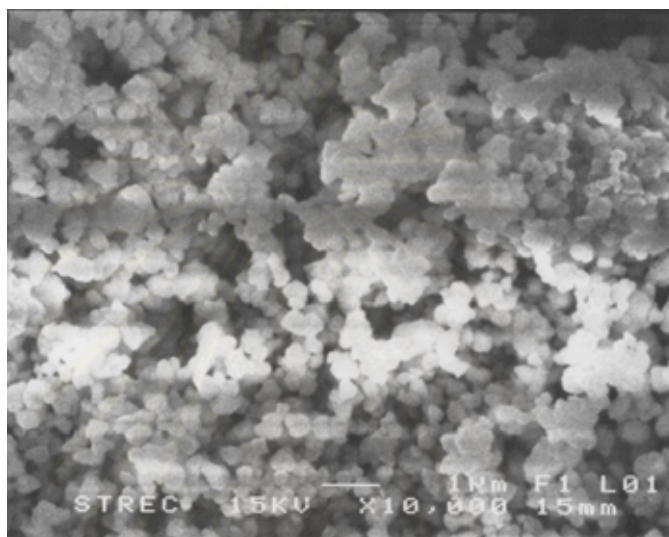


Figure 5.13 SEM micrograph of ZrO_2-Cl

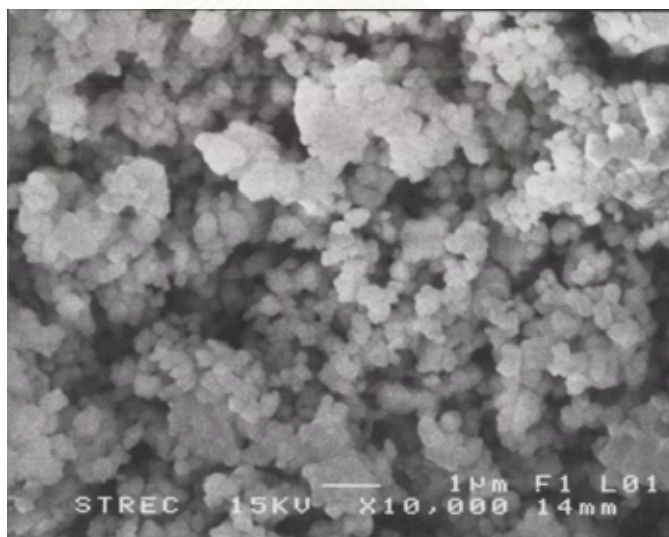


Figure 5.14 SEM micrograph of 0.75% SZ (ZrO_2-Cl)

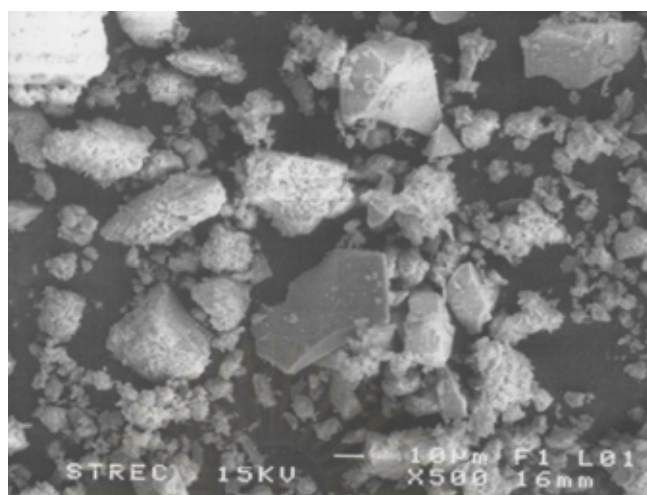


Figure 5.15 SEM micrograph of ZrO_2-N

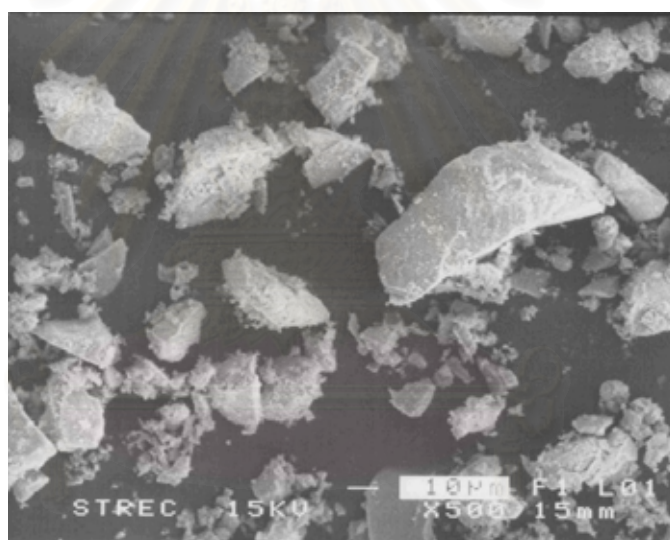


Figure 5.16 SEM micrograph of 0.75% SZ (ZrO_2-N)

5.1.2 Catalytic Performance of Isosynthesis over Zirconia and Sulfated Zirconia Catalysts

The ZrO_2 and SO_4-ZrO_2 catalysts were tested for their isosynthesis activity and selectivity at $400^\circ C$, atmospheric pressure and CO/H_2 of 1. A previous study showed that the steady-state rate was reached after 20 h. Table 5.5 show that catalytic activity from CO hydrogenation. In addition, the product selectivity was listed in

Table 5.6. It was found that catalytic activities of zirconia and sulfated zirconia synthesized by ZrO_2Cl were higher than the other catalysts, whereas the selectivity of isobutene in hydrocarbons was lower. The catalytic activity of zirconia and sulfated zirconia from zirconyl nitrate were influenced by the fraction of monoclinic phase, but catalysts synthesized by zirconyl chloride were governed by the relative intensity of Zr^{3+} . The reaction rate and percentage of tetragonal phase had the similar trend according to the base/acid sites. Moreover, amount of sulfuric acid loaded on surface area of catalysts rendered higher selectivity of isobutene. It can be described that sulfur content affects the physical properties of catalysts, base/acid site, specific surface area and tetragonal phase. The tetragonal phase rendered not only increased catalytic activities of catalysts, but also the product selectivity depending on base and acid site, which were proportional to sulfur content as shown in Figures 5.17 and 5.18.

Table 5.5 Catalytic activity results from isosynthesis

Catalysts	CO conversion (%)	Reaction rate ($\mu\text{mol kg cat}^{-1} \text{ s}^{-1}$)
ZrO_2-N	3.16	106.0
0.1%SZ (ZrO_2-N)	3.49	117.0
0.25%SZ (ZrO_2-N)	2.65	88.8
0.5%SZ (ZrO_2-N)	2.72	91.1
0.75%SZ (ZrO_2-N)	2.70	90.5
ZrO_2-Cl	2.53	84.9
0.1%SZ (ZrO_2-Cl)	3.97	133.1
0.25%SZ (ZrO_2-Cl)	3.51	117.7
0.5%SZ (ZrO_2-Cl)	3.63	121.7
0.75%SZ (ZrO_2-Cl)	3.85	129.2

Table 5.6 Product selectivity results from isosynthesis

Catalysts	Product selectivity in hydrocarbons ^a (mol%)			
	C ₁	C ₂	C ₃	<i>i</i> -C ₄ H ₈
ZrO ₂ -N	11.0	5.5 (95.6)	10.1 (96.8)	73.4
0.1%SZ (ZrO ₂ -N)	1.1	0.5 (77.3)	8.0 (99.6)	90.4
0.25%SZ (ZrO ₂ -N)	0.7	0.7 (85.7)	8.2 (99.5)	90.4
0.5%SZ (ZrO ₂ -N)	0.3	0.4 (82.7)	8.1 (99.6)	91.1
0.75%SZ (ZrO ₂ -N)	0.7	0.5 (78.5)	8.1 (99.5)	90.6
ZrO ₂ -Cl	5.5	3.9 (75.3)	8.6 (95.9)	82.0
0.1%SZ (ZrO ₂ -Cl)	0.4	0.5 (89.1)	8.1 (99.7)	91.0
0.25%SZ (ZrO ₂ -Cl)	1.5	0.8 (85.1)	8.2 (99.5)	89.5
0.5%SZ (ZrO ₂ -Cl)	0.8	0.6 (81.2)	8.2 (99.5)	90.3
0.75%SZ (ZrO ₂ -Cl)	1.6	0.9 (75.7)	8.2 (99.2)	89.3

^a Parentheses are the selectivity of olefin.

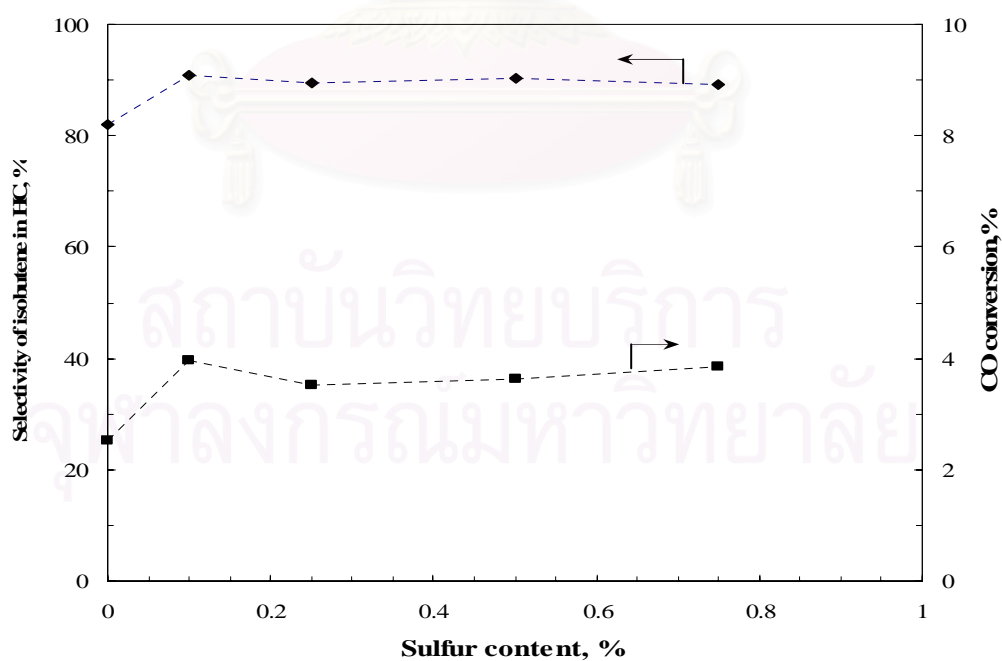


Figure 5.17 Relationship between CO conversion and selectivity of isobutene with sulfur content in SO₄/ZrO₂-Cl

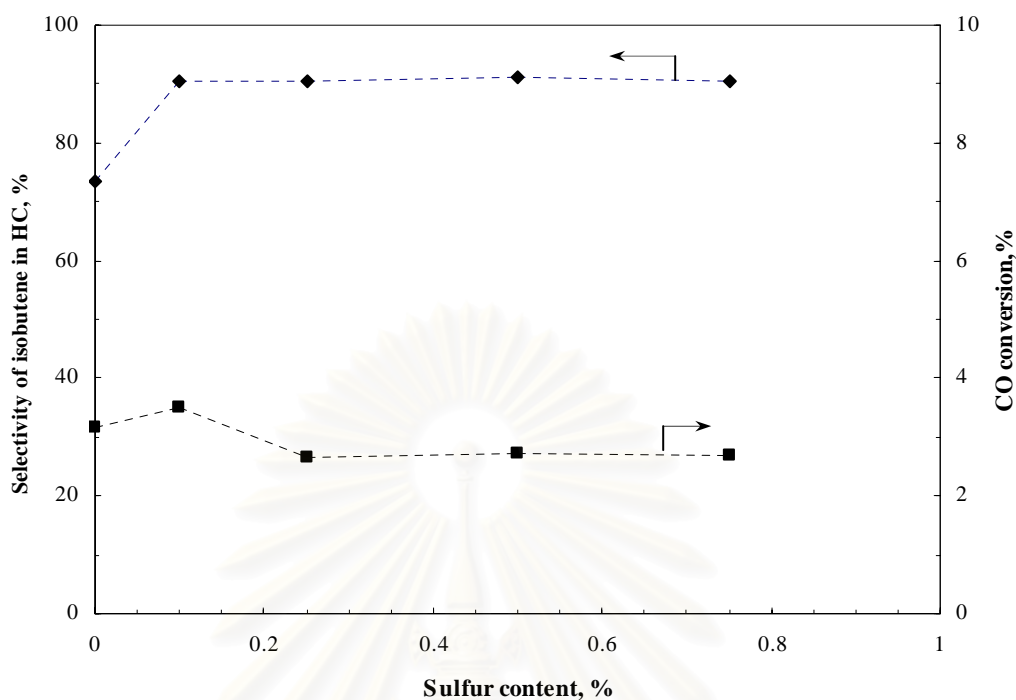


Figure 5.18 Relationship between CO conversion and selectivity of isobutene with sulfur content in $\text{SO}_4/\text{ZrO}_2\text{-N}$

5.2 The Effect of Temperature during Calcinations on Characteristics of Sulfated Zirconia and Their Application as a Catalyst for Isosynthesis.

To study the effect of temperature during calcinations step, 0.75% $\text{SO}_4/\text{ZrO}_2\text{-N}$ from Section 5.1 and commercial sulfated zirconia were used to study by varying the calcinations temperature at 450, 600 and 750 °C. The catalysts were denoted by 0.75%SZ (N-450), 0.75%SZ (N-600), 0.75%SZ (N-750), SZ (450), SZ (600) and SZ (750), respectively.

5.2.1 Catalyst Characterization

5.2.1.1 X-ray Diffraction (XRD)

The varied temperatures during calcination resulted in changes in both crystallite size and crystal phase. The XRD spectra of those sulfated zirconia catalysts

are illustrated in Figures 5.19 and 5.20. Table 5.7 indicated that the crystal size in monoclinic phase was increased with increased temperature during calcinations step. Considering the characteristic peak areas of monoclinic and tetragonal phases (Figure 5.20), it was observed that the former was more dominant than the latter upon increase in temperature during calcination. In addition, the phase composition of each 0.75% $\text{SO}_4/\text{ZrO}_2\text{-N}$ catalyst can be calculated as shown in Table 5.7. The results showed that the fraction of monoclinic phase increased with increased temperature. Moreover, calcination temperature affected the commercial SZ as shown in Figure 5.20. The XRD patterns of catalyst exhibited tetragonal-monoclinic phase transformation. The tetragonal phase decreased with increased calcinations temperature. Most published studies agree that sulfation retards crystallization of zirconia support and then the transition from the tetragonal to the monoclinic form (Fărcașiu *et al.*, 1997) occurs. According to monoclinic-tetragonal phase transformation of zirconia, the tetragonal phase should be formed above 1170°C , but the zirconia prepared by precipitation from aqueous salt solution can be occurred as a metastable tetragonal phase at lower temperature. Moreover, the transformation of the metastable tetragonal form into the monoclinic form was probably due to the lower surface energy of the tetragonal phase compared to monoclinic phase (Tani, *et al.*, 1982, Osendi *et al.*, 1985). In fact, phase transformation of catalyst can be occurred by varying the calcination temperature. In this case, lower calcination temperature would correlate with the alteration of crystal structure and sulfated migration into the bulk phase of the solid (Fărcașiu *et al.*, 1997). Moreover, calcination serves to bind the sulfated groups to the surface (Vera *et al.*, 1997).

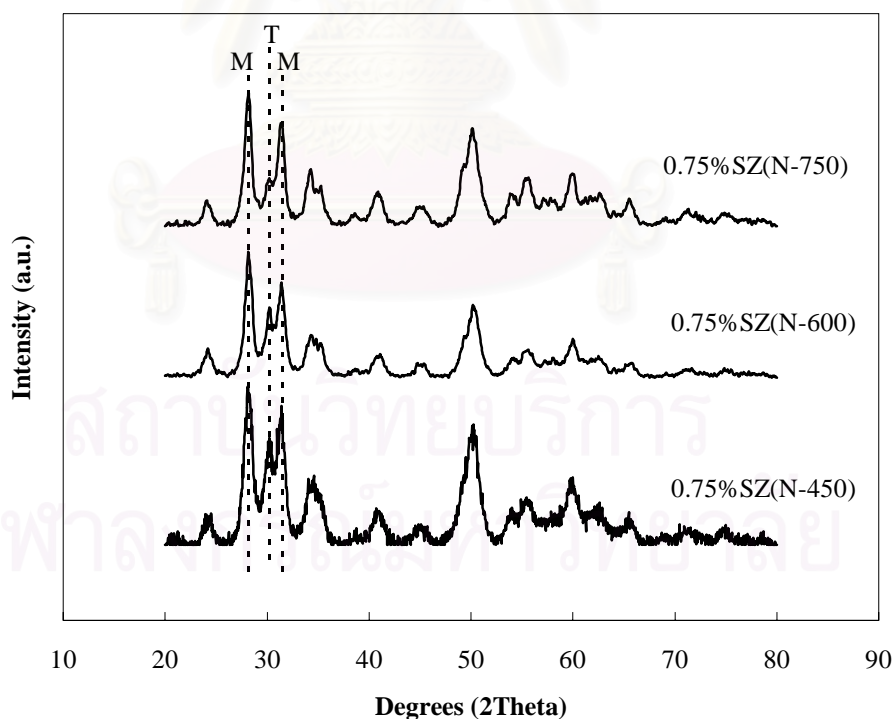
Table 5.7 Characteristics of ZrO₂ with various calcination temperatures

Catalysts	Phase	Crystal Size (nm) ^a		% tetragonal phase ^a
		M ^b	T ^c	
0.75%SZ(N-450)	M, T	9.1	8.1	28.9
0.75%SZ(N-600)	M, T	9.7	8.1	27.5
0.75%SZ(N-750)	M, T	11.0	6.5	25.6
SZ(450)	T	n.d.	7.1	100.0
SZ(600)	M, T	5.4	8.5	78.3
SZ(750)	M, T	19.5	10.7	11.3

^a Based on XRD line broadening.

^b Monoclinic phase in ZrO₂.

^c Tetragonal phase in ZrO₂.

**Figure 5.19** XRD patterns of 0.75%SZ (N) various calcination temperatures

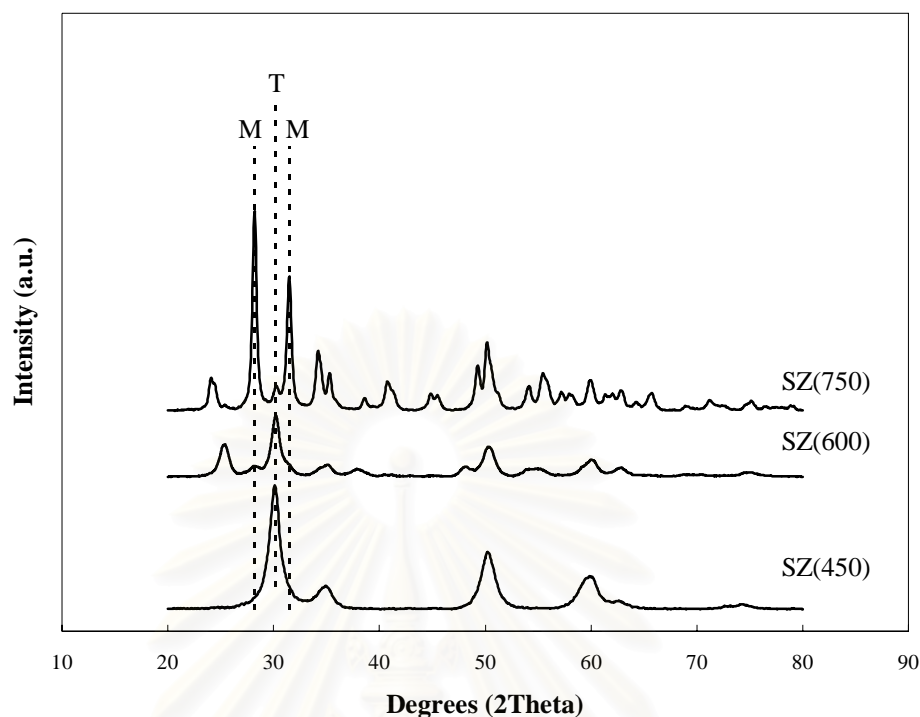


Figure 5.20 XRD patterns of SO_4/ZrO_2 commercial various calcination temperature

5.2.1.2 N_2 Physisorption

Figure 5.21 shows that the specific surface area of sulfated zirconia immediately decreases with the increased calcination temperature. The decrease in surface area with temperature is almost linear. The physical properties of ZrO_2 catalysts characterized by means of N_2 physisorption such as BET surface area, cumulative pore volume and average pore diameter are summarized in Table 5.8. The surface area calculated from adsorption isotherm using BET equation was in the range of 29.4–232.2 m^2/g . These sulfated zirconia catalysts calcined at the lowest temperature exhibited higher specific surface areas than the other ones. Furthermore, average pore diameter was dramatically increased with increased calcination temperature. Considering, pore size distribution of catalysts as shown in Figure 5.22, these peaks of 0.75% $\text{SO}_4/\text{ZrO}_2\text{-N}$ were shifted to higher pore diameter whereas the SZ commercial peaks were decreased. However, these catalysts showed the similar distribution curve. Therefore, it can be concluded that the temperature during calcination significantly affected these physical properties.

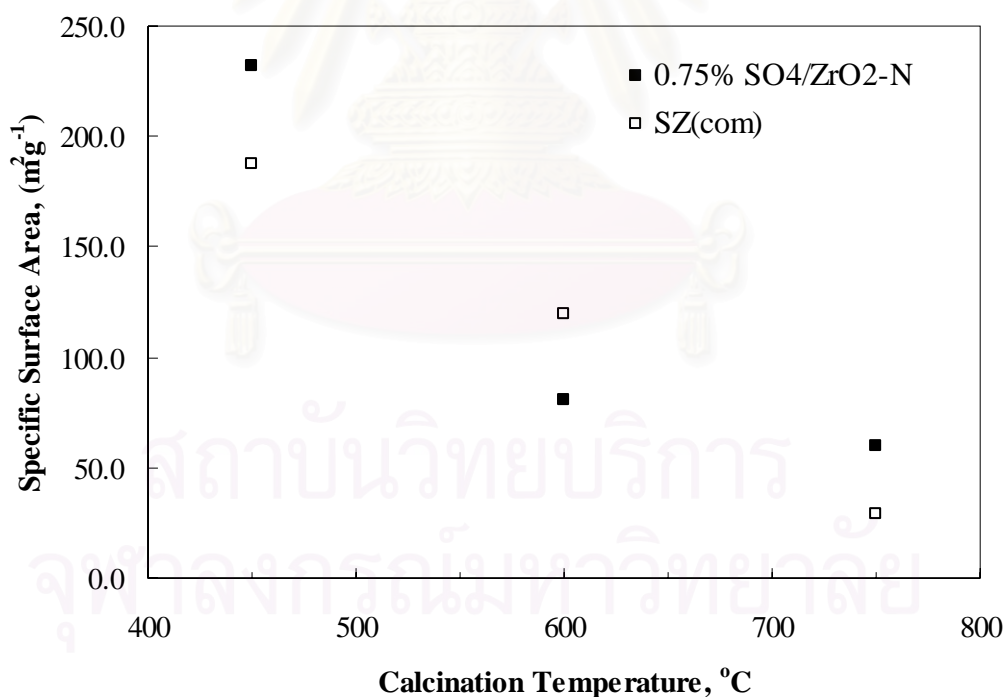
Table 5.8 N₂ Physisorption results

Catalysts	BET Surface Area ^a (m ² /g)	Cumulative Pore Volume ^b (cm ³ /g)	Average Pore Diameter ^c (nm)
0.75%SZ(N-450)	232.2	0.351	4.8
0.75%SZ(N-600)	80.5	0.171	5.1
0.75%SZ(N-750)	60.0	0.157	6.3
SZ(450)	187.1	0.172	3.1
SZ(600)	119.3	0.180	3.7
SZ(750)	29.4	0.067	7.0

^a Error of measurement = $\pm 5\%$.

^b BJH desorption cumulative volume of pores between 1.7 and 300 nm diameter.

^c BJH desorption average pore diameter.

**Figure 5.21** Surface areas of the catalysts as a function of calcination temperature

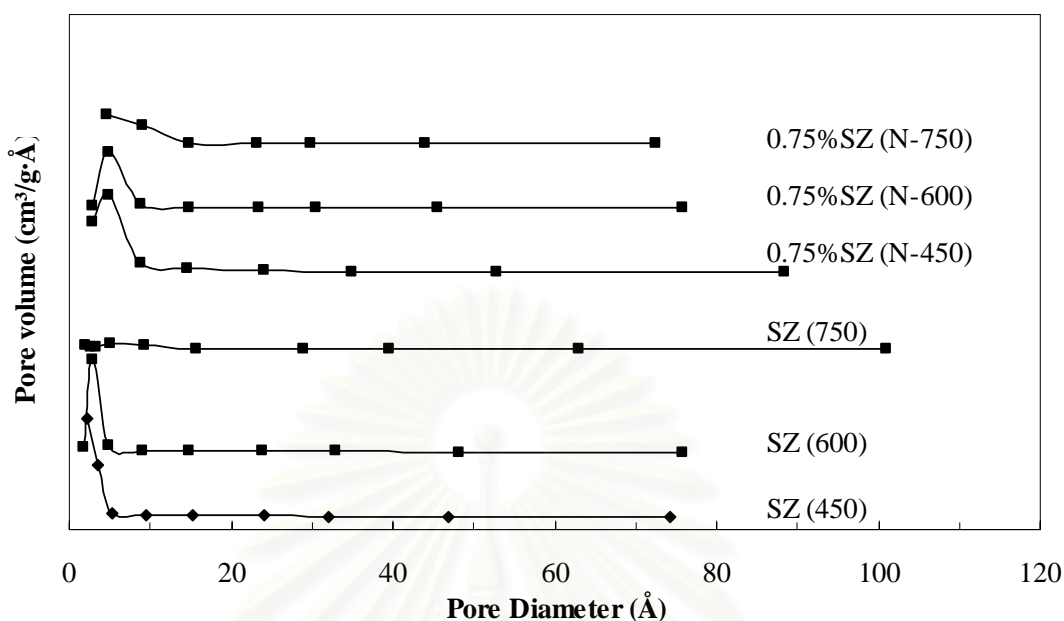


Figure 5.22 Pore size distribution of sulfated zirconia catalysts

5.2.1.3 Temperature Programmed Desorption (TPD)

NH_3 -TPD profiles of 0.75% $\text{SO}_4/\text{ZrO}_2\text{-N}$ and sulfated zirconia catalysts are illustrated in Figures 5.23 and 5.24, respectively. As seen in Figure 5.23, a calcination temperature rise apparently affects the properties of catalysts. Acid and base sites were calculated by based on the characteristic of sulfated zirconia. It indicated that the presence of weak and moderate acid sites related to the characteristic peaks of desorption temperature. With increased calcination temperature, the profiles did not change, but the amount of acid sites decreased. The amounts of acid sites of sulfated zirconia catalysts are listed in Table 5.9. The other studies showed that the amount of sulfated retained decreased with the increase calcination temperature as shown in Figure 5.25. Because the sulfated group on sulfated zirconia was labile sulfates, which can be reduced by washing with water, calcinations temperature and duration during calcination step. As a mentioned by Hino *et al* (2005), the structural model of sulfate species contained mainly three or four S atoms with two ionic bonds of S-O-Zr in addition to coordination bonds of S=O. The results showed that the acidity of sulfated zirconia commercial catalyst was higher than another one. The acid sites at lower

calcination temperature of catalysts were higher than other catalysts because sulfated groups were still remained on surface of catalysts.

The CO_2 -TPD profiles for the $0.75\%\text{SO}_4/\text{ZrO}_2\text{-N}$ catalysts are shown in Figure 5.24. Considering, the profiles of the $0.75\%\text{SO}_4/\text{ZrO}_2\text{-N}$ catalysts, they changed the patterns indicating higher amount of moderate base sites along with the disappearance of weak base sites. Sulfated zirconia commercial was super strong acid catalyst. Figure 5.25 indicated that base sites increased with increased calcination temperature but acid sites were decreased. Li *et al.* (2006) showed that the monoclinic phase is able to retain more sulfur than tetragonal phase, suggesting that the monoclinic form may be basic than the tetragonal as shown in Figure 5.26.

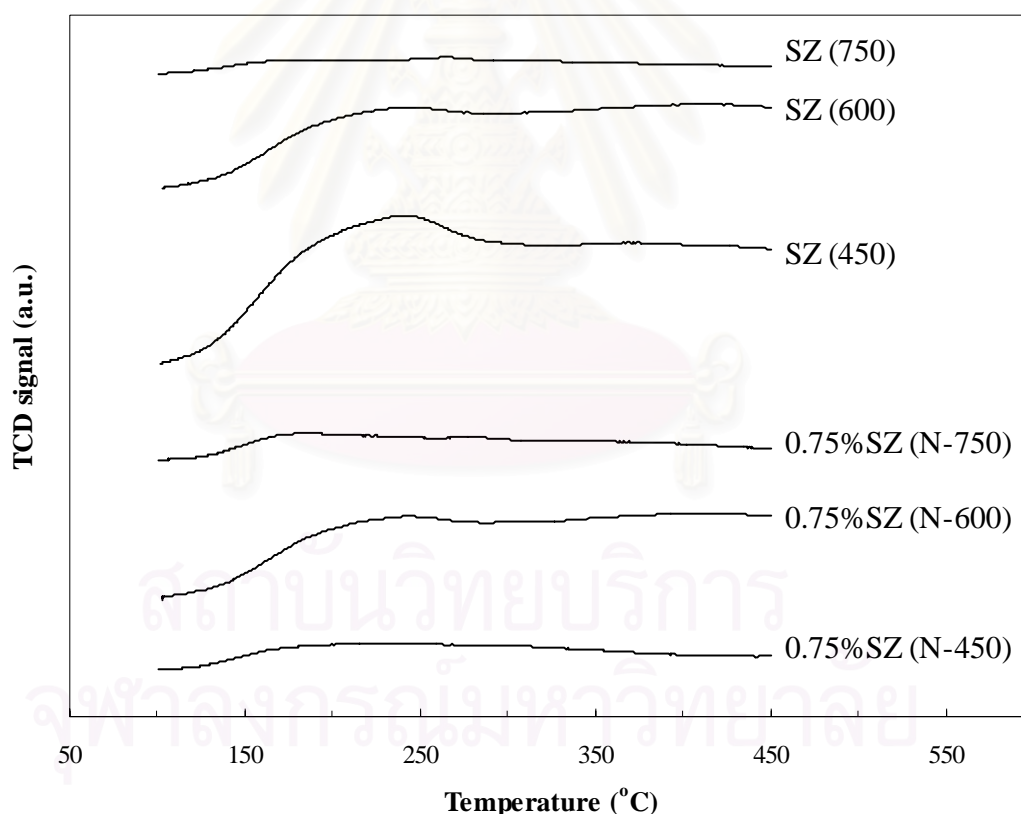


Figure 5.23 NH_3 -TPD profiles of $\text{SO}_4\text{-ZrO}_2$ catalysts

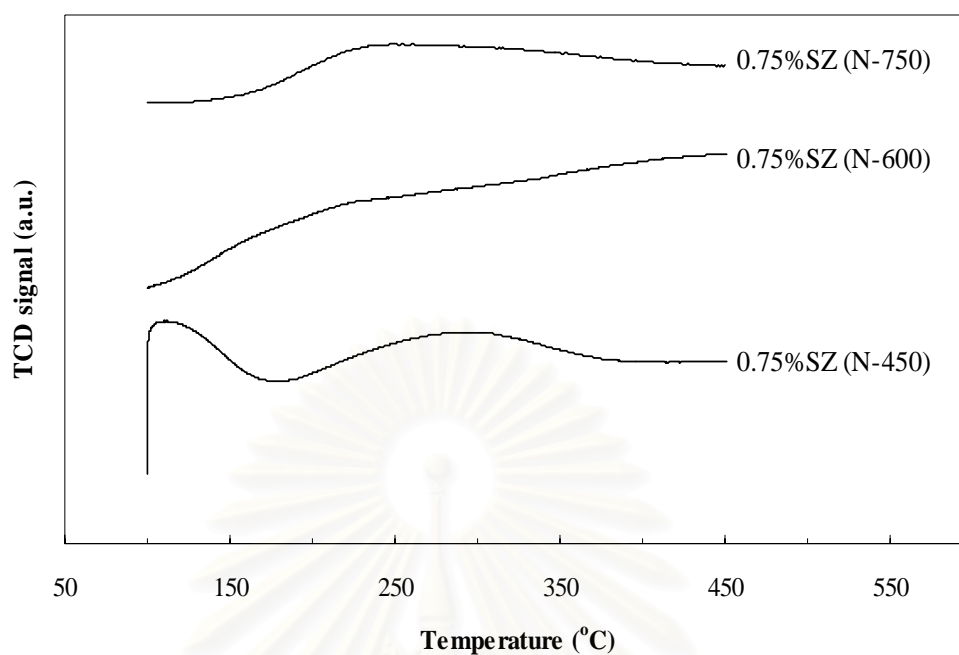


Figure 5.24 CO₂-TPD profiles of SO₄-ZrO₂ catalysts

Table 5.9 Results from NH₃- and CO₂-TPD

Catalysts	Total Sites (μmole/g)	
	Acid Sites ^a	Base Sites ^b
0.75%SZ(N-450)	917	39
0.75%SZ(N-600)	712	46
0.75%SZ(N-750)	432	53
SZ(450)	1881	n.d.
SZ(600)	1032	n.d.
SZ(750)	58	n.d.

^a From NH₃-TPD.

^b From CO₂-TPD.

n.d., not determined.

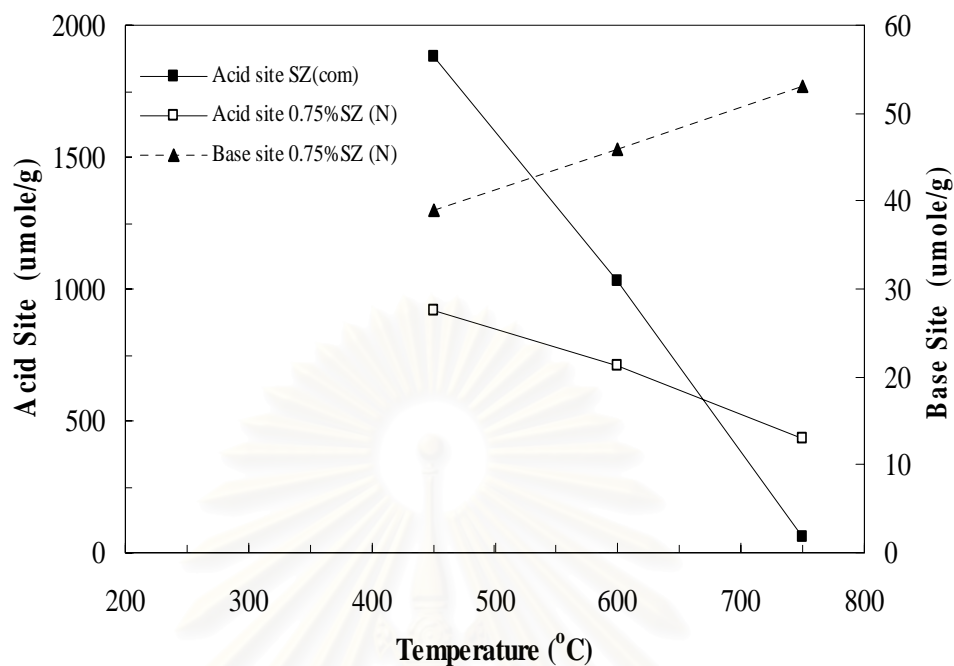


Figure 5.25 Relationship between calcinations temperature and acid and base sites in sulfated zirconia

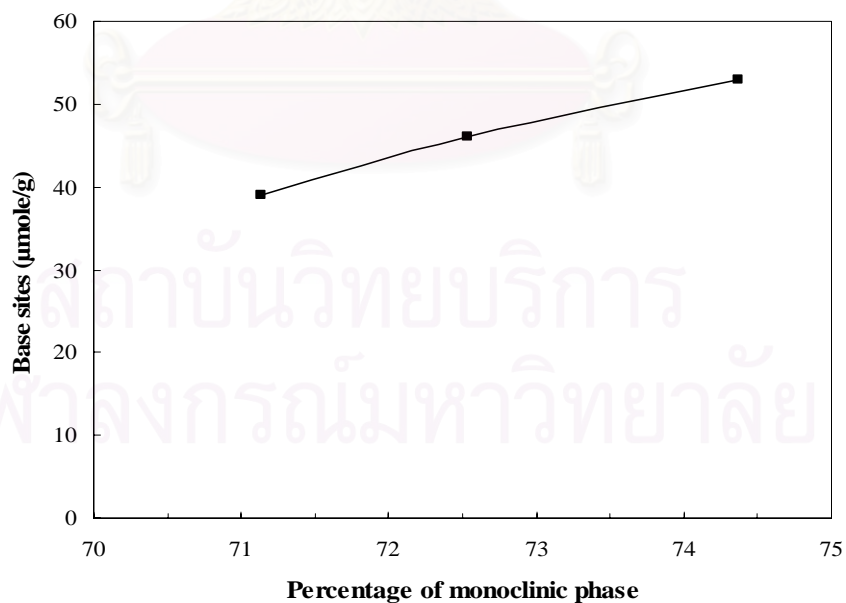


Figure 5.26 Relationship between percentage of monoclinic phase and base sites on 0.75% SZ (ZrO_2-N)

5.2.1.4 Electron Spin Resonance Spectroscopy (ESR)

Figure 5.27 showed the relative ESR intensity at various calcination temperatures of sulfated zirconia. It was found that increased calcination temperatures resulted in the increased intensity of Zr^{3+} was increased. Considering commercial sulfated zirconia and 0.75% SZ (ZrO_2-N), it indicated that the 0.75% SZ (ZrO_2-N) samples with various calcination temperatures have higher intensity of Zr^{3+} than that of the commercial one.

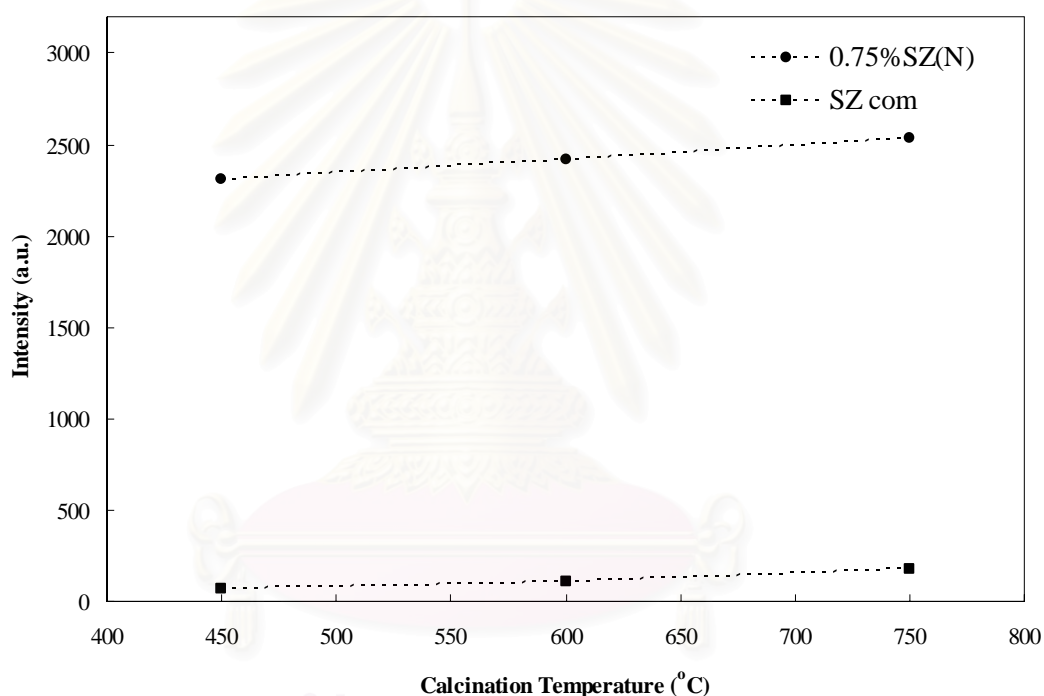


Figure 5.27 Relative ESR intensity of various calcination temperatures in sulfated zirconia catalysts

5.2.1.5 X-ray Photoelectron Spectroscopy (XPS)

The XPS results showed the possibility of bearing high acidity on the surface of SO_4-ZrO_2 . The spectra of S $2p$ and Zr $3d$ for SO_4-ZrO_2 that binding energies were 154.480 and 186.700, respectively.

Table 5.10 Results from XPS

Catalysts	Atomic conc%			
	O 1 _s	C 1 _s	Zr 3 _d	S 2 _p
0.75%SZ(N-450)	52.27	22.26	25.05	0.42
0.75%SZ(N-600)	49.95	26.31	23.35	0.21
0.75%SZ(N-750)	51.19	25.57	23.07	0.17
SZ(450)	49.65	34.15	15.77	0.43
SZ(600)	44.72	41.09	13.89	0.29
SZ(750)	38.85	48.62	12.65	0.15

5.2.2 Catalytic Performance of Isosynthesis over Sulfated Zirconia Catalysts

Tables 5.11 and 5.12 show the rate and selectivity of the isosynthesis for SO₄-ZrO₂ operated at 400 °C, atmospheric pressure and CO/H₂ of 1. It was found that commercial sulfated zirconia catalysts exhibited higher reaction rates than the synthesized ones. For commercial sulfated zirconia, reaction rate increased with increased calcination temperatures. However, for the 0.75% SZ (ZrO₂-N), firstly it increased when calcination temperature rose after at a certain point, and then suddenly decreased. Moreover, CO conversion of both types of sulfated zirconia catalysts had the similar trend as seen for the reaction rates. The relation between TOS and reaction rate is showed in Figure 5.28. Considering the 0.75% SZ (ZrO₂-N) samples calcined at different temperatures, the patterns of reaction rate the curves similar trend. Moreover, not only reaction rates of the commercial sulfated zirconia exhibited the increased with increased TOS while slowly decreased with TOS after that, but also it increased when calcination temperature increased.

Furthermore, the variation of selectivity of isobutene with calcination temperatures was also considered as shown in Figures 5.29 and 5.30. The results from 0.75% SZ (ZrO₂-N) selectivity of isobutene receded with increased calcination temperature. This was due to the effect of active sites. However, the selectivity of

isobutene on commercial sulfated zirconia catalysts rose when calcination temperature increased. The 0.75% SZ (ZrO_2) samples after calcined at 450 °C was highest isobutene selectivity (90.6 mol%), but the commercial sulfated zirconia calcined at 450 °C showed the highest CO conversion and reaction rate (43.39 % and 1454.3 $\mu\text{mol kg cat}^{-1}\text{s}^{-1}$, respectively). Figures 5.29 and 5.30 show the isobutene selectivity and CO conversion of commercial sulfated zirconia having being indirectly proportional. The results of 0.75% SZ ($\text{ZrO}_2\text{-N}$) for both isobutene selectivity and CO conversion firstly increased and then decreased with the increase in calcination temperature from 450 °C to 750 °C at constant time (3 h) and ramp rate (5.0).

The fact that catalytic activities depend strongly on the calcination temperature suggested that the temperature during calcinations had effect on the crystalline structure and acid and base sites. The concentration of the sulfated groups was a function of percentages of monoclinic phase because monoclinic form may be basic than the tetragonal (Li *et al.*, 2006). The trend is also seen in the acid sites of sulfated zirconia at various calcination temperatures. The uptake of acid sites increased with increasing concentration of monoclinic phase (Figure 5.31). A previous study suggests that stronger basic sites allow binding sulfated group more effectively on monoclinic zirconia than on tetragonal zirconia. Now turn our attention to the role of calcination temperature that affects to specific surface areas. Increasing in calcination temperature led to smaller surface area. In line with this reason, the catalytic activity, isobutene selectivity and the fraction of tetragonal phase of commercial sulfated zirconia were directly proportional. But for 0.75% SZ ($\text{ZrO}_2\text{-N}$) samples, both isobutene selectivity and CO conversion were directly proportional.

จุฬาลงกรณ์มหาวิทยาลัย

Table 5.11 The catalytic activity results from isosynthesis

Catalysts	CO conversion (%)	Reaction rate ($\mu\text{mol kg cat}^{-1} \text{ s}^{-1}$)
0.75%SZ(N-450)	2.70	90.5
0.75%SZ(N-600)	3.60	120.7
0.75%SZ(N-750)	2.67	89.5
SZ(450)	43.39	1454.3
SZ(600)	9.24	309.9
SZ(750)	4.76	159.6

Table 5.12 Product selectivity results from isosynthesis

Catalysts	Product selectivity in hydrocarbons ^a (mol%)			
	C ₁	C ₂	C ₃	<i>i</i> -C ₄ H ₈
0.75%SZ(N-450)	0.7	0.5 (78.5)	8.1 (99.5)	90.6
0.75%SZ(N-600)	1.11	0.8 (81.1)	8.0 (99.4)	90.1
0.75%SZ(N-750)	4.21	3.2 (88.1)	9.7 (98.2)	82.9
SZ(450)	77.32	19.3 (57.9)	3.3 (0.0)	0
SZ(600)	17.87	7.9 (80.9)	12.1 (94.5)	62.1
SZ(750)	1.69	2.3 (94.0)	9.3 (99.29)	86.7

^a Parentheses are the selectivity of olefin.

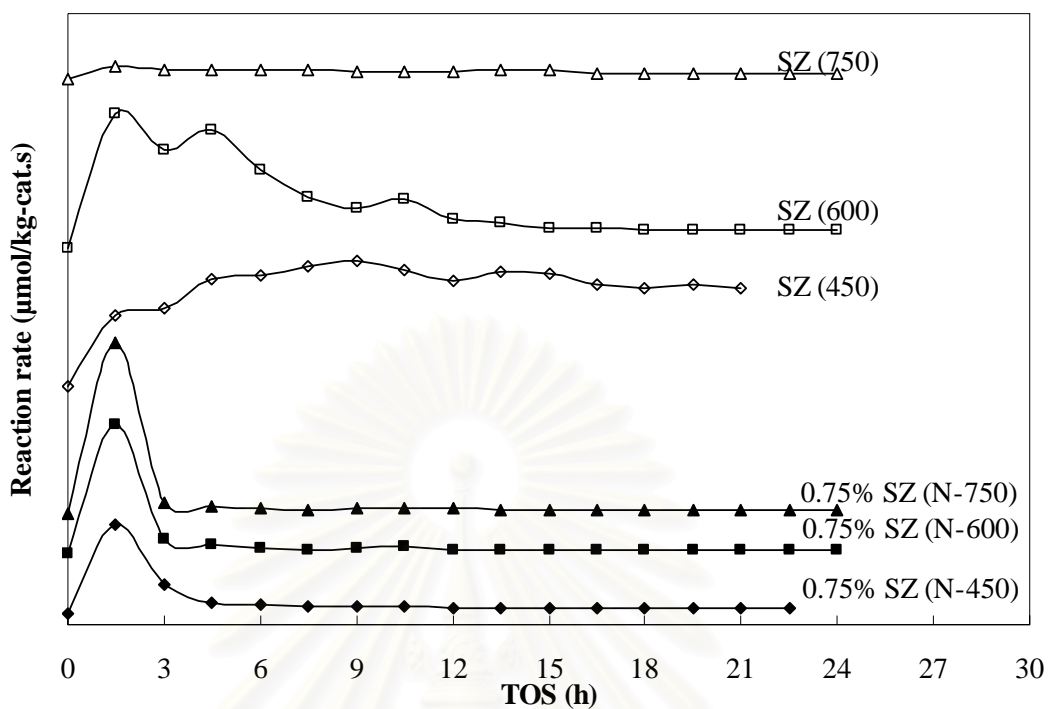


Figure 5.28 Relationship between reaction rate and time on stream

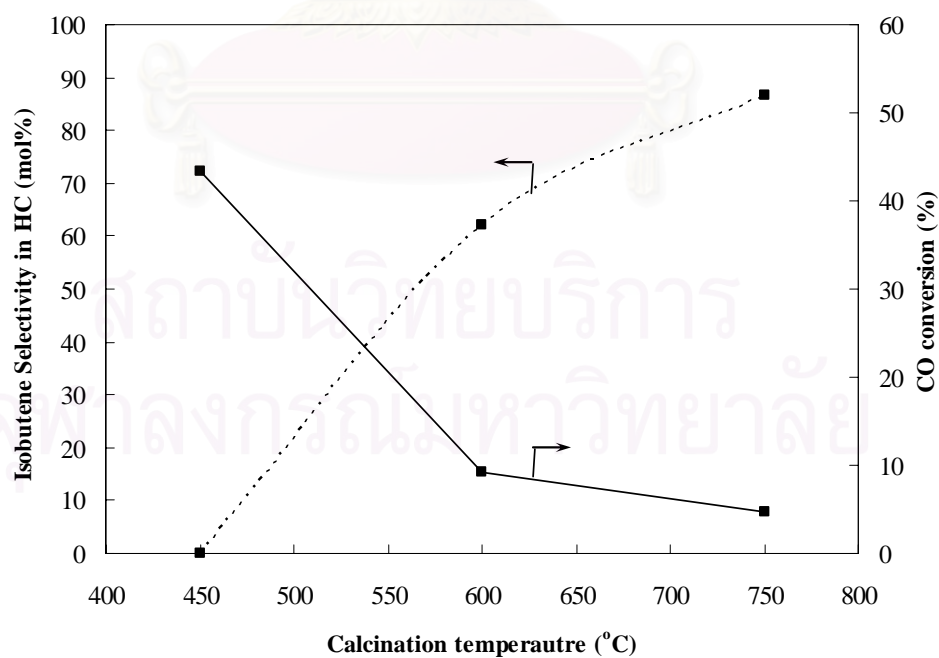


Figure 5.29 Relationship between CO conversion and selectivity of isobutene for commercial sulfated zirconia at various calcination temperatures

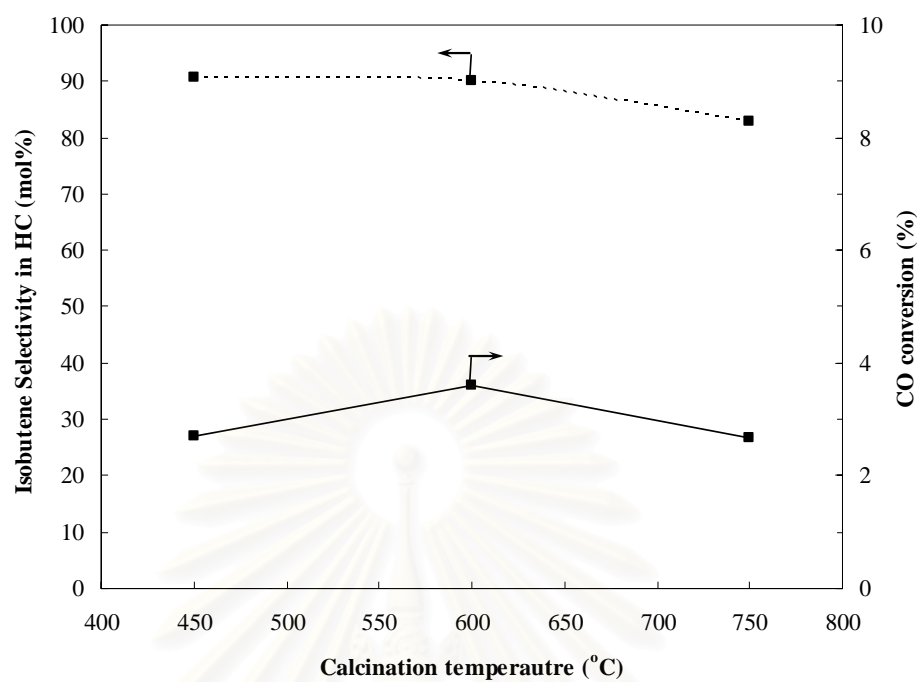


Figure 5.30 Relationship between CO conversion and selectivity of isobutene for 0.75% SZ (ZrO_2-N) at various calcinations temperatures

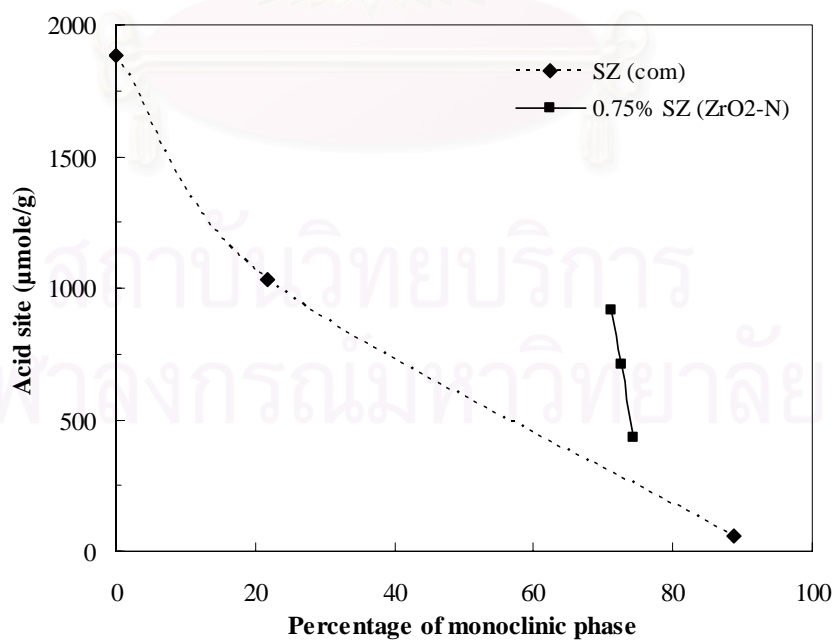


Figure 5.31 Relationship between percentage of monoclinic phase and acid sites

CHAPTER VI

CONCLUSIONS AND RECOMMENDATION

6.1 Conclusions

The conclusions of the present research are as follows:

1. The sulfated zirconia exhibited better catalytic activity and selectivity of isobutene in hydrocarbons than zirconia. The sulfur loading, acid-base properties the fraction of monoclinic phase and relative intensity of Zr^{3+} in zirconia affected the catalytic properties. It was found that the 0.75% SZ (ZrO_2-N) was the suitable catalyst for isosynthesis at 400 °C.

2. The difference in calcination temperature from 450 to 750 °C can result in changes in phase composition for sulfated zirconia and acid-base properties. The product selectivity of isobutene was dependent on fraction of monoclinic phase. The result revealed that for the commercial sulfated zirconia, the isobutene selectivity and CO conversion were indirect proportional. Moreover, the 0.75% SZ (ZrO_2-N) samples were not significant change in isobutene selectivity and CO conversion. Both isobutene selectivity and CO conversion were directly proportional.

3. The commercial sulfated zirconia exhibited higher catalytic activity than the 0.75% SZ (ZrO_2-N). However, the 0.75% SZ (ZrO_2-N) achieved higher selectivity of isobutene in hydrocarbons than the commercial ones due to larger amount of Zr^{3+} being present.

6.2 Recommendation for future studies

From the previous conclusions, the following recommendations for the future study are proposed.

1. The effect of the other preparation techniques for synthesizing sulfated zirconia catalysts on the catalytic performance over isosynthesis should be further investigated.
2. The kinetic parameters and relationship between reaction rate and partial pressure of reactant for isosynthesis should be further investigated.



สถาบันวิทยบริการ
จุฬาลงกรณ์มหาวิทยาลัย

REFERENCES

- Ekerdt, J.G., and Jackson, N.B. The surface characteristics required for isosynthesis over zirconium dioxide and modified zirconium dioxide. *J. Catal.* 126 (1990): 31-45.
- Ekerdt, J.G., and Jackson, N.B. Isotope studies of the effect of acid sites on the reactions of C₃ intermediates during isosynthesis over zirconium dioxide and modified zirconium dioxide. *J. Catal.* 126 (1990): 46-56.
- Ekerdt, J.G., Tseng, S.C., and Jackson, N.B. Isosynthesis reactions of CO/H₂ over zirconium dioxide. *J. Catal.* 109 (1988): 284-297.
- Fărcașiu, D., Qi Li, J. and Cameron, S. Preparation of sulfated zirconia catalysts with improved control of sulfur content, II Effect of sulfur content on physical properties and catalytic activity. *App. Cat. A.* 154 (1997):173-184.
- Fărcașiu, D. and Qi Li, J. Preparation of sulfated zirconia catalysts with improved control of sulfur content, III. Effect of conditions of catalyst synthesis on physical properties and catalytic activity. *App. Cat. A.* 175 (1998):1-9.
- Hammache, S. and Goodwin, Jr., G. Characteristic of the active sites on sulfated zirconia for n-butane isomerization. *J. Catal.* 218 (2003):258-266.
- Hammache, S. and Goodwin, Jr., G. Elucidation of n-butane isomerization on sulfated zirconia using olefin addition. *J. Catal.* 211 (2002):316-325.
- Hino, M., Kurashige, M., Matsushashi, H. and Arata, K. The surface structure of sulfated zirconia: Studies of XPS and thermal analysis. *Thermochimica.* 441 (2006):35-41.
- Kim, S.Y., Goodwin, Jr., G., Hammache, S., Auroux, A., and Galloway, D. The impact of Pt and H₂ on n-butane isomerization over sulfated zirconia: Change in intermediates coverage and reactivity. *J. Catal.* 201 (2001):1-12.
- Kim, S. Y., Goodwin, Jr., G., and Fărcașiu, D. The effect of reaction conditions and catalyst deactivation on the mechanism of n-Butane isomerization on sulfated zirconia. *App. Cat. A.* 207 (2001):281-286.
- Kim, S.Y., Goodwin, Jr., G., and Galloway, D. n-Butane isomerization on sulfated zirconia: active site heterogeneity and deactivation. *Catal. Today.* 63 (2000): 21-32.

- Kim, S.Y., Lohitharn, N., Goodwin, Jr., G., Olindo, R., Pinna, F., and Canton, P. The effect of Al₂O₃-promotion of sulfated zirconia on *n*-butane isomerization: An isotropic transient kinetic analysis. *Catal. Com.* 7 (2006):209-213.
- Li, Xuebing., Nagaoka, K., Olindo, R., and Lercher J. A., Synthesis of highly active sulfated zirconia by sulfation with SO₃. *J. Catal.* 238 (2006):39-45.
- Li, Y.W., He, D.H., Cheng, Z.X., Su, C.L., Li, J.R., and Zhu, Q.M. Effect of calcium salts on isosynthesis over ZrO₂ catalysts. *J. Mol. Catal. A: Chem.* 175 (2001): 267-275.
- Li, Y.W., He, D.H., Yuan, Y.B., Cheng, Z.X., and Zhu, Q.M. Influence of acidic and basic properties of ZrO₂ based catalysts on isosynthesis. *Fuel.* 81 (2002): 1611- 1617.
- Li, Y.W., He, D.H., Zhang, Q.J., Xu, B.Q., and Zhu, Q.M. Influence of reactor materials on *i*-C₄ synthesis from CO hydrogenation over ZrO₂ based catalysts. *Fuel. Process.Tech.* 83 (2003): 39-48.
- Li, Y.W., He, D.H., Zhu, Q.M., Zhang, X., and Xu, B.Q. Effects of redox properties and acid-base properties on isosynthesis over ZrO₂-based catalysts. *J. Catal.* 221 (2004): 584-593.
- Liu, H., Zhang, X., and Xue, Q. ESR Characterization of ZrO₂ nanopowder. *J. Phys. Chem.* 99 (1995): 332-334.
- Lohitharn, N., Lotero, E., and Goodwin, Jr., G. A comprehensive mechanistic pathway for *n*-butane isomerization on sulfated zirconia. *J. Catal.* 241 (2006):328-341.
- Maruya, K., Kawamura, M., Aikawa, M., Hara, M., and Arai, T. Reaction path of methoxy species to isobutene and its dependence on oxide catalysts in CO hydrogenation. *J. Organ. Chem.* 551 (1998): 101-105.
- Maruya, K., Komiya, T., Hayakawa, T., Lu, L., and Yashima, M. Active sites on ZrO₂ for the formation of isobutene from CO and H₂. *J. Mol. Catal. A: Chem.* 159 (2000): 97-102.
- Maruya, K., Takasawa, A., Haraoka, T., Domen, K., and Onishi, T. Role of methoxide species in isobutene formation from CO and H₂ over oxide catalysts Methoxide species in isobutene formation. *J. Mol. Catal. A: Chem.* 112 (1996):143-151.
- Mishara, H.K., Dalai, A.K., Das, D. D., Parida, K.M. and Pradhan, N.C. Sulfated nanozirconia: an investigation on acid-base properties and *n*-butane isomerization activity. *J Colloid.* 272 (2004):378-383.

- Prescott, H. A., Wloka, M. And Kemnitz, E. Supported sulfated zirconia catalysts and their properties. *J. Mol. Catal. A: Chem.* 223 (2004):67-74.
- Pichler, H. Twenty five years of synthesis of gasoline by catalytic conversion of carbon monoxide and hydrogen. *Adv. Catal.* 4 (1952): 271-341.
- Pichler, H., and Ziesecke, K.H. Some properties of solid paraffins produced from carbon monoxide and hydrogen at high pressures. *Brennst. Chem.* 30 (1949): 1-13.
- Pârvulescu, V., Coman, S. and Grange, P. Preparation and characterization of sulfated zirconia catalysts obtained via various procedures. *App. Cat. A.* 176 (1999):27-43.
- Sofianos, A. Production of branched-chain hydrocarbons via isosynthesis. *Catal. Today.* 15 (1992): 149-175.
- Srinivasan, R., and Davis, B.H. Influence of zirconium salt precursors on the crystalstructures of zirconia. *Catal. Lett.* 14 (1992): 165.
- Stichert, W., Schüth, F., Kuba, S. and Knözinger, H. Monoclinic and tetragonal high surface area sulfated zirconias in butane isomerization: CO adsorption and catalytic results. *J. Catal.* 198 (2001):227-285.
- Su, C.L., He, D.H., Li, J.R., Cheng, Z.X., and Zhu, Q.M. Influences of preparation parameters on the structural and catalytic performance of zirconia in isosynthesis. *J.Mol. Catal. A: Chem.* 153 (2000): 139-146.
- Su, C.L., Li, J.R., He, D.H., Cheng, Z.X., and Zhu, Q.M. Synthesis of isobutene from synthesis gas over nanosize zirconia catalysts. *Appl. Catal. A: General* 202 (2000): 81-89.
- Wender, I. Reactions of synthesis gas. *Fuel Proc.* 48 (1996): 189-297.



APPENDICES

สถาบันวิทยบริการ
จุฬาลงกรณ์มหาวิทยาลัย

APPENDIX A

CALCULATION OF CRYSTALLITE SIZE

Calculation of crystallite size by Debye-Scherrer equation

The crystallite size was calculated from the half-height width of the diffraction peak of XRD pattern using the Debye-Scherrer equation.

From Scherrer equation:

$$D = \frac{K\lambda}{\beta \cos\theta} \quad (\text{A.1})$$

where D = Crystallite size, Å

K = Crystallite-shape factor (= 0.9)

λ = X-ray wavelength (= 1.5418 Å for CuK α)

θ = Observed peak angle, degree

β = X-ray diffraction broadening, radian.

The X-ray diffraction broadening (β) is the pure width of powder diffraction free from all broadening due to the experimental equipment. α -Alumina is used as a standard sample to observe the instrumental broadening since its crystallite size is larger than 2000 Å. The X-ray diffraction broadening (β) can be obtained by using Warren's formula.

From Warren's formula:

$$\beta = \sqrt{B_M^2 - B_S^2} \quad (\text{A.2})$$

where B_M = the measured peak width in radians at half peak height

B_S = the corresponding width of the standard material.

Example: Calculation of the crystallite size of zirconia

The half-height width of 111_m diffraction peak = 0.25° (from Figure A.1)

$$= \left(\frac{2\pi}{360} \right) \cdot (0.25)$$

$$= 0.0044 \text{ radian}$$

The corresponding half-height width of peak of α -alumina (from the B_s value at the 2θ of 28.36° in Figure A.2) = 0.0039 radian

$$\begin{aligned} \text{The pure width, } \beta &= \sqrt{B_M^2 - B_S^2} \\ &= \sqrt{0.0044^2 - 0.0039^2} \\ &= 0.0021 \text{ radian} \end{aligned}$$

$$\beta = 0.0021 \text{ radian}$$

$$2\theta = 28.36^\circ$$

$$\theta = 14.18^\circ$$

$$\lambda = 1.5418 \text{ \AA}$$

$$\text{The crystallite size} = \frac{0.9 \times 1.5418}{0.0021 \times \cos 14.18^\circ}$$

$$= 678 \text{ \AA}$$

$$= 67.8 \text{ nm}$$

สถาบันวิทยบริการ
จุฬาลงกรณ์มหาวิทยาลัย

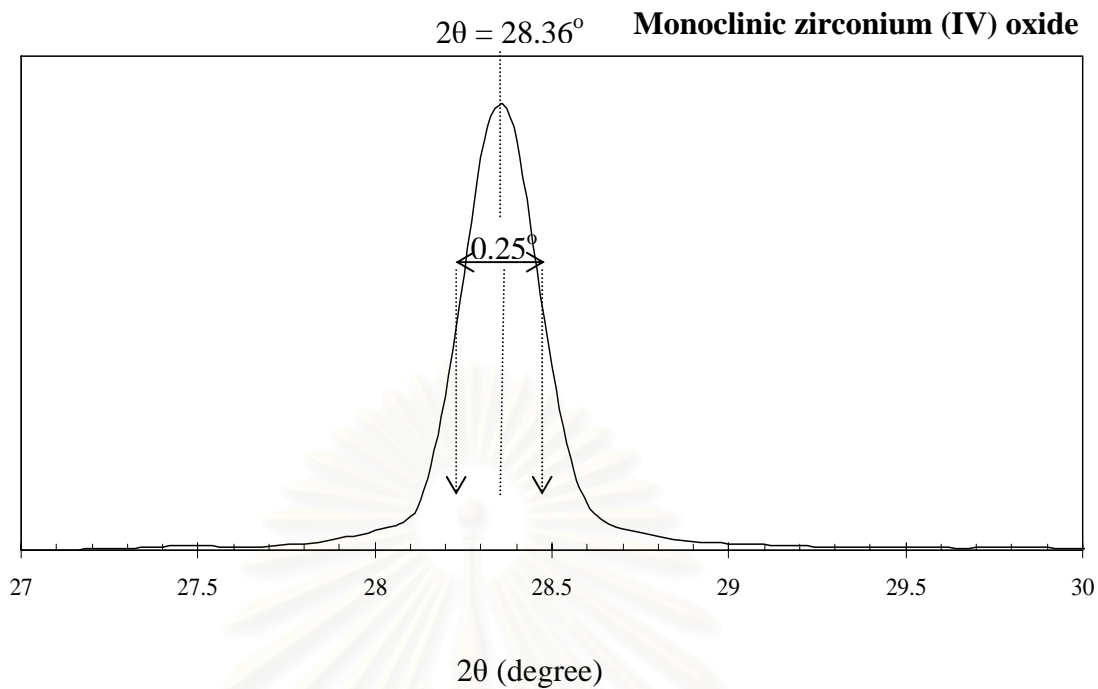


Figure A.1 The 111_m diffraction peak of zirconia for calculation of the crystallite size.

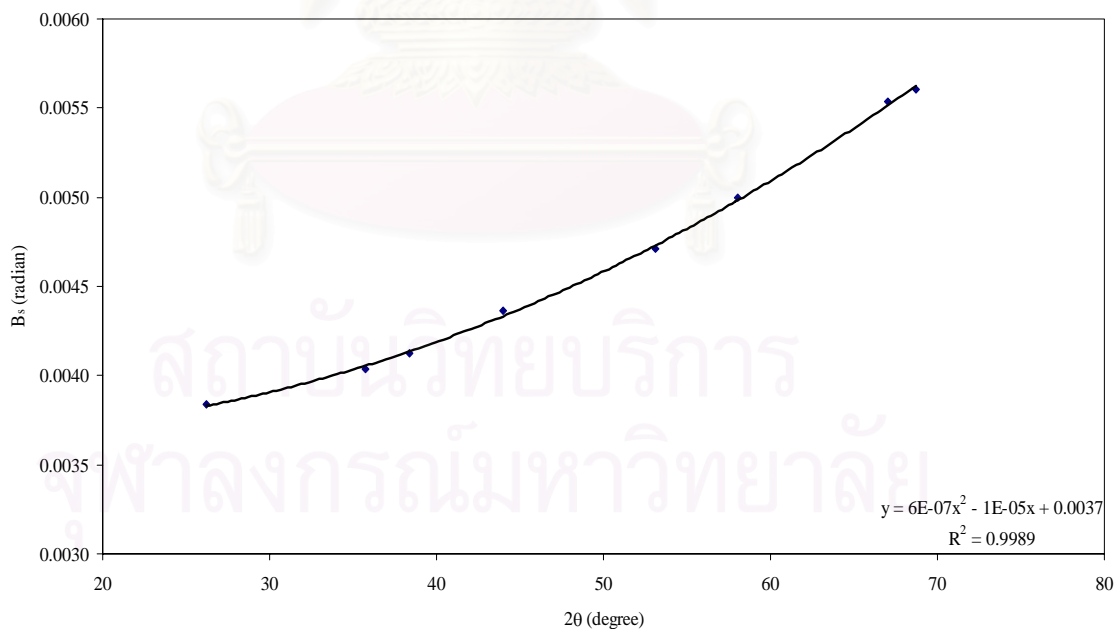


Figure A.2 The plot indicating the value of line broadening due to the equipment (data were obtained by using α -alumina as a standard).

APPENDIX B

CALCULATION OF FRACTION OF CRYSTAL PHASE OF ZIRCONIA

The fraction of crystal phase of zirconia was estimated from X-ray diffraction (XRD) profile. The amounts of tetragonal and monoclinic phase present in the zirconia were estimated by comparing the areas of characteristic peaks of the monoclinic phase ($2\theta = 28$ and 31 for (111) and (111) reflexes, respectively) and the tetragonal phase ($2\theta = 30$ for the (111) reflex). The fraction composition of each phase was calculated from the Gaussian areas $h \times w$.

$$\text{Fraction of monoclinic phase} = \frac{\sum (h \times w) \text{ monoclinic phase}}{\sum (h \times w) \text{ monoclinic and tetragonal phase}} \quad (\text{B.1})$$

$$\text{Fraction of tetragonal phase} = \frac{\sum (h \times w) \text{ tetragonal phase}}{\sum (h \times w) \text{ monoclinic and tetragonal phase}} \quad (\text{B.2})$$

where h = the height of X-ray diffraction pattern at the characteristic peaks

w = the half-height width of X-ray diffraction pattern at the characteristic peaks.

สถาบันวิทยบริการ
จุฬาลงกรณ์มหาวิทยาลัย

Example: Calculation of the fraction of crystal phase of zirconia

Table B.1 Calculation of the fraction of crystal phase of zirconia

Crystal phase	2θ	h	w	$h \times w$	Fraction of crystal phase
Monoclinic	28.24	2577	0.29	747.33	
	31.56	1837	0.32	587.84	
	Total			1335.17	
Tetragonal	30.28	8348	0.37	3088.76	0.70
Total				4423.93	1.00

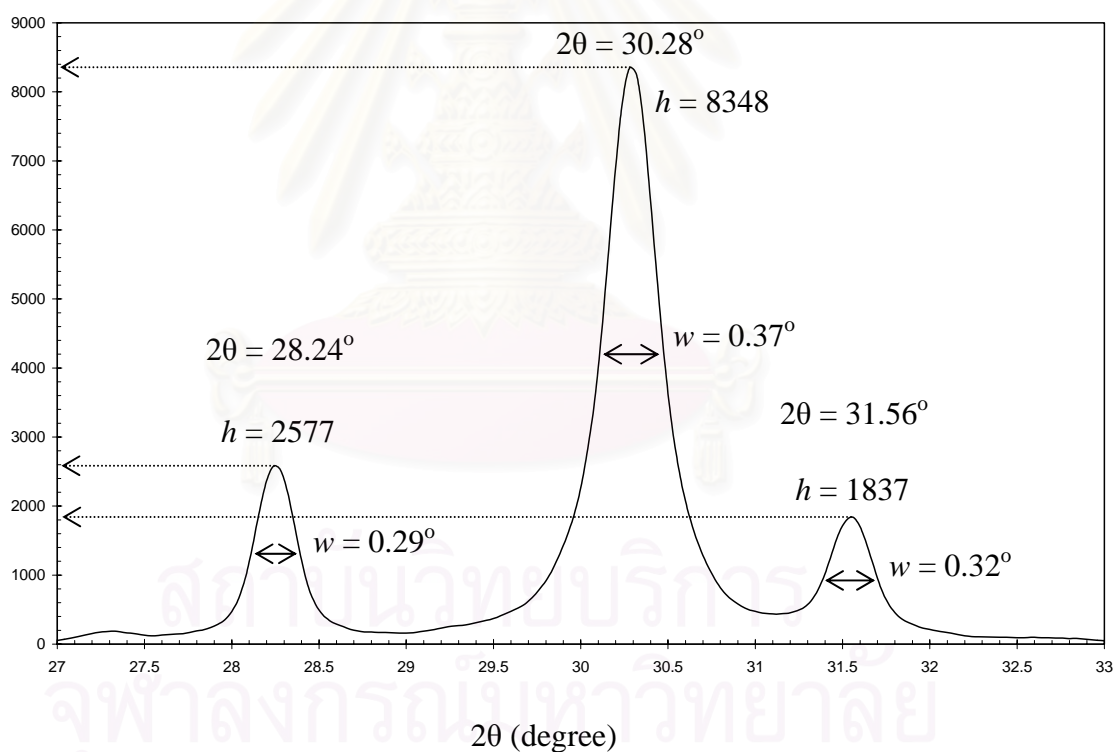


Figure B.1 The X-ray diffraction peaks of zirconia (nanopowder) for calculation of the fraction of crystal phase of zirconia.

APPENDIX C

CALIBRATION CURVES

This appendix showed the calibration curves for calculation of reactant and product compositions in isosynthesis. The reactants are carbon monoxide and hydrogen while the products are carbon dioxide and hydrocarbons consisting of C₁-C₄ such as methane, ethane, ethylene, propane, propylene, n-butane, isobutane, isobutene. For isosynthesis, the main product in hydrocarbons is isobutene.

The gas chromatography with a thermal conductivity detector (TCD), Shimadzu model 8A was used for analyzing the concentration of carbon monoxide and carbon dioxide by using Molecular sieve 5A column and Porapak-Q column, respectively.

The VZ-10 column was used in a gas chromatography equipped with a flame ionization detector (FID), Shimadzu model 14B, for analyzing the concentration of products including of methane, ethane, ethylene, propane, propylene, n-butane, isobutane, isobutene. Conditions used in both GCs are illustrated in Table B.1.

The calibration curves exhibit the relationship between mole of gas component (y-axis) and peak area reported from gas chromatography (x-axis). The calibration curves of carbon monoxide, carbon dioxide, methane, ethane, ethylene, propane, propylene, n-butane, isobutane and isobutene are shown in the following figures.

Table C.1 Conditions of Gas chromatography, Shimadzu model GC-8A and GC-14B.

Parameters	Condition	
	Shimadzu GC-8A	Shimadzu GC-14B
Width	5	5
Slope	50	50
Drift	0	0
Min. area	10	10
T.DBL	0	0
Stop time	30	90
Atten	5	0
Speed	2	2
Method	41	41
Format	1	1
SPL.WT	100	100
IS.WT	1	1

สถาบันวิทยบริการ
จุฬาลงกรณ์มหาวิทยาลัย

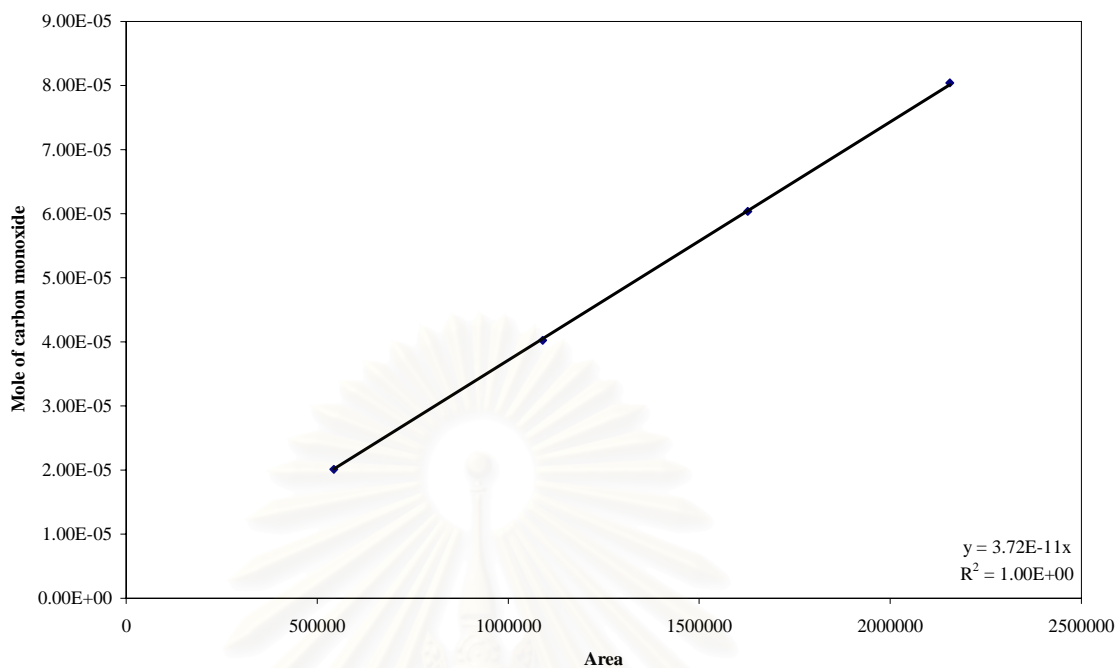


Figure C.1 The calibration curve of carbon monoxide.

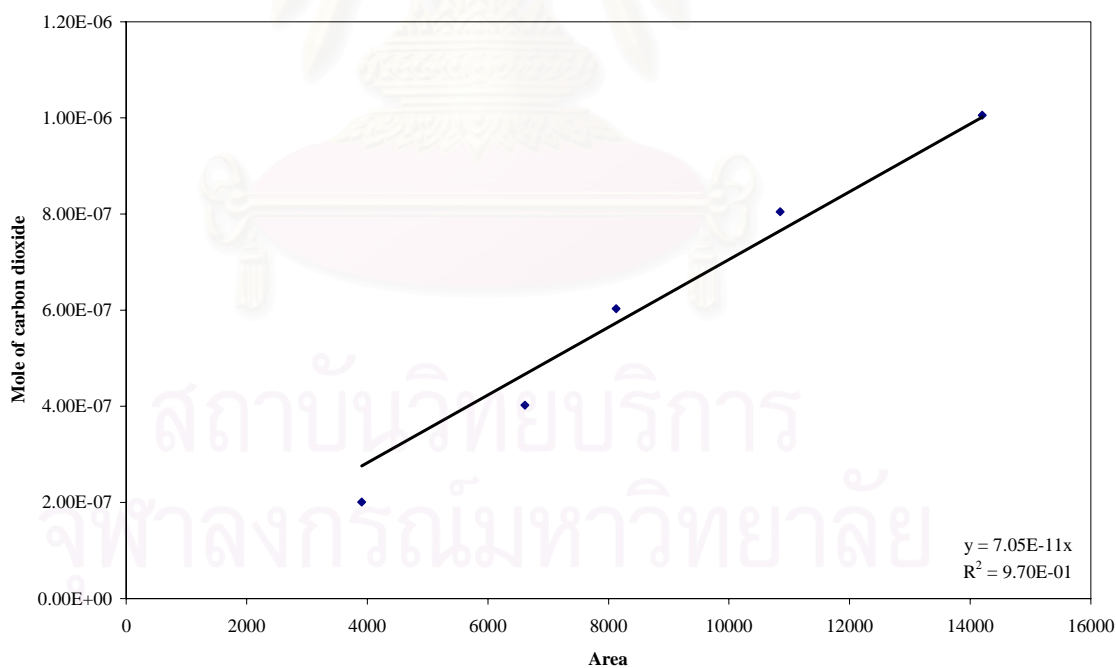


Figure C.2 The calibration curve of carbon dioxide.

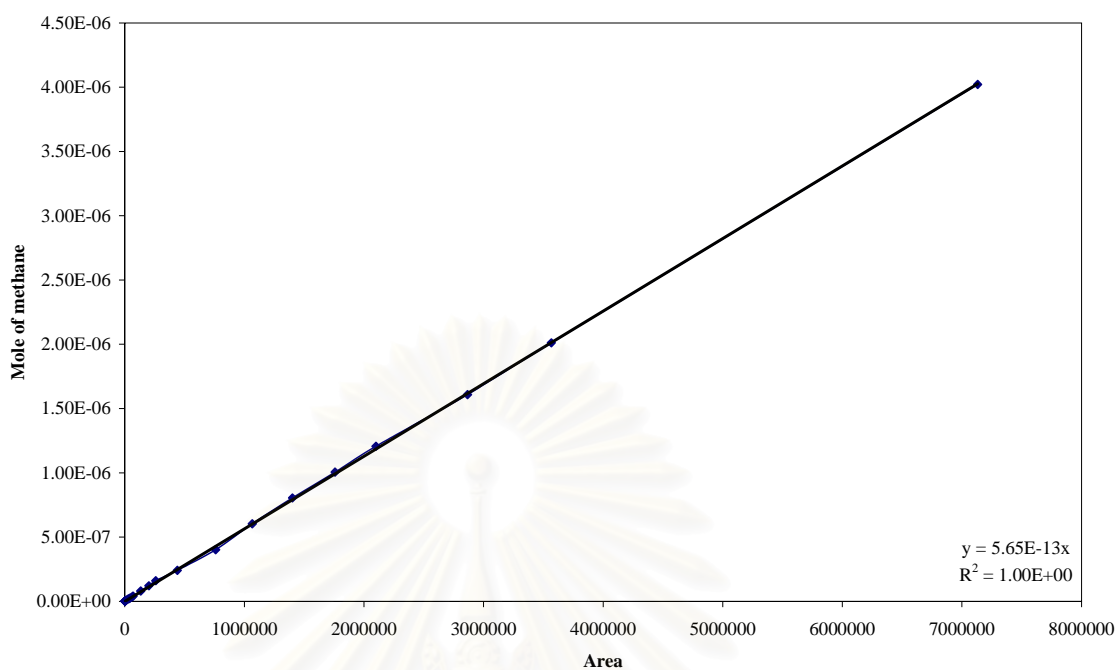


Figure C.3 The calibration curve of methane.

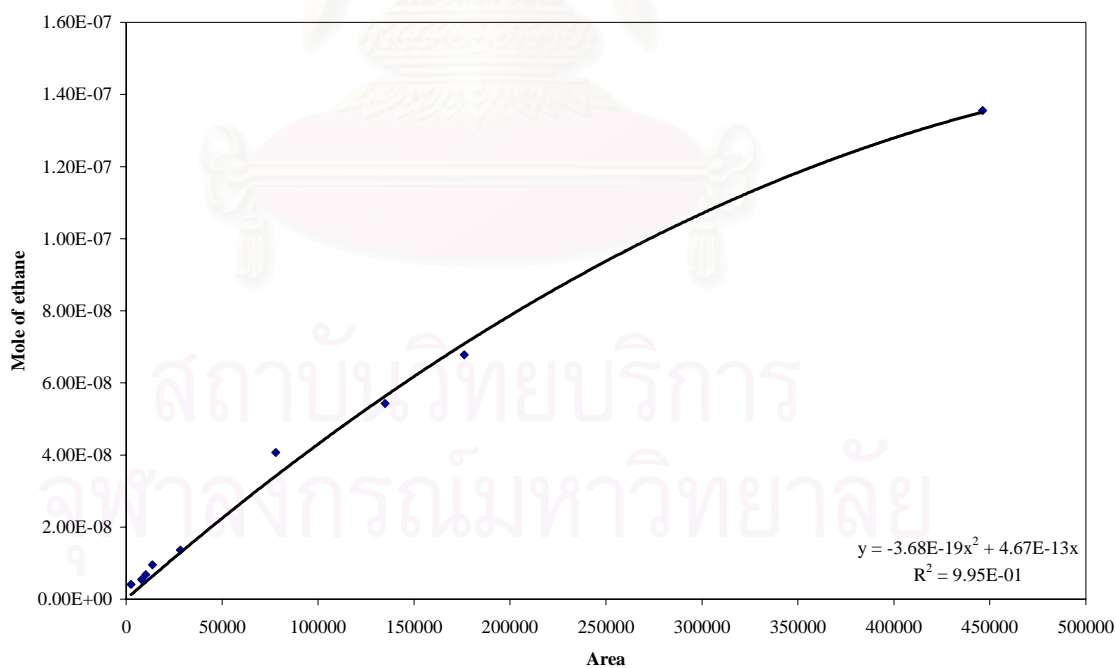


Figure C.4 The calibration curve of ethane.

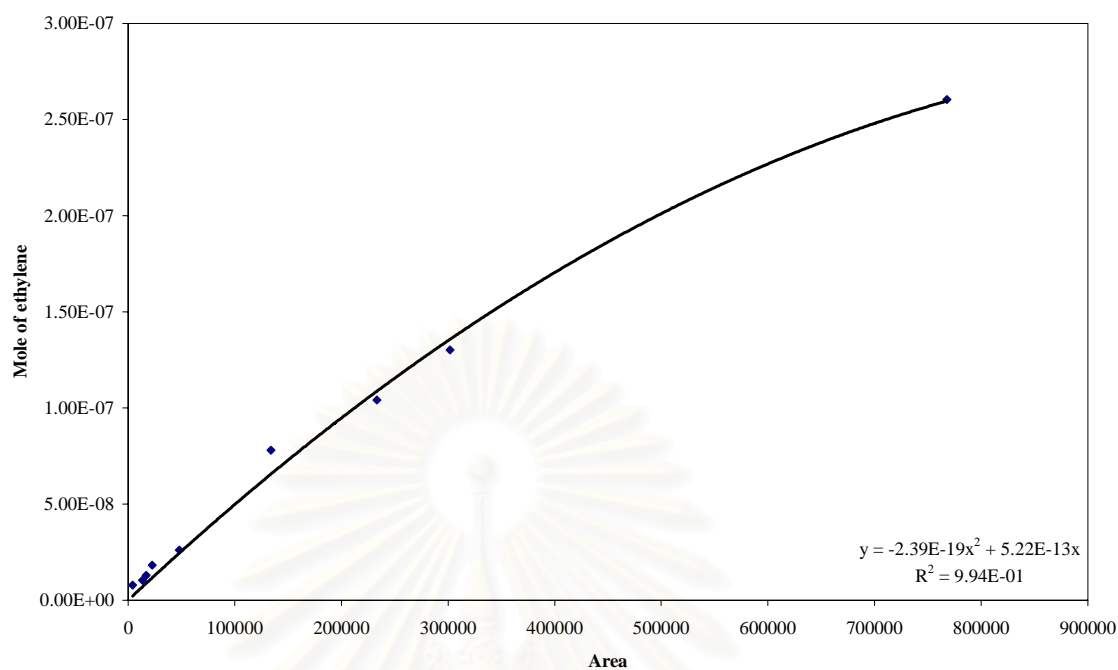


Figure C.5 The calibration curve of ethylene.

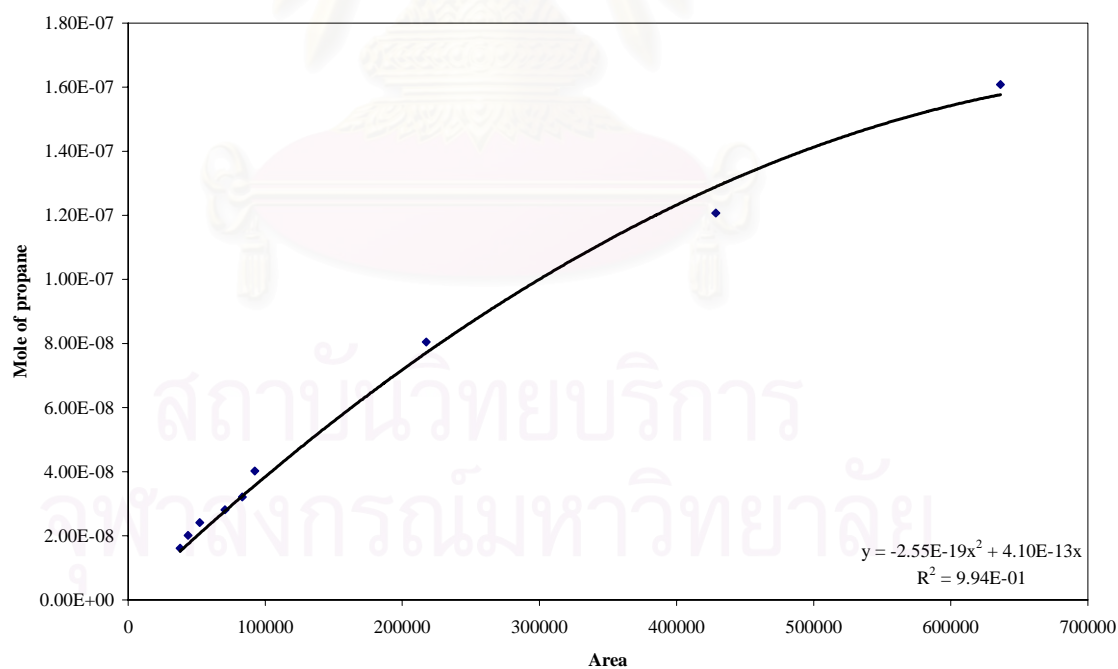


Figure C.6 The calibration curve of propane.

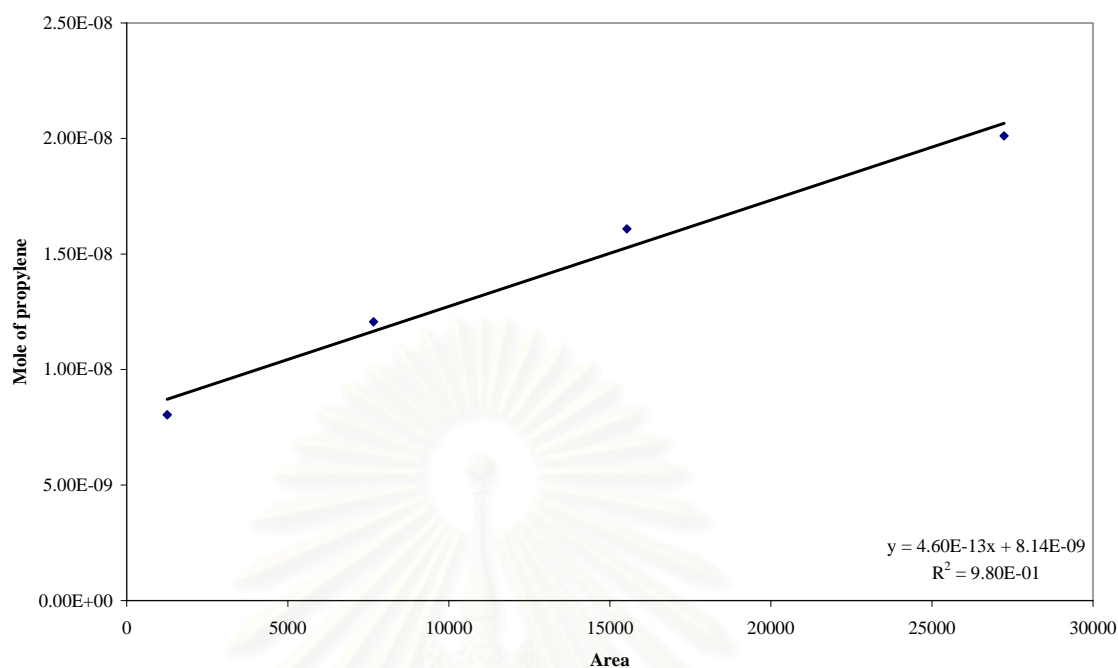


Figure C.7 The calibration curve of propylene.

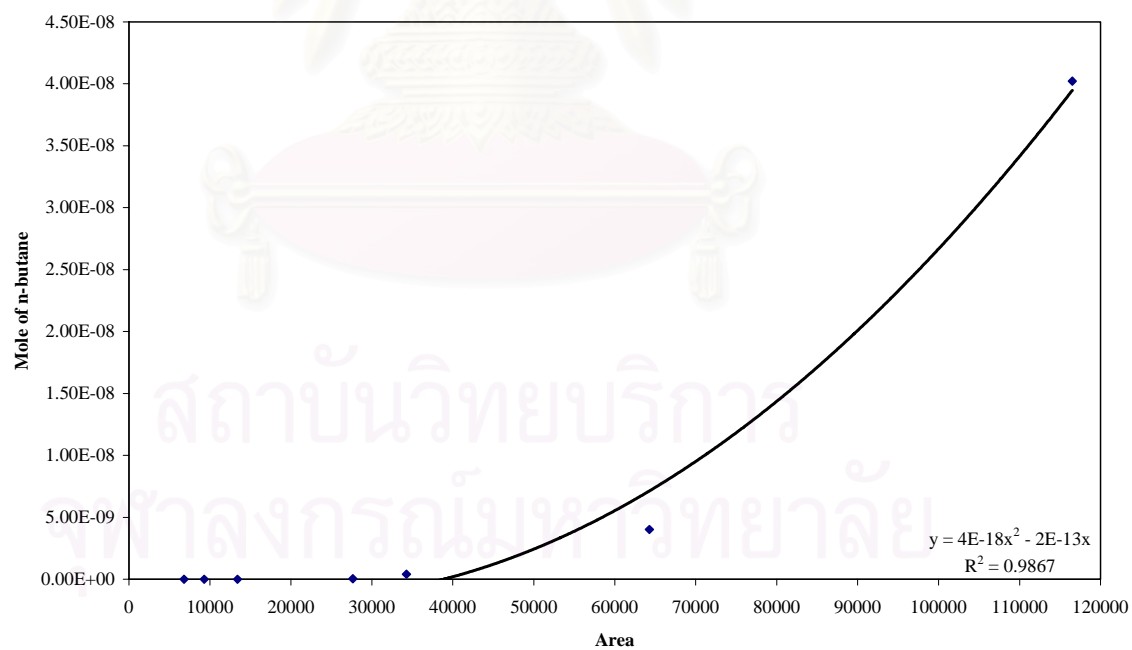


Figure C.8 The calibration curve of n-butane.

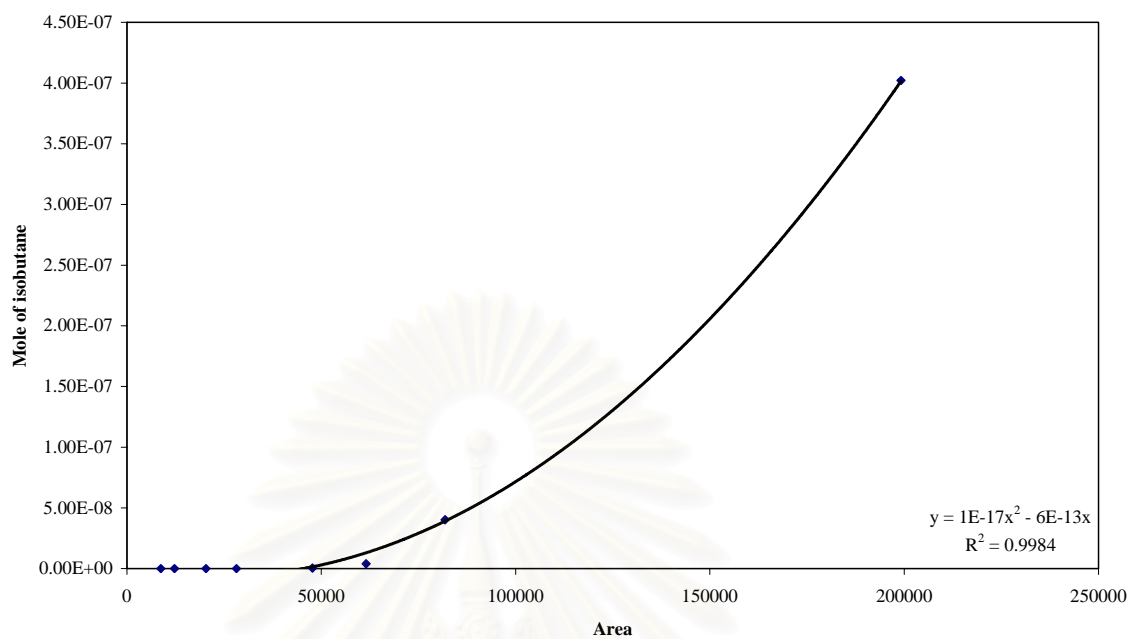


Figure C.9 The calibration curve of isobutane.

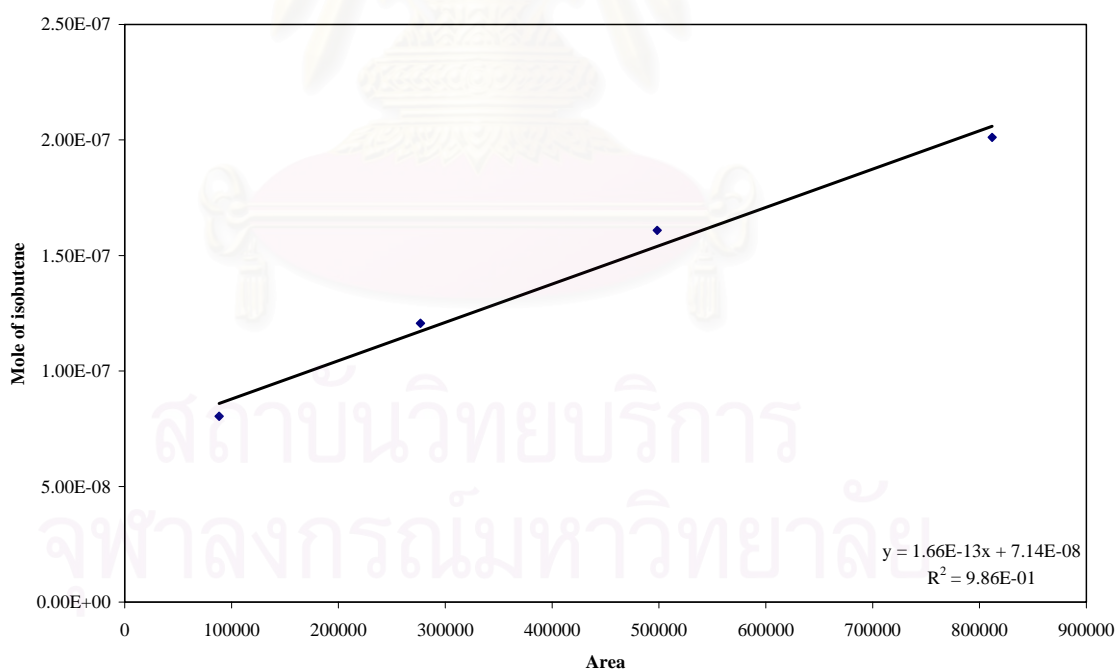


Figure C.10 The calibration curve of isobutene.

APPENDIX D

CALCULATIONS OF CARBON MONOXIDE CONVERSION, REACTION RATE AND SELECTIVITY

The catalytic performance for the isosynthesis was evaluated in terms of CO conversion, reaction rate and selectivity.

CO conversion is defined as moles of CO converted with respect to moles of CO in feed:

$$\text{CO conversion (\%)} = \frac{\text{moles of CO converted to product}}{\text{moles of CO in feed}} \times 100 \quad (\text{D.1})$$

where mole of CO can be determined from CO peak area of the product gas and the calibration curve of CO (Figure C.1 in Appendix C).

$$\text{Mole of CO} = (\text{Area of CO peak from integrator plot on GC - 8A}) \times 3.72 \times 10^{-11} \quad (\text{D.2})$$

Reaction rate was calculated from CO conversion as follows:

Let the weight of catalyst used	=	W	g
Flow rate of CO	=	10	cm ³ /min
Volume of 1 mole of gas at STP	=	22400	cm ³
Temperature of gas at STP	=	273	K
Room temperature of gas	=	303	K

$$\text{Reaction rate (\mu\text{mole/kg catalyst/s})} = \frac{[\% \text{conversion of CO}/100] \times 22400 \times 303 \times 10^6}{W \times 10 \times 60 \times 273} \quad (\text{D.3})$$

Selectivity of product is defined as moles of carbon in the product of interest (B) with respect to moles of CO converted:

$$\text{Selectivity of B (\%)} = \frac{\text{moles of B formed}}{\text{moles of CO converted}} \times 100 \quad (\text{D.4})$$

where B is product, mole of B can be measured employing the calibration curves of products such as CO₂ and hydrocarbon C₁-C₄ such as methane, ethane, ethylene, propane, propylene, n-butane, isobutane and isobutene as shown in Figures C.2-C.10 of Appendix C.

$$\text{Mole of methane} = (\text{Area of methane peak from integrator plot on GC - 14B}) \times 5.65 \times 10^{-13} \quad (\text{D.5})$$

สถาบันวิทยบริการ
จุฬาลงกรณ์มหาวิทยาลัย

VITA

Miss Nicha Tangchupong was born on October 17, 1983 in Bangkok, Thailand. She received her Bachelor Degree of Chemical Engineering from Faculty of Engineering, King Monkult's Institute of Technology Ladkrabang, Bangkok, Thailand in March 2005. She continued her Master study in the same major at Chulalongkorn University, Bangkok, Thailand in June 2005.



สถาบันวิทยบริการ
จุฬาลงกรณ์มหาวิทยาลัย